HIGHWAY RESEARCH RECORD

Number 319

Application of Aerial Surveys and Photogrammetry

7 Reports

Subject Areas

21 Photogrammetry
22 Highway Design
26 Pavement Performance
61 Exploration-Classification (Soils)

HIGHWAY RESEARCH BOARD
DIVISION OF ENGINEERING NATIONAL RESEARCH COUNCIL
NATIONAL ACADEMY OF SCIENCES—NATIONAL ACADEMY OF ENGINEERING
WASHINGTON, D.C. 1970

Standard Book Number 309-01818-8

Price: $2.80

Available from

Highway Research Board
National Academy of Sciences
2101 Constitution Avenue
Washington, D.C. 20418

Department of Design

W.B. Drake, Chairman
Kentucky Department of Highways, Lexington

L.F. Spaine
Highway Research Board Staff

GENERAL DESIGN DIVISION

M.D. Shelby, Chairman
Texas Transportation Institute, Texas A M University College Station

COMMITTEE ON PHOTOGRAMMETRY AND AERIAL SURVEYS
(As of December 31, 1969)

Glenn Anschutz, Chairman
Kansas State Highway Commission, Topeka

William T. Pryor, Secretary
Bureau of Public Roads, Washington, D.C.

Robert L. Alston
Fred B. Bales
Forrest G. Bentley
H.L. Brantley
Richard H. Burke
James J. Byrne
Roger R. Chamard
J.E. Colcord, Jr.
Richard A. Coleman
John Oran Eichler
Hubert A. Henry
Lloyd O. Herd
David S. Johnson, Jr.
George P. Katibah
Gottfried Konecny
M.H. MacLeod
Charles E. McNoldy
Robert D. Miles
Olin W. Mintzer
Grover W. Parrott
Arthur C. Quinnell
Harold Rib
Vernon H. Schultz
James I. Taylor
Robert D. Turpin
John Waller
Robert J. Warren
James I. Webster
Dwight E. Winsor
Marshall S. Wright, Jr.

PAVEMENT DIVISION

Milton E. Harr, Chairman
Purdue University, Lafayette, Indiana

COMMITTEE ON PAVEMENT CONDITION EVALUATION
(As of December 31, 1969)

Malcolm D. Graham, Chairman
New York Department of Transportation, Albany

Frederick E. Behn
W. B. Drake
Karl H. Dunn
Leroy D. Graves
Ralph C. G. Haas
W. S. Housel
Ronald W. Hudson
C. S. Hughes
James W. Lyon, Jr.
Alfred W. Maner
Phillip L. Melville
A. B. Moe
Frank P. Nichols
Bayard E. Quinn
G. Y. Sebastyan
Foster A. Smiley
Elson B. Spangler
Bertram D. Tallamy
W. E. Teske
Allan P. Whittemore
Eldon J. Yoder

Foreword

Notable advances have been made in recent years in the application and utilization of aerial photography and photogrammetry in various phases of highway engineering. The 7 papers comprising this RECORD will be of interest to those responsible for the application of new developments in these areas to a wide variety of engineering procedures.

The first 2 papers deal with analytical aerial triangulation for aerial surveys. The investigation reported in the abridged paper by Karara and Marks indicates the suitability of analytical aerial triangulation for highway location and design. An approach is recommended as being sufficiently accurate and practical for implementation. Knowles presents a mathematical solution of an aerotriangulation procedure that can be applied successfully to the problem of vertical control extension for large-scale photographs. The solution was found to be exact to within limits that are negligible in their effect on the resulting errors obtained from using actual photographic data.

Maxwell's paper describes a computer software system that furnishes the highway engineer with a method for approximating the terrain surface with a numerical surface. The use of the numerical surface approach has promise for the elimination of some of the terrain representation problems associated with the traditional cross section method. McNoldy discusses the current use of terrain data obtained through photogrammetric procedures for highway location and design and describes in some detail equipment and computer programs that are available.

The paper, by Stoeckeler, introduces the use of color photography for the evaluation of distress in flexible pavements. The author concludes that the maximum amount of information on pavement distress features can be extracted from infrared color transparencies.

The application of multispectral remote sensing to engineering soils mapping was investigated by Tanguay and Miles. Their study included 15-channel imagery and 4 types of aerial photographs. Color film was judged to be the best and most economical of the media for mapping soils and soil conditions. Computer analysis of multispectral data proved to be efficient and practical.

The final paper, by Taylor and Carter, is concerned with developing photogrammetric techniques for measuring traffic kinematics in a manner appropriate for use in the mathematical expressions utilized in traffic gap acceptance analyses. The accuracy of the methodology was determined to be suitable for the analyses to be performed.

Contents

Analytical Aerial Triangulation for Highway Location and Design

H. M. KARARA and G. W. MARKS, University of Illinois

ABRIDGMENT

•THIS IS A SUMMARY REPORT on a study conducted by the University of Illinois in cooperation with the Illinois Division of Highways and the U.S. Department of Transportation, Federal Highway Administration, Bureau of Public Roads (1HR-804). The report is available through the Clearinghouse for Federal Scientific and Technical Information, Springfield, Virginia 22151, PB 186 495.

The investigation reported here pertains to the application of analytical aerial triangulation for aerial surveying to accomplish highway location and design. Three basic approaches distinguished by the number of photographs used as a unit in the relative orientation phase (2-photo, 3-photo, and simultaneous solutions) were compared through the analysis of both fictitious and real data. The 3-photo (triplet) analytical aerial triangulation approach was recommended as the one most suitable for the implementation of analytical photogrammetry to the highway location and design task. This approach can provide the results needed for the determination of supplemental photogrammetric control, with feasible requirements for analyst data handling and with an optimum facility for observational blunder detection.

The monocular and stereoscopic approaches to analytical photogrammetry were also compared in this project. The results indicated that both approaches yield essentially the same order of accuracy, and this led to the recommendation of the monocular observational system for operational utilization, inasmuch as such a system would be significantly lower in price than a stereoscopic observational system.

Experimentations with various densities and distributions of ground control demonstrated the extremely important influence these 2 parameters have on the results of aerial triangulation projects. The use of a minimum of 3 control points at both ends of the bridged strip or substrip was strongly recommended. These control points should be positioned in a triangular fashion such that 2 points are placed along a line approximately perpendicular to the strip axis at one side of the stereoscopic model and the third point near the centerline of the strip near the opposite side of the stereoscopic model.

To meet accuracy requirements of map compilation products, a bridging distance of not more than 6 stereoscopic models was recommended. For strips longer than 6 models, the control should be placed at equal intervals along the strip, with the maximum interval between control points being 6 stereoscopic models in length. The analysis and adjustment of such continuous strips may be accomplished in either of 2 ways: (a) Each substrip is to be treated separately; or (b) the continuous strip is treated as a whole, and the adjustment is based on all available control provided at the ends of each substrip. On the basis of the investigators' previous experience in this matter, the separate substrip approach was recommended.

Results of the investigation indicated the extreme care with which photographic points are to be transferred, particularly in the monocular approach.

For optimum operation utilization, the electronic computer programs for the monocular 3-photo solution were developed and assembled into a single systems computer programming package, with emphasis placed on the inclusion of program and operator checks within the system to ensure minimization of operator data handling blunders.

Paper sponsored by Committee on Photogrammetry and Aerial Surveys and presented at the 49th Annual Meeting.

The investigation indicated the suitability of analytic aerial triangulation for highway location and design, and pointed out a number of areas where further research is highly recommended, including the design of photographic targets (panels), and the development of design criteria for aerial triangulation projects involving large-scale photography.

Analytic Aerotriangulation for Large-Scale Photography

DAVID R. KNOWLES, Department of Civil Engineering, Texas A&M University

Much effort the past several years has been directed toward the use of analytic aerotriangulation as a tool to help solve some of the highway mapping problems. Some of these efforts in the area of vertical control extension for large-scale photographs have been discouraging. This paper presents in a simplified and detailed manner a mathematical solution of an analytic aerotriangulation procedure that is exact to within limits that are negligible in their effect on the resulting errors obtained from using actual large-scale photographic data. The procedure is of the cantilever strip assembly type where relative and absolute orientation is performed on the first model with the remaining models being relatively oriented and scaled, similar to an analog aerotriangulation procedure as used with a Zeiss C-8 stereoplanigraph. This procedure can be used in production or as a research tool to study and evaluate control extension errors that can be attributed to the photography, measurement of photograph coordinates, ground control, and adjustment procedures.

•ANALYTIC AEROTRIANGULATION procedures have been developed that give satisfactory results for small-scale photography, but when applied to large-scale photography the results do not always meet the requirements desired for compiling large-scale topographic maps that are commonly used in highway work. This raises the question as to whether or not a mathematical solution to the aerotriangulation problem that has been developed for small-scale photography can be successfully applied to a procedure for large-scale photography.

For small-scale photography the relative orientation solution can assume that differences in elevation of the relative orientation points are small compared to the flying height, and the resulting errors in the orientation motions are negligible compared to errors caused by other factors such as errors in measuring photograph coordinates; therefore, these differences in elevation can be neglected in the solution. For large-scale photography this assumption may not be applicable. For example, for 1:40,000 photography taken with a 6-in. focal length camera, the flying height would be 20,000 ft above the average ground elevation. If there is a 100-ft difference in elevation between the low and high points, the maximum neglected elevation would be 50 ft. This elevation difference would be 1:400 of the flying height. For 1:3,000 photography taken with the same camera of the same area, this neglected elevation difference would be 1:30 of the flying height or a difference by a factor of more than ten.

In the relative orientation solution the orientation motions are not exactly independent variables; however, they approach independence as they approach zero. For low-flying heights, the air tends to be less stable resulting in larger orientation motions that consequently increase the importance of taking into account the interdependency of the orientation motions.

Paper sponsored by Committee on Photogrammetry and Aerial Surveys and presented at the 49th Annual Meeting.

Considering the 2 differences between large-scale and small-scale photography just mentioned, it seems worthwhile to develop an exact solution to the analytic aerotriangulation problem.

RELATIVE ORIENTATION

If 2 aerial photographs having overlapping coverage are taken such that the second photograph lies in the same plane as the first with its x-axis coinciding with a line defined by the x-axis of the first photograph, then a point in the overlapping area will have the same y-coordinate on both photographs. Any deviation of this ideal orientation of the second photograph with respect to the first will cause a difference in y-photo coordinates. These differences are referred to as y-parallaxes. If y-parallaxes at 5 points are known, it is possible to determine 5 orientation elements, dY, dZ, dκ, dω, and dφ, that will define this deviation of the second photograph (Fig. 1). Such a determination is known as relative orientation. Once the orientation elements have been determined, it is possible to rectify the second photograph (i.e., change the x- and y-photo coordinates of the photo images) so as to produce a hypothetical photograph that would be identical with one that was taken with ideal orientation to the first photograph.

In order to determine the relationship between y-parallax at a point and the orientation elements, each orientation element is first treated independently. Y-parallax, Py, is defined so as to also be a correction to be applied to the y-coordinate of the right photograph (i.e., $Py = y' - y''$).

TIP (dφ)

From Figure 2,

$$Py_{\phi} = y' - y''$$

$$r = \frac{f}{\cos\alpha} \text{ where } \alpha = \arctan\left(-\frac{x''}{f}\right)$$

$$r + \Delta r = \frac{f}{\cos(\alpha + d\phi)}$$

$$\Delta r = \frac{f}{\cos(\alpha + d\phi)} - r$$

$$\Delta r = f\left[\frac{1}{\cos(\alpha + d\phi)} - \frac{1}{\cos\alpha}\right]$$

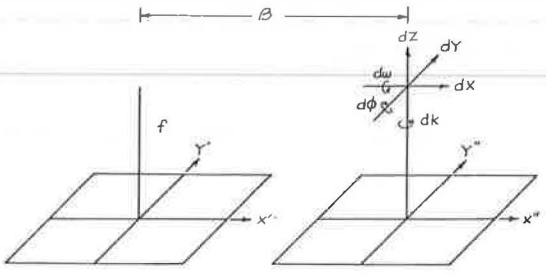

Figure 1.

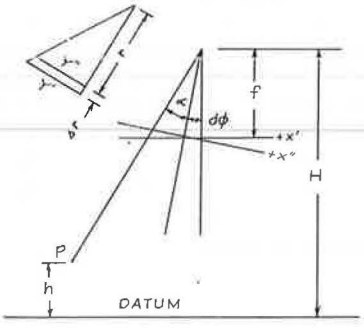

Figure 2.

From similar triangles,

$$\frac{Py_\phi}{\Delta r} = \frac{y''}{r}$$

$$Py_\phi = \frac{y''}{r}\,\Delta r$$

$$Py_\phi = \frac{y''\cos\alpha}{f} f\left[\frac{1}{\cos(\alpha + d\phi)} - \frac{1}{\cos\alpha}\right]$$

$$Py_\phi = y''\left[\frac{\cos}{\cos(\alpha + d\phi)} - 1\right] \qquad (1)$$

TILT ($d\omega$)

From Figure 3,

$$Py_\omega = y' - y''$$

$$y' = f\tan(\beta + d\omega) \text{ where } \beta = \arctan\left(\frac{y''}{f}\right)$$

$$y'' = f\tan\beta$$

$$Py_\omega = f\left[\tan(\beta + d\omega) - \tan\beta\right] \qquad (2)$$

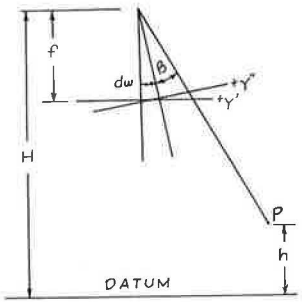

Figure 3.

SWING ($d\kappa$)

From Figure 4,

$$Py_\kappa = y' - y''$$

$$r = \sqrt{y''^2 + x''^2}$$

$$y' = r\sin(\gamma + d\kappa) \text{ where } \gamma = \arcsin\left(\frac{y''}{r}\right)$$

$$y'' = r\sin\gamma$$

$$Py_\kappa = \sqrt{y''^2 + x''^2}\left[\sin(\gamma + d\kappa) - \sin\gamma\right] \qquad (3)$$

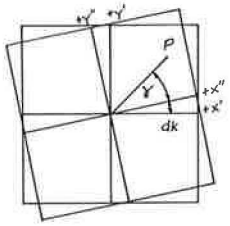

Figure 4.

dZ

From similar triangles (Fig. 5),

$$\frac{Y}{y'} = \frac{H - h}{f}$$

$$\frac{Y}{y''} = \frac{H - h + dZ}{f}$$

$$Y = \frac{y'(H - h)}{f} = \frac{y''(H - h + dZ)}{f}$$

$$y''(H - h) = y''(H - h) + y''dZ$$

$$(y' - y'')(H - h) = y''dZ$$

$$Py_Z = y' - y''$$

$$Py_Z = \frac{y''dZ}{H - h} \qquad (4)$$

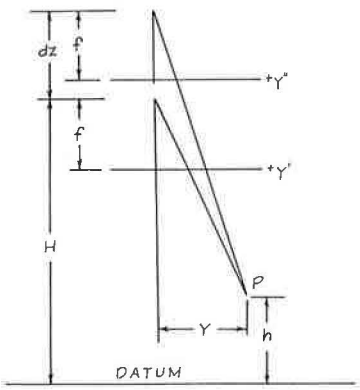

Figure 5.

dY

From similar triangles (Fig. 6),

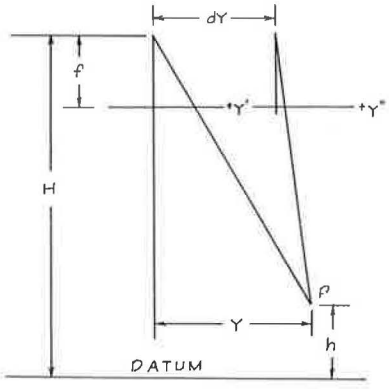

Figure 6.

$$\frac{Y}{y'} = \frac{H - h}{f}$$

$$\frac{Y + dY}{y} = \frac{H - h}{f}$$

$$y' = \frac{fY}{H - h}$$

$$y'' = \frac{f(Y - dY)}{H - h}$$

$$Py_Y = y' - y''$$

$$Py_Y = \frac{fY}{H - h} - \frac{fy - fdY}{H - h}$$

$$Py_Y = \frac{fdY}{H - h} \qquad (5)$$

These relationships between y-parallax and the 5 relative orientation motions are derived assuming no interdependency. In actuality, interdependency between the orientation motions must be taken into account. That is to say, if a photograph is moved through an angle $d\phi$, the correction in y due to $d\phi$ must be taken into account when computing the change in y due to a rotation through $d\omega$. A sequence of relative orientation motions is taken to be $d\phi$, $d\omega$, $d\kappa$, dZ, and dY. This sequence makes calculations much simpler because the first 2 motions render a rectified photograph that lies in a plane parallel to the plane of the photograph to which it is being oriented.

The new set of relationships between y-parallaxes and the relative orientation motions, taking into account interdependency, are as follows:

TIP ($d\phi$)

$$Py_\phi = y'' \left[\frac{\cos \alpha}{\cos(\alpha + d\phi)} - 1 \right] \text{ where } \alpha = \arctan\left(-\frac{x''}{f}\right) \qquad (6)$$

TILT ($d\omega$)

$$Py_\omega = f\left[\tan(\beta + d\omega) - \tan \beta\right] \text{ where } \beta = \arctan\left(\frac{y'' + Py_\phi}{f}\right) \qquad (7)$$

SWING ($d\kappa$)

$$Py_\kappa = r\left[\sin(\gamma + d\kappa) - \sin \gamma\right] \text{ where } r = \sqrt{(y'' + Py_\phi + Py_\omega)^2 + (x'' + Cx_\phi + Cx_\omega)^2} \qquad (8)$$

$$\gamma = \arcsin\left(\frac{y'' + Py_\phi + Py_\omega}{r}\right)$$

Cx_ϕ = correction to x due to $d\phi$
Cx_ω = correction to x due to $d\omega$

dZ

$$Py_Z = \frac{(y'' + Py_\phi + Py_\omega + Py_\chi)dZ}{H - h} \tag{9}$$

dY

$$Py_Y = \frac{fdY}{H - h} \tag{10}$$

The y-parallax at any one point due to the 5 orientation motions is equal to the sum of the y-parallaxes due to each motion. Therefore,

$$Py_t = Py_\phi + Py_\omega + Py_\chi + Py_Z + Py_Y \tag{11}$$

In order to rectify a photograph it is also necessary to correct the x-photo coordinates. A relationship between the x-photo coordinate correction at a point and the 5 relative orientation motions is obtained in a similar fashion as for the y-photo coordinate correction. This analysis yields the following:

TIP (dϕ)

$$Cx_\phi = f\left[\tan\alpha - \tan(\alpha + d\phi)\right] \tag{12}$$

TILT (dω)

$$Cx_\omega = (x'' + cx_\phi)\left[\frac{\cos\beta}{\cos(\beta + d\omega)} - 1\right] \tag{13}$$

SWING (dχ)

$$Cx_\chi = r\left[\cos(\gamma + d\chi) - \cos\gamma\right] \tag{14}$$

dZ

$$Cx_Z = \frac{(x'' + Cx_\phi + Cx_\omega + Cx_\chi)dZ}{H - h} \tag{15}$$

dY

$$Cx_Y = 0 \tag{16}$$

where α, β, γ, and r are the same values as used in the y-photo coordinate correction equation.

The total correction for the x-photo coordinate of a point due to the 5 relative orientation motions is

$$Cx_t = Cx_\phi + Cx_\omega + Cx_\chi + Cx_Z \tag{17}$$

If a change in the air base is taken into consideration where

$$Cx_X = \frac{fdX}{H - h} \tag{18}$$

then

$$Cx_t = Cx_\phi + Cx_\omega + Cx_\chi + Cx_Z + Cx_X \tag{19}$$

For the purpose of developing an analytical relative orientation procedure, it is assumed that the flying height of the initial photograph has been assumed or computed by the absolute orientation procedure and that the air base has also been assumed or computed by the scaling procedure. In the expanded form of Eq. 11, $d\phi$, $d\omega$, $d\kappa$, dZ, dY, and h are unknown with Py_t being the measured y-parallax at a point. Six observation equations obtained by measuring the x- and y-photo coordinates of 6 points on the overlapping area of 2 photographs will not yield a solution of the orientation elements because each point may have a different value of h (elevation). This means there will always be 5 more unknowns than observations equations. This problem can be surmounted by using 5 observation equations, solving for approximate orientation values, using these values to apply approximate corrections to x-photo coordinates, and then using these x-photo coordinates to compute approximate values of elevations that can be used in resolving the observation equations. This process can be iterated until convergence is reached.

The expanded form of Eq. 11 is nonlinear making a direct solution of a set of observation equations impossible. To obtain a solution, a linear equation is developed that will approximate Eq. 11 and will approach exactness when the orientation motions approach zero.

The derivation of this linear equation is as follows:

TIP ($d\phi$)

$$Py_\phi = y'' \left[\frac{\cos \alpha}{\cos(\alpha + d\phi)} - 1 \right]$$

$$= y'' \left[\frac{\cos \alpha}{\cos \alpha \cos d\phi - \sin \alpha \sin d\phi} - 1 \right]$$

$$= y'' \left[\frac{f/r}{(f/r)\cos d\phi - (-x''/r)\sin d\phi} - 1 \right] \qquad (6)$$

Assuming $\cos d\phi = 1$; $\sin d\phi = d\phi$,

$$Py_\phi = y'' \left[\frac{f/r}{f/r + (x''/r)d\phi} - 1 \right]$$

$$= y'' \left[\frac{f - (f + x''d\phi)}{f + x''d\phi} \right]$$

Assuming $x''d\phi$ is small compared to f,

$$Py_\phi = -\frac{y''x''}{f} d\phi \qquad (20)$$

TILT ($d\omega$)

$$Py_\omega = f \left[\tan(\beta + d\omega) - \tan \beta \right]$$

$$= f \left[\frac{\tan \beta + \tan d\omega}{1 - \tan \beta \tan d\omega} - \tan \beta \right] \qquad (7)$$

Assuming $Py_\phi = 0$, then $f \tan \beta = y''$, and

$$Py_\omega = \frac{y'' + f \tan d\omega}{1 - (y''/f)\tan d\omega} - y''$$

$$= \frac{fy'' + f^2 \tan d\omega - fy'' + y''^2 \tan d\omega}{f - y'' \tan d\omega}$$

Assuming $\tan d\omega = d\omega$,

$$Py_\omega = \frac{f^2 d\omega + y''^2 d\omega}{f}$$

$$Py_\omega = \left(f + \frac{y''^2}{f}\right) d\omega \tag{21}$$

SWING ($d\varkappa$)

$$Py_\varkappa = r\left[\sin(\gamma + d\varkappa) - \sin\gamma\right]$$

$$= r\left[\sin\gamma \cos d\varkappa + \cos\gamma \sin d\varkappa - \sin\gamma\right] \tag{8}$$

Assuming $Py_\phi = 0$, $Py_\omega = 0$, $Cx_\phi = 0$, $Cx_\omega = 0$, then $r \sin\gamma = y''$ and $r \cos\gamma = x''$ and

$$Py_\varkappa = y'' \cos d\varkappa + x'' \sin d\varkappa - y''$$

Assuming $\cos d\varkappa = 1$ and $\sin d\varkappa = d\varkappa$,

$$Py_\varkappa = x'' d\varkappa \tag{22}$$

dZ

$$Py_Z = \frac{(y'' + Py_\phi + Py_\omega + Py_\varkappa)\, dZ}{H - h} \tag{9}$$

Assuming $Py_\phi = 0$, $Py_\omega = 0$, $Py_\varkappa = 0$,

$$Py_Z = \frac{y''}{H - h}\, dZ \tag{23}$$

dY

$$Py_Y = \frac{f}{H - h}\, dY \tag{10}$$

The sum of the changes in y due to each orientation motion yields

$$Py_t = -\frac{y''x''}{f}\, d\phi + \left(f + \frac{y''^2}{f}\right) d\omega + x'' d\varkappa + \frac{y''}{H - h}\, dZ + \frac{f}{H - h}\, dY \tag{23}$$

An iteration procedure is used with 5 linear observation equations and their corresponding exact nonlinear observation equations to compute the orientation motions. Assuming values for elevations, the linear equations yield approximate values of the computed values of y-parallaxes. These parallaxes are compared with the measured y-parallaxes, and the differences are used in the linear equations to obtain corrections to the originally computed orientation motions. As the differences in computed and measured parallaxes become small, the orientation corrections become small making the linear equations approach the exact equations, and convergence is reached. Corrections are then computed for the x-photo coordinates, and these corrected coordinates are used to compute corrected elevations. The iterating process from approximate to exact equations is then repeated with the corrected elevations, computing more nearly correct elevations after convergence. This process is continued until values of elevations converge.

After the relative orientation motions have been computed and the corrections applied to the coordinate of points lying in the overlapping area, the correction to the coordinates of the points not lying in the overlapping area must also be computed if these points are to be used in a succeeding model. Even though the orientation motions are known, the corrections for the coordinates of these points cannot be computed using the expanded forms of Eqs. 11 and 19 without knowing the elevations of these points. Therefore, elevations must be assumed for these points, partial corrections applied to the coordinates, relative orientation applied to the succeeding photograph, an air base computed for the succeeding model, and then elevations of the points computed. This procedure is iterated until convergence of the coordinate corrections for these points is reached.

The linear observation equations enable one to use a least squares adjustment procedure where more than 5 relative orientation points in a model can be used. Using matrix notation, the least squares solution to the observation equations is as follows:

$$x = (A^T A)^{-1} A^T b$$

where

$$x = \begin{bmatrix} d\phi \\ d\omega \\ d\varkappa \\ dZ \\ dY \end{bmatrix}, \quad b = \begin{bmatrix} Py_1 \\ Py_2 \\ \cdot \\ \cdot \\ Py_n \end{bmatrix}, \text{ and}$$

A = the coefficient matrix.

ABSOLUTE ORIENTATION

Absolute orientation is defined as the scaling, leveling, and orientation to ground control of a relative oriented stereoscopic model or group of models. For the cantilever strip assembly, this is accomplished by rectifying the first photograph to yield a truly vertical photograph, relatively orienting the second photograph with respect to the first, which yields a rectified vertical second photograph, and then scaling the model comprised of the 2 photographs to yield an absolutely oriented model. The orientation of the remainder of the strip is accomplished by relatively orienting each succeeding photograph and scaling each succeeding model.

The earth's curvature (curvature of a level surface) is neglected in the absolute orientation procedure, and the level datum for the first model is considered to be a secant plane. For large-scale photography at a nominal scale of 1 in. = 200 ft, the ground coverage of the first model is approximately 1,800 ft by 1,100 ft. For typical ground control distribution, the maximum error in elevation due to the secant plane is about 0.01 ft. For a cantilevered strip 5 models long (approximately 3,500 ft for

1 in. = 200 ft photograph), the error in elevation in the last model is about 0.2 ft and varies with the square of the distance from the first model. This error is significant and can be corrected for after the strip assembly. Because, for real data, the errors in the computed ground coordinates are such that a strip adjustment is necessary, the correction for the earth's curvature is accomplished in the various strip adjustment procedures available.

The absolute orientation motions required to yield the rectified vertical photograph are a rotation about the y axis, $d\eta$, and a rotation about the x axis, $d\epsilon$. Also, a change in the flying height above the datum, dH, is necessary to index the elevations. If before absolute orientation is accomplished the first model is relatively oriented and scaled, the Z-distance to a point can be computed where this distance is the perpendicular distance above the tilted datum (see h′ in Figure 7). The difference between this computed distance and the true elevation for the point, dh, is a function of the 3 orientation motions. To determine this relationship, each orientation motion is first treated independently.

$d\eta$ (Fig. 7)

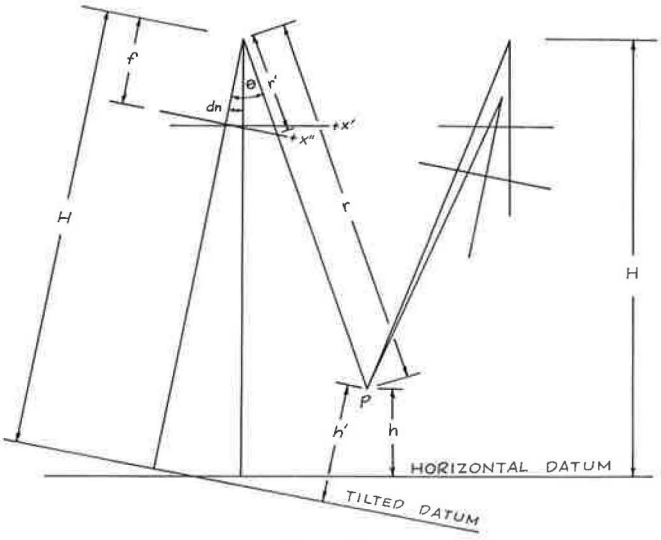

Figure 7.

$$dh_\eta = h - h'$$

$$\cos\theta = \frac{H - h'}{r} \text{ where } \theta = \arctan\left(-\frac{x''}{f}\right)$$

$$\cos(\theta + d\eta) = \frac{H - h}{r}$$

$$\frac{H - h'}{\cos\theta} = \frac{H - h}{\cos(\theta + d\eta)}$$

$$H - h' = (H - h)\frac{\cos\theta}{\cos(\theta + d\eta}$$

$$H - h + d\eta = (H - h)\frac{\cos\theta}{\cos(\theta + d\eta)}$$

$$dh_\eta = (H - h)\frac{\cos\theta}{\cos(\theta + d\eta)} - (H - h)$$

$$dh_\eta = (H - h)\left[\frac{\cos\theta}{\cos(\theta + d\eta)} - 1\right] \tag{24}$$

$d\epsilon$ (Fig. 8)

$$dh_\epsilon = h - h'$$

$$\cos\lambda = \frac{H - h'}{r} \text{ where } \lambda = \arctan\left(\frac{y''}{f}\right)$$

$$\cos(\lambda + d_\epsilon) = \frac{H - h}{r}$$

$$\frac{H - h'}{\cos\lambda} = \frac{H - h}{\cos(\lambda + d\epsilon)}$$

$$H - h' = \frac{(H - h)\cos\lambda}{\cos(\lambda + d\epsilon)}$$

$$H - h + dh_\epsilon = \frac{(H - h)\cos\lambda}{\cos(\lambda + d\epsilon)}$$

$$dh_\epsilon = \frac{(H - h)\cos\lambda}{\cos(\lambda + d\epsilon)} - (H - h)$$

$$dh_\epsilon = (H - h)\left[\frac{\cos\lambda}{\cos(\lambda + d\epsilon)} - 1\right] \tag{25}$$

dH (Fig. 9)

$$dh_H = h - h'$$
$$dH = h - h'$$
$$dh_H = dH \tag{26}$$

When the photograph is rectified by the $d\eta$ and $d\epsilon$ rotations, the x- and y-photo coordinates must be corrected correspondingly. Because $d\eta$ is analogous to $d\phi$, and $d\epsilon$ is analogous to $d\omega$, the following relationships can be written:

$d\eta$ (from Eq. 1)

$$Cy_\eta = y''\left[\frac{\cos\theta}{\cos(\theta + d\eta)} - 1\right] \tag{27}$$

$d\eta$ (from Eq. 12)

$$Cx_\eta = f[\tan\theta - \tan(\theta + d\eta)] \tag{28}$$

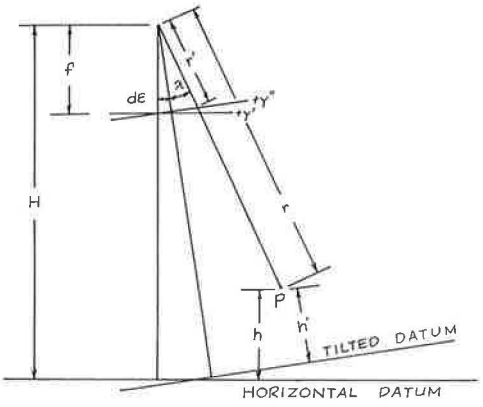

Figure 8.

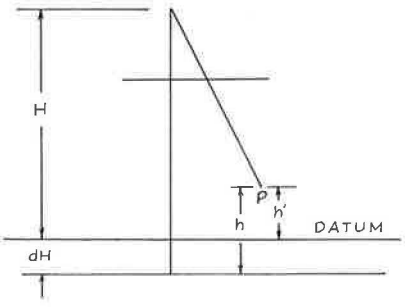

Figure 9.

dη (from Eq. 12)

$$Cy_\epsilon = f[\tan(\lambda + d\epsilon) - \tan\lambda] \quad (29)$$

dε (from Eq. 13)

$$Cx_\epsilon = x''\left[\frac{\cos\lambda}{\cos(\lambda + d\epsilon)} - 1\right] \quad (30)$$

Because dH is actually a change in the datum and the distance from the photograph to the ground does not change, there are no corrections to be applied to the x- and y-photo coordinates for dH.

To take into account interdependency such as was done for relative orientation, the sequence of motions is taken to be dη, dε, and dH. Equations 24 through 30 can then be rewritten as follows:

dη

$$dh_\eta = (H - h)\left[\frac{\cos\theta}{\cos(\theta + d\eta)} - 1\right] \quad (31)$$

$$Cy_\eta = y''\left[\frac{\cos\theta}{\cos(\theta + d\eta)} - 1\right] \quad (32)$$

$$Cx_\eta = f[\tan\theta - \tan(\theta + d\eta)] \text{ where } \theta = \arctan\left(-\frac{x''}{f}\right) \quad (33)$$

dε

$$dh_\epsilon = (H - h)\left[\frac{\cos\lambda}{\cos(\lambda + d\epsilon)} - 1\right] \quad (34)$$

$$Cy_\epsilon = f[\tan(\lambda + d\epsilon) - \tan\lambda] \quad (35)$$

$$Cx_\epsilon = (x'' + Cx_\eta)\left[\frac{\cos\lambda}{\cos(\lambda + d\epsilon)} - 1\right] \text{ where } \lambda = \arctan\left(\frac{y'' + Cy_\eta}{f}\right) \quad (36)$$

dH

$$dh_H = dH \quad (37)$$

The difference between the computed elevation and the known elevation at any one point due to the 3 absolute orientation motions is equal to the sum of the differences due to each motion.

Therefore,

$$dh_T = dh_\eta + dh_\epsilon + dH \quad (38)$$

The expanded form of Eq. 38 is nonlinear making a direct solution of a set of observation equations impossible. In order to obtain a solution, a linear equation is developed that will approximate Eq. 38 and will approach exactness when the orientation motions approach zero.

The derivation of this linear equation is as follows:

$d\eta$

$$dh_\eta = (H - h)\left[\frac{\cos\theta}{\cos(\theta + d\eta)} - 1\right]$$

$$= (H - h)\left[\frac{\cos\theta}{\cos\theta\cos d\eta - \sin\theta\sin d\eta} - 1\right] \qquad (31)$$

From Figure 7,

$$\cos\theta = f/r'$$
$$\sin\theta = -x''/r'$$
$$dh_\eta = (H - h)\left[\frac{f/r''}{(f/r')\cos d\eta - (-x''/r')\sin d\eta} - 1\right]$$

Assuming $\cos d\eta = 1$; $\sin d\eta = d\eta$,

$$dh_\eta = (H - h)\left[\frac{f/r'}{f/r' + (x''/r')d\eta} - 1\right]$$

$$= (H - h)\frac{f - (f + x''d\eta)}{f + x''d\eta}$$

Assuming $x''d\eta$ is small compared to f,

$$dh_\eta = \frac{-(H - h)x''d\eta}{f} \qquad (39)$$

$d\epsilon$

$$dh_\epsilon = (H - h)\left[\frac{\cos\lambda}{\cos(\lambda + d\epsilon)} - 1\right]$$

$$= (H - h)\left[\frac{\cos\lambda}{\cos\lambda\cos d\epsilon - \sin\lambda\sin d\epsilon} - 1\right] \qquad (34)$$

From Figure 8 and assuming interdependency is negligible,

$$\cos\lambda = f/r'$$
$$\sin\lambda = y''/r'$$
$$dh_\epsilon = (H - h)\left[\frac{f/r'}{(f/r')\cos d\epsilon - (y''/r')\sin d\epsilon} - 1\right]$$

Assuming $\cos d\epsilon = 1$; $\sin d\epsilon = d\epsilon$,

$$dh_\epsilon = (H - h)\left[\frac{f/r'}{f/r' - (y''/r')d\epsilon} - 1\right]$$

$$= (H - h)\frac{f - (f - y''d\epsilon)}{f - y''d\epsilon}$$

Assuming $y''d\epsilon$ is small compared to f,

$$dh_\epsilon = \frac{(H - h)y''}{f} d\epsilon \tag{40}$$

dH

$$dh_H = dH \tag{37}$$

Because Eq. 37 is already linear, it remains unchanged. The sum of the difference in elevation due to each orientation motion yields

$$dh_T = -\frac{(H - h)x''}{f} d\eta + \frac{(H - h)y''}{f} d\epsilon + dH \tag{41}$$

In Eq. 41, $d\eta$, $d\epsilon$, and dH are unknowns with dh_T being the difference in the known elevation of a point (vertical control point) and the computed Z-distance to this point, computed from the relative oriented first model. Three observation equations obtained from 3 vertical control points yield approximate solutions to the 3 motions. These motions are used in the exact equations (expanded form of Eq. 38) to obtain computed differences in elevation. These differences are compared with the original differences obtaining residuals due to the approximate equations to compute corrections to the original computed motions. This procedure is iterated until convergence is reached. After the final motions are obtained, these motions are used to correct x- and y-photo coordinates and to correct the flying height above the datum.

The original computed Z-distances (computed from the relative oriented model) were computed using an air base and flying height that were obtained using the titled datum; therefore, the final absolute orientation motions obtained earlier are not exact. In order to approach exactness, the second photograph is relatively oriented again to the almost exact horizontal datum from which an air base and flying height can be computed. Absolute orientation is then computed. This procedure is iterated until convergence is reached.

After final absolute orientation of the first photograph is determined, the remaining photographs can be relatively oriented and the resulting models scaled. This yields an absolutely oriented cantilevered strip from which ground coordinates of any point measured on the photographs can be computed.

CONCLUSIONS

The theory and equations just developed have been incorporated into a computer program and tested with hypothetical data. The results of the testing show that the programmed procedure is exact to within limits that are negligible in their effect on the resulting errors obtained from using actual photographic data. Errors incurred when using this program with actual data can then be attributed to the photography, measurement of photograph coordinates, and ground control; and efforts to improve the results can be concentrated in these areas. The relative and absolute orientation equations are mathematical models of conventional stereoscopic mapping instruments such as the Kelsh plotter and can, therefore, be used to study and analyze the errors involved in the use of these pieces of equipment.

Mathematical Surface Approximation of the Terrain

DONALD A. MAXWELL, The Computer Sciences Corporation,
Falls Church, Virginia

Although the systems approach to design is usually thought of as having applications mainly in the field of hardware systems design, systems methodology and philosophy are also applicable to the design of computer software systems. The NGI (numeric ground image) systems design study is an example of the systems approach to the design of a computer software system. The NGI system furnishes the highway engineer with a method for approximating the terrain surface with a numerical surface. Traditional highway design practice has required the use of cross sections to represent the terrain. The use of the numerical surface approach instead of the cross-sectional method eliminates some terrain representation problems associated with the traditional cross-sectional method. For example, if the horizontal alignment of a roadway is shifted, a new and separate set of cross sections corresponding to the new alignment must be obtained. This new set of cross sections is necessary because the old set was directly referenced to the old alignment. This is not true of the numerical surface approach because it is not directly referenced to any specific alignment.

The NGI system is designed to interface with FORTRAN "driver" programs. In general, whenever the interfacing program requires an elevation for a specific horizontal position, it passes the X- and Y-coordinates of that position to the NGI system through the appropriate interface. The NGI system computes the Z(elevation) corresponding to the X and Y and passes it back to the original program through the same interface. The nature of the interfacing program can vary from, say, earthwork analysis to contour plotting. At this stage of development the NGI system is not a general purpose engineering tool to be used by the unwary. However, once the operating characteristics of the NGI system are determined and surface technology is extended into engineering design, it holds the promise of becoming a highly effective highway design technique. The technique has been successfully applied to compute graphic applications such as perspective drawings and contour maps of the terrain and to alternate route evaluation calculation.

•DURING THE PAST DECADE a great deal of research effort has been directed toward the development and implementation of computer-aided highway design systems. Two of the most ambitious efforts are the Bureau of Public Roads TIES (total integrated engineering system) project and the M.I.T. ICES (integrated civil engineering

Paper sponsored by Committee on Photogrammetry and Aerial Surveys and presented at the 49th Annual Meeting.

system) project. In addition, several of the state highway departments and various private consultants have developed and are presently writing their own systems. The primary objective of these efforts is generally the same: the more effective use of the information storage capacity and processing speed of the modern, digital computer systems as an engineering design tool.

One of the results of these efforts has been the recognition of some of the problems involved with applying optimization techniques to present highway engineering design technology. For example, if we could approximate both the terrain and the design roadway with corresponding degrees of accuracy, then operations research techniques could be used to optimize the design of the facility (in terms of cost, safety, aesthetics, and the like) with respect to its environment. This is particularly true in the design of complex interchanges using iterative optimization techniques.

Using the current state of the art, it is possible to describe the design roadway in terms of a mathematical model to any degree of accuracy required. Unfortunately, the terrain cannot be represented with a mathematical model that is based on cross-sectional terrain data to a corresponding degree of accuracy. Thus, in order to apply efficient optimization techniques, some alternative method must be developed to approximate the terrain.

In the fall of 1966 personnel from the Texas Highway Department, Division of Automation, expressed an interest in developing such an alternative technique for approximating the terrain. A study to develop such a technique entitled, "Numerical Ground Image," was subsequently conducted by the Texas Transportation Institute during fiscal year 1968. This study was sponsored by the Texas Highway Department in cooperation with the U. S. Department of Transportation, Federal Highway Administration, Bureau of Public Roads. An addendum to the study, the application of the NGI study to an actual design situation, was conducted as an in-house research effort of the Bureau of Public Roads, Engineering System Division.

The purpose of the NGI study was to develop and evaluate a technique for approximating the terrain with a mathematical surface. From the onset of the project it was assumed that the technique must be general enough to be used at all levels of computer-assisted design and be suitable for use with iterative optimization techniques that might be employed in the future. In addition, the technique should be able to accommodate large design projects as well as small ones.

The level of effort involved during the conduct of the study was 1 professional man-year and 1½ technician man-years expended over a time span of 12 calendar months. Except for the review and approval cycle for the final report, the study was completed within these constraints. The activities completed during the conduct of the study were as follows:

1. Review of existing literature to determine the current state of the art;
2. Collection of test data for debugging and evaluation purposes;
3. Analysis of alternate numeric surface techniques to determine the optimum system;
4. Design and development of the necessary computer programs to effect the use of this system; and
5. Evaluation of this system to determine its applicability to computer-aided design systems.

The following sections of this presentation describe briefly what the study hoped to accomplish, how the study was conducted, some results, and some conclusions about the NGI system itself. These sections are as follows:

1. Cross-section approach versus numeric-surface approach,
2. Development of the proposed NGI system,
3. Application of the NGI system to highway design, and
4. Conclusions and recommendations.

THE CROSS-SECTION APPROACH VERSUS THE NUMERIC-SURFACE APPROACH

When highway design technology was orginally programmed for digital computers, the existing hand-calculation methods were simply translated into machine calculations with very little change in concept. Such was the case with terrain approximation techniques, i.e., the cross-sectional method was simply carried forward with the rest of the design methodology. The following paragraphs discuss some of the problems associated with using cross sections in a computer-aided design system and how these problems can be overcome by using a numeric surface as an alternate approximation technique.

The Cross-Section Approach

Traditional and current highway design practice has required that the terrain be represented by cross sections taken with respect to a previously established horizontal alignment. The usual sequence for the collection of cross-sectional data is shown in Figure 1. Although other feasible schemes for representing the terrain (such as the M.I.T. digital terrain model) have been developed and used with some degree of success, none has gained the universal acceptance that the cross-sectional method still enjoys. This widespread use of cross sections continues in spite of some very serious limitations.

These limitations are inherent to the cross-sectional method itself and are more or less independent of how the sections are measured or how they are subsequently used. In brief, these limitations are as follows:

1. The horizontal alignment must be established before the cross-sectional data can be measured. This is true no matter what method is used to obtain the cross-sectional data.
2. A unique set of cross sections is required for each and every horizontal alignment. Thus for every horizontal alignment shift, a new and separate set of cross sections must be obtained either by mathematically shifting the original set to the new alignment or by measuring new sections.
3. Gaps in the terrain coverage caused by conventional cross-sectional spacing practice create a situation where significant terrain features may be poorly represented or omitted entirely from the terrain data.
4. The cross-sectional method does not easily lend itself to freeway interchange design. The existence of horizontal alignments that are parallel and the resulting overlapping of their respective cross sections create a confusing situation during both the design and the layout of the facility.

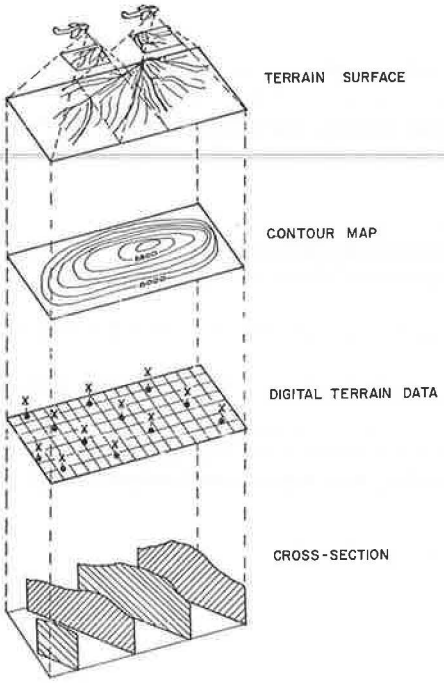

Figure 1. Cross-section terrain approximation.

However, cross sections do have some strong points; otherwise, they would never have gained the universal acceptance that they have. Three very obvious advantages are as follows:

1. The technology of cross sections is well known and highly developed, and for this reason the design engineer would feel "comfortable" working with cross sections.
2. Cross sections lend themselves to the design of rural highways where the design geometry is straightforward, the occurrence of roadway intersections is minimal, and only the vertical alignment need be optimized.
3. The errors in terrain approximation tend to be accidental rather than systematic; thus,

errors in earthwork quantities, for example, tend to cancel themselves over the long run.

The Numeric-Surface Approach

All of the 4 limitations of the cross-sectional method mentioned could be eliminated if the terrain could be represented by a surface as shown in Figure 2. In addition, some of the advantages of such a numeric surface are as follows:

1. The surface could be referenced independently of the horizontal alignment, and terrain data could be collected before the horizontal alignment is firmly established.
2. Furthermore, there would be no need to obtain new terrain data every time the horizontal alignment is revised because the terrain data are independent of the alignment.
3. There would be no gaps in terrain coverage due to spacing conventions because the surface would yield a continuous coverage as opposed to the intermittent terrain coverage associated with cross sections.

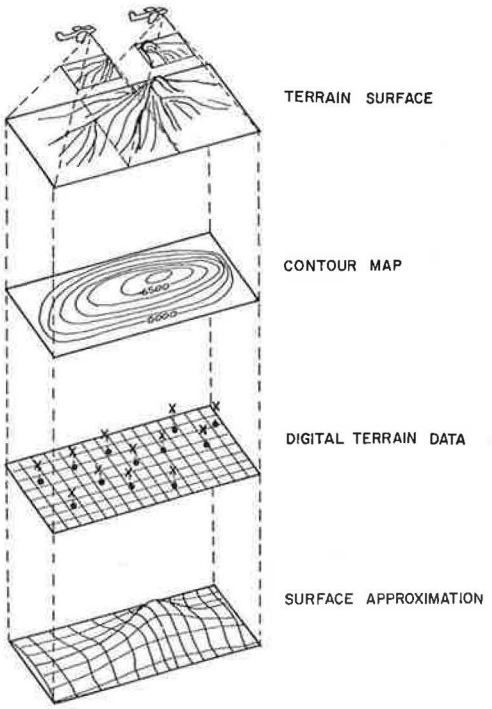

Figure 2. Numeric-surface terrain approximation.

While the numeric-surface approach would eliminate the major limitations of cross sections, a new set of problems would materialize. Some of the more obvious problems are as follows:

1. The technology of numeric-surface techniques applied to highway design is scant when compared to cross-sectional technology.
2. Numeric-surface techniques will require a large (as compared to cross-sectional methodology) number of calculations. In fact, efficient use of these techniques would almost require a digital computer to perform the necessary arithmetic.
3. There is no mathematical function that is suitable for use as a general case approximation to the terrain surface. For example, a linear approximation is often suitable for approximating "man-made" features but not suitable for sand dunes.

DEVELOPMENT OF THE NGI SYSTEM

The development of the NGI system could be considered as a 2-phase process. The first phase is the analysis phase that involves 4 basic activities: development of the system specification, generation of alternative systems, evaluation of these alternatives, and description of the optimum system. The purpose of this phase is to select the optimum system, vis-a-vis the system requirements, from the large number of possible systems.

The second phase or design phase involves 3 activities: the decomposition of the optional system into independent (but interrelated) program modules or functional elements, design of the overall program architecture to link these modules together, and programming and debugging of the appropriate software to effect the system's use.

Analysis Phase

System Specification—The development of the system specification is an iterative process that results in the definition of the system input, output, environment, and performance criteria. The process is iterative because it proceeds in a trial-and-error sequence (from initial formulation of the specification to evaluation of the specification

in light of the system requirements) until the system specification and system requirements mesh. The system specification for the NGI system is as follows:

1. Input—(a) The terrain surface is represented by a representative sample of X-Y-Z coordinates; and (b) the horizontal position of the point where an elevation is required is defined by its X-Y coordinates.
2. Output—(a) The elevation of the required point is given by its Z-coordinate; and (b) a code indicating whether or not a blunder in the computational procedure has been detected, e.g., an attempt to extrapolate an elevation from outside the range of the data.
3. Environment—All calculations and data manipulations must be accomplished by a digital computer without operator intervention.
4. Performance criteria—(a) That alternative which produces the most accurate results is the optimum alternative; and (b) in case of a tie between alternatives, then the one with the highest throughput rate is optimal.

Generation of Alternative Systems—In separating the optimum system from the very large number of possible systems, the chances for selecting the optimum system are increased in proportion to the number of alternatives evaluated. This is because the alternatives any individual investigator might select for possible evaluation are usually discipline-oriented and because the first alternative receives the greatest attention. Therefore, some systematic method must be used to generate a large number of alternatives that are not the result of personal bias for subsequent evaluation. The method employed to select the optimum alternative for the NGI system is briefly described as follows:

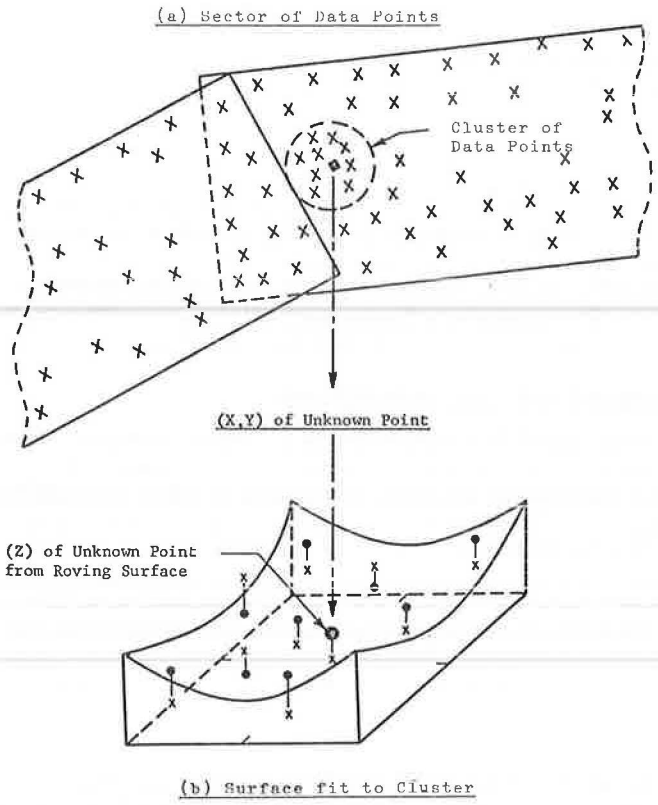

Figure 3. Data point grouping for interpolation.

1. Decompose the system into functional classes that describe the functional attributes of the proposed system. In this case they are surface type, surface fitting method, and data aggregation scheme.
2. Within each class define class members as follows: surface type—triangles, polynomials, Fourier, and Spline; surface fitting method—least squares, weighted least squares, and exact; and data aggregation scheme—by sector, by cluster (Fig. 3).
3. From the set of alternatives formed by all combinations of classes and class members select the most feasible alternatives, in light of project constraints, for technical evaluation. For the NGI system these were as follows: Type I—triangle surface, exact fit, by sector; Type II—polynomial surface, least squares fit, by sector; Type III—Fourier series surface, least squares fit, by sector; Type IV—parabolic surface, least squares fit, by cluster; and Type V—cubic surface, least squares fit, by cluster.

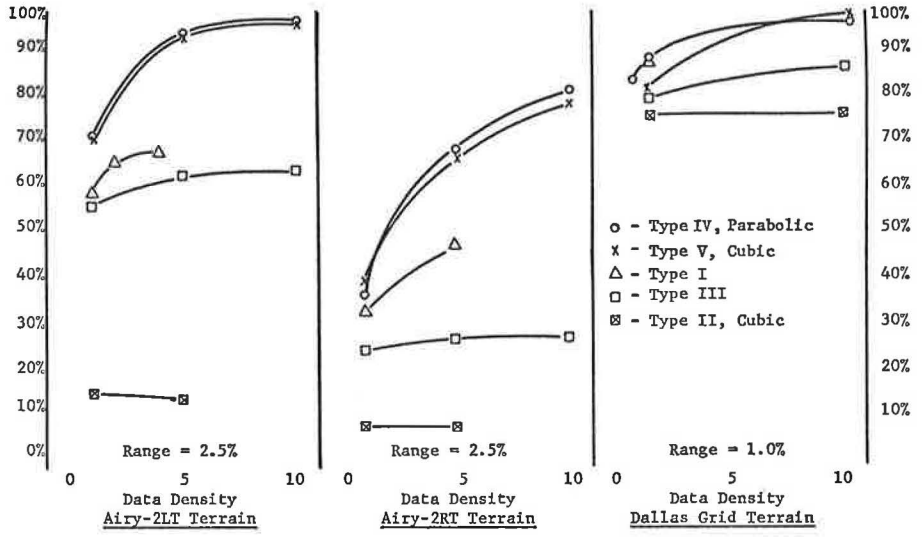

Figure 4. Results of accuracy tests.

Evaluation of the Alternatives—The object of this activity is to determine which of the alternative systems, i.e., Type I, II, III, IV, or V, is the optimum system. The system that exhibits the greatest accuracy for various data densities is considered to be the optimum system. Any ties between equally accurate systems are broken in favor of the system having the greatest throughput rate.

Test runs using Types I, II, III, IV, and V were processed using Airy-2LT, Airy-2RT, and Dallas Grid terrain data samples with data densities varying between 1.0 and 10.0 points per 10,000 sq ft. The terrain data used for evaluation consisted of fictitious terrain data calculated from mathematical surfaces and actual terrain data measured from the actual terrain situations by photogrammetric methods. The relief pattern for the Airy samples conform to the relief pattern displayed by an Airy function. The Dallas Grid sample conforms to the relief pattern of an actual terrain situation. Regardless of the terrain, each sample represents the terrain over a rectangular area 500 ft long and 250 ft wide. All samples drawn from the fictitious terrain surfaces are made up of data points that are randomly distributed in horizontal position regardless of the relief pattern. The actual terrain samples are selected from the Dallas Grid terrain master sample, which is a 2,601-data-point sample measured in a 10- by 50-ft grid superposed over an actual terrain area. During the test both accuracy and throughput data were collected for evaluation purposes.

The accuracy test results are shown in Figure 4. The data points are plotted both by terrain sample and by system type such that they become points along accuracy versus data density curves. The accuracy test performed during each test run consists of (a) selecting 5 samples of 30 different points within the terrain test area, (b) comparing the actual elevation at each point with the elevation obtained by the NGI system and computing the error, and (c) calculating the accuracy of the sample. Accuracy here is defined as the percentage of errors that fall within the interval ±0.5 ft.

The throughput rate results are shown in Figure 5 for both the Type IV and the Type V systems as points along throughput rate versus sector data curves. The data are based on the time required (as measured by the internal clock of the computer) to calculate the 150 test elevation required by the accuracy tests.

On the basis of accuracy, either the Type IV or V system can be identified as the optimum alternative by inspection of Figure 4, thus eliminating Types I, II, and III from further consideration. Because the Type IV and Type V systems have similar accuracy characteristics, the throughput rate curves shown in Figure 5 must be used to break the tie between them. On the basis of throughput rate, the cubic option is eliminated.

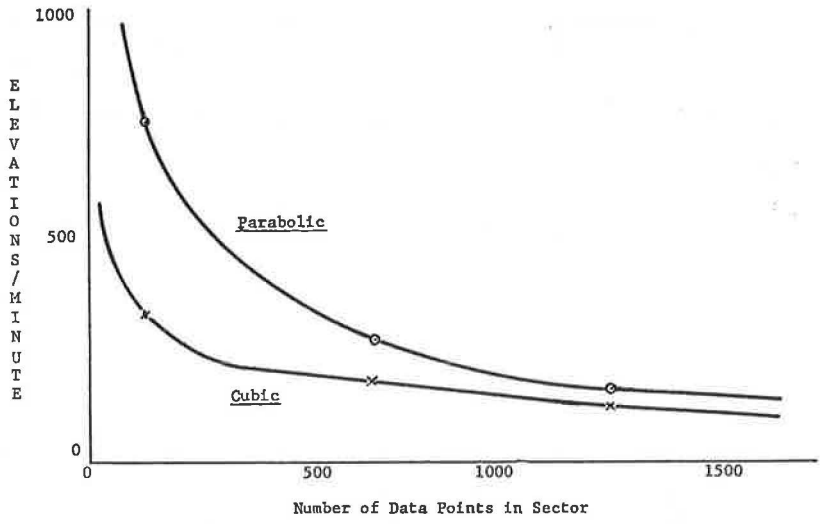

Figure 5. Results of throughput tests.

Therefore, the Type IV system using a parabolic surface becomes the optimum system by virtue of being the last remaining alternative.

Descritpion of the Optimum System

The description of the attributes of the optimum system is complete if the properties of the system are described and its operating characteristics are determined. The physical properties of a software system are not pertinent to this design process so the discussion is limited to the functional characteristics of the system. The discussion of the operating properties is also limited to a discussion of the functional properties. The functional properties are as follows:

1. Coordinate system—The NGI system uses a local coordinate system for each sector of data points. The origin (0, 0, 0) of the system is located at the lower left (southwest) corner of the sector. Each sector coordinate system is then related to the coordinate system of the project by appropriate translation, rotation, and scale constants.
2. Data grouping scheme—The terrain data for the entire project is subdivided into sectors of not more than 1,000 points. These sectors may be overlapping, nonparallel, or askew to the coordinate axis. The only requirements are that they completely enclose all of the data points and they must be rectangular in shape.
3. Extent of the surface fit—A set ordering technique is used to select the cluster of 9 data points closest to the desired horizontal position. (The cluster size of 9 is based on experimental results not included in this presentation; it represents 1½ times the minimum data required for a least squares fit.)
4. Type of surface—The NGI system uses a parabolic surface to approximate the terrain surface. This surface is fit to the roving cluster of 9 data points.
5. Type of fit—The surface is fit to the cluster of terrain data points by a conventional least squares surface fitting technique.

The exact operational properties of the system cannot be determined until the final NGI system is implemented and observed while operating in a design environment. However, two of these properties can be discussed in general terms, which gives an idea of what to expect so far as actual operation of the NGI system is concerned.

1. Throughput rate—The expected throughput rates of the optimum system for various sector sizes can be determined from Figure 5. This is probably a conservative value

because the final NGI system will exhibit generally larger throughput rates than the text systems because of a more efficient object code. For example, for a sector of 500 points a throughput rate of 350 elevations per minute can be expected.

2. Data density—The data density required to achieve a given accuracy (sensitivity) is a function of the relief of the terrain surface and the characteristics of the terrain sample data points. However, in general, as the data density for a given area is increased, the accuracy achieved by the system is increased. In fact, as the data density increases, the sensitivity versus data density curve approaches 100 percent sensitivity as a limit. The shape of this curve and its position in relation to the axis is a function of terrain relief and sample characteristics.

Design of the NGI System

The objective of this design effort is to develop an engineering tool to be used for terrain approximation while operating in a computer-aided design environment. As a result, development of the NGI system is more strongly influenced by generality of engineering applicability than by mathematical convenience. The scope of this development is limited to design of a feasible system and not necessarily an optional one.

The success or failure of the NGI system as a useful tool will depend on a number of factors. The one overriding consideration is the maintenance of engineering integrity, i.e., an engineer controlled, not a so-called automatically controlled, data processing system. Another primary consideration is the ease with which the NGI system can be interfaced with other systems. Several other considerations of less importance are the ease of program debugging, modification, and maintenance, and the minimizing of the system throughput rate.

The NGI system has 3 subsystems. Each subsystem, although an integral part of the total system, functions more or less independently of the others. The only communication link between these 3 subsystems is the NGI master data file, which resides on a system direct access input-output device (disk pack). The NGI system architecture is defined by the flow chart shown in Figure 6.

NGI Data Subsystem—The function of the NGI data subsystem is to establish the NGI system master data file on the appropriate disk pack. A "driver" program that is interfaced with the NGI data package reads, edits, and arranges the sector parameters and terrain data in the proper sequence, then passes these data to the NGI data subsystem through the correct interface. The NGI data subsystem checks the data for correctness and writes the NGI master data file located on the proper direct access input-

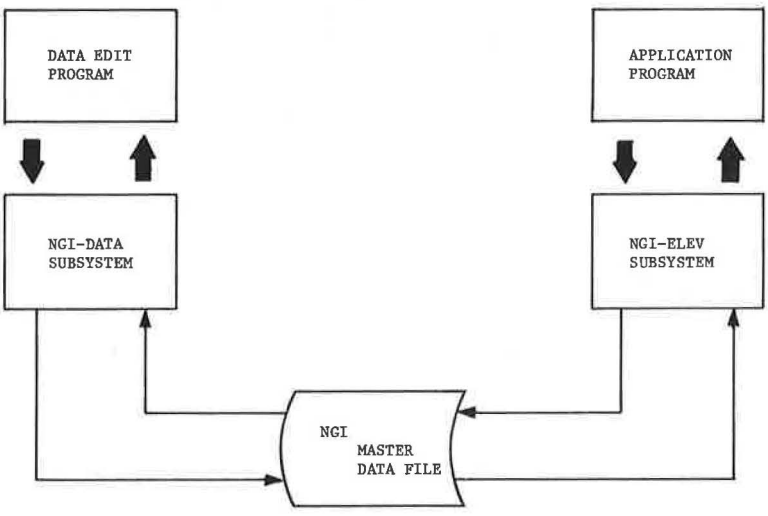

Figure 6. System architecture.

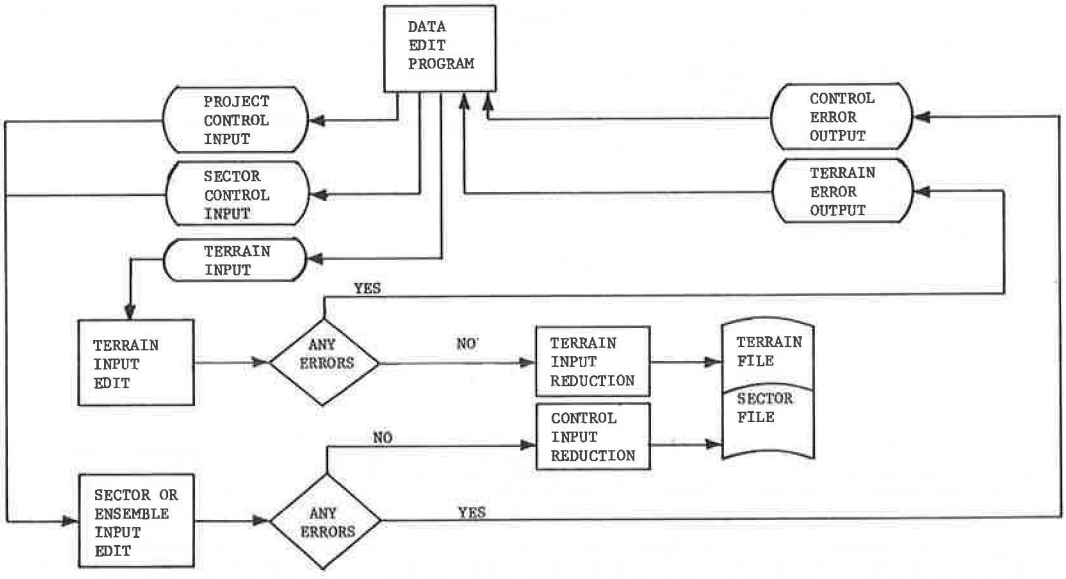

Figure 7. NGI data subsystem architecture.

output device. Once this data file has been properly formed, the NGI data subsystem has completed its function. A flow chart of this process is shown in Figure 7.

NGI Master Data File—The function of the NGI master data file is to store all of the pertinent terrain and control data required by the NGI system. These data can then be accessed by the NGI test and NGI elevation subsystems whenever desired. The intent is to "roller towel" data into the core, sector by sector, from the NGI master data file as required by the other subsystems.

NGI Elevation Subsystem—This subsystem provides an interface between the NGI system and application programs so that the NGI elevation package can return an elevation corresponding to any valid horizontal position desired by the application program. The flow chart shown in Figure 8 illustrates the logic and function of this subsystem.

Inasmuch as a procedure for predicting the accuracy of the elevations calculated by the NGI system when it is operating in a design situation has yet to be developed, the accuracy tests used to evaluate the competing alternatives are no longer pertinent. However, a procedure for detecting blunders, e.g., extrapolating instead of interpolating an elevation, can be designed so as to predict whether or not the NGI system will yield elevations free from blunders. This will prevent aborting a future processing because of an excessive number of blunders while the NGI elevation package is interfaced with an application program.

APPLICATION OF THE NGI SYSTEM TO HIGHWAY DESIGN

Background

The highway design process can be thought of as having 3 levels of detail: macro, meso, and micro. As the design progresses from the macro stage through the micro stage, the level of detail and hence the required accuracy increases. This relates to highway engineering in the following manner. The process of selecting the proper corridor for a highway location is an example of design at the macro level. The meso level of design is illustrated by the route selection process where several routes within a corridor are evaluated and the optimum route is determined. Micro level of design involves the calculation of plan quantities for the construction process. At this stage of development numeric-surface techniques do not yield results that are satisfactory for the micro level of design. The following gives 2 examples of how the NGI system can be applied to the macro or meso level of design.

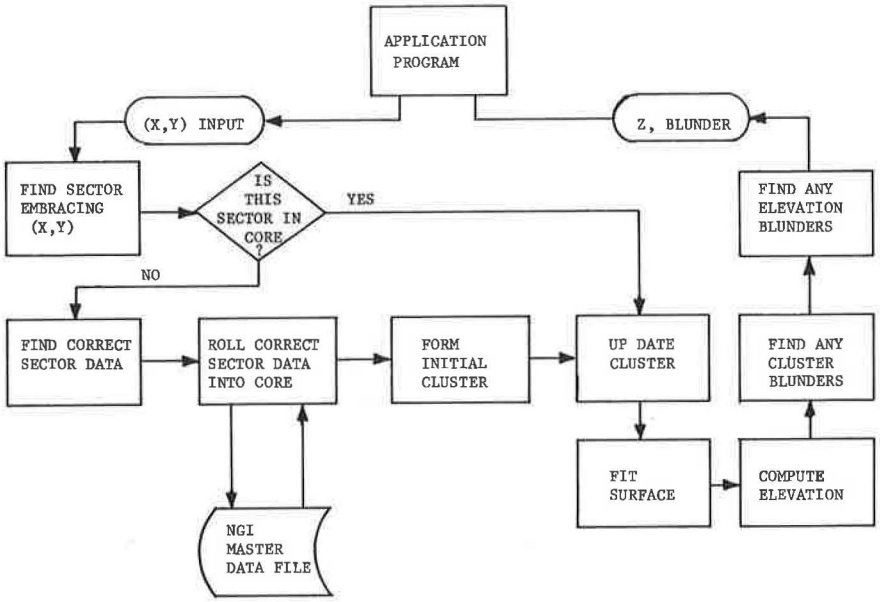

Figure 8. NGI elevation subsystem architecture.

Computer Graphics Applications

In the past when the highway engineer determined the horizontal and vertical alignment for the highway location he had the benefit of on-site experience. The present-day locator does not enjoy this advantage; he is often "desk bound" and must rely on remote-sensing techniques to gather terrain data for inputs to his computer-aided de-

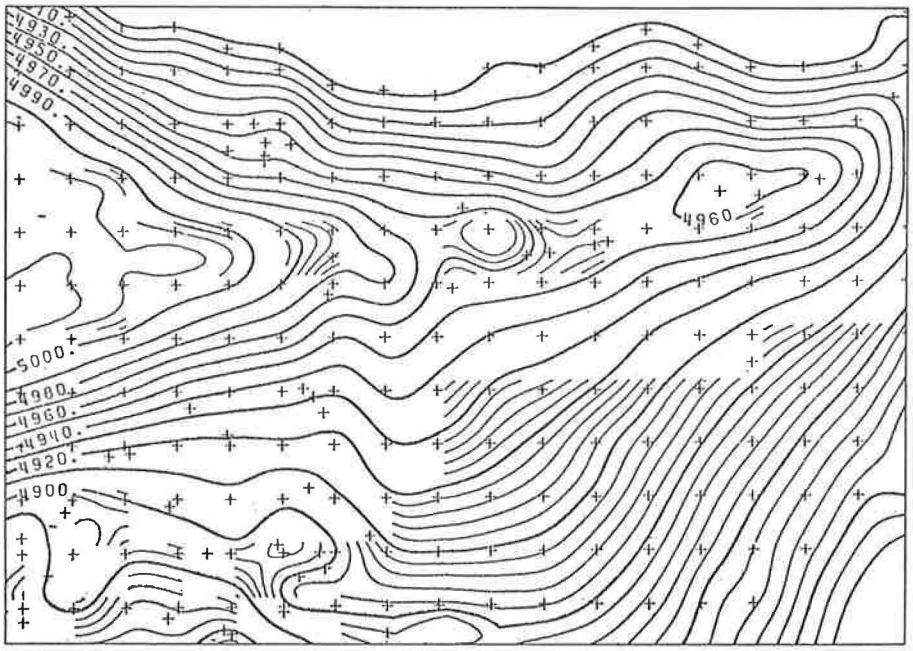

Figure 9. Contour map of Dino test area.

sign processes. Unfortunately, these data are all too often available only in numeric form (usually centerline profile and cross sections). This form is usually adequate for earthwork calculation, but not for alignment location purposes where some "feel" for the terrain must be communicated to the location engineer. This is particularly true at the meso level of design.

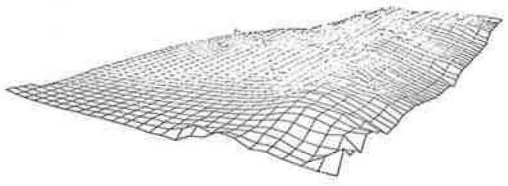

Figure 10. Perspective view over southwest corner of Dino test area.

Contour maps (Fig. 9) are often used to give the locator some insight as to the shape of the terrain surface. The technique of centerline project from topographic maps is well known and has proved very successful for both corridor and route selection. While this technique has proved successful for alignment purposes in regard to cut-and-fill, hydraulic, and alignment considerations, it has proved not as powerful for communicating the aesthetic ramifications of a particular design. This consideration has become extremely important so far as modern freeway design is concerned, especially in regard to public acceptance of such a facility.

Perspective views (Fig. 10) of the terrain serve to give the locator added insight into the shape of the relief of a given area. This is especially true when a broad overview of the terrain is required for the corridor and route selection process. Using a perspective viewing technique, it is possible to "place" the locator on the proposed location so he can actually visualize what the driver will see when the highway is constructed. In addition, the locator can be placed so that he can evaluate the location from a remote point of view.

A perspective view of the terrain or a contour map can be obtained from numeric data by using a digital computer and a digital plotter. A summary of the technique used to produce the drawings in this report is as follows:

1. Obtain representative terrain data in X-Y-Z format.
2. Superpose (mathematically) a regular grid (mesh) over the area to be drawn.
3. Interpolate the elevations of the mesh points (grid intersections) using the NGI system.
4. For perspective drawings, determine the visibility of the mesh points, i.e., eliminate the hidden lines and calculate their X-Y perspective coordinates with respect to the viewing plane, and plot the resulting perspective mesh using a digital plotter.
5. For contour maps, determine where the desired contour lines cross the superposed grid lines, determine the order in which the points should be connected, and plot the resulting contours using the digital plotter.

Earthwork Quantities

In addition earthwork quantities with accuracies suitable for meso level of design (i.e., the evaluation of alternative routes) may be calculated by the following technique:

1. Project the highway centerline along the desired route and determine its orientation with respect to the coordinate system.
2. Determine the spacing and length of each cross section and calculate its trace in the horizontal plane.
3. Calculate the corresponding elevations for each cross section.
4. Determine the earthwork quantities in a standard fashion with existing earthwork programs using the cross section obtained earlier as terrain data.

The accuracy of the results may not be suitable for the exact amount of earthwork for any one alternative route because of systematic errors. However, the relative differences in volume may be quite accurate because of the cancellation effect of the accidental errors.

CONCLUSIONS AND RECOMMENDATIONS

Conclusions

These general conclusions should be considered as preliminary, not final, inasmuch as the final conclusions about the value of the NGI system as an engineering tool can be made only after its operating characteristics have been observed in an actual operating environment. These conclusions in light of this situation are as follows:

Accuracy of Results—The accuracy obtained by the NGI system is limited by 3 factors: round-off noise, the errors caused by assuming that the earth is parabolic in shape, and errors created by unrepresentative terrain data. The errors caused by round-off noise are insignificantly small, i.e., less than 0.01 ft. The errors introduced by the last 2 factors can be reduced by increasing the data density, because in general, as the density increases, the accuracy increases. How much they can be reduced by increasing the data density depends on the amount of terrain relief over the area in question. In practice, however, the resulting accuracy will be limited by data acquisition and processing constraints.

However, in the case of discontinuities in the terrain surface the assumption that an increase in data density will yield an increase in accuracy may not be valid. Unfortunately, the terrain data used to evaluate the system did not contain any discontinuities so any prediction of how the NGI system behaves in the neighborhood of a discontinuity is speculative. However, several contrived situations can be shown to exist where the system will not achieve the expected results. This problem might be overcome if a method for describing a discontinuity in terms of the usual X-Y-Z input to the system could be developed.

Distribution of the Data—The NGI system makes the most effective use of uniformly distributed terrain data, allowing for slight increase in data density in the more difficult terrain situations, i.e., rough spots. The experience resulting from this study indicates that the "strength of figure" of the data points (the uniformity of their distribution) counts for as much as the "intelligence" (placement of the terrain data points in regard to the relief pattern of the terrain) of the sample. For example, if the data submitted to the NGI system were originally measured in cross-sectional format, i.e., along lines perpendicular to the centerline at even stationing, the system fails to obtain the accuracy expected with this data density. This decrease in accuracy occurs because the "strength of figure" of the terrain data is inadequate to support a fitted surface.

Applicability—The results obtained from the NGI system are consistent with those obtained from cross sections when used with present computer-aided design practice. However, the value of the NGI system does not lie in its ability to directly substitute for cross sections in such design phases as earthwork calculations and slope staking. The value of this new technology lies instead in its ability to represent the earth's surface as a numeric surface. By treating both the design roadway and the terrain as surfaces, computer-aided design technology can be drawn into new areas of application. For example, once the roadway surface has been designed, it can then be combined with the terrain surface such that perspective drawings of the design can be generated and displayed for easy reference during the design process. Alternate designs can be developed without remeasuring or shifting the terrain data for each alternate design, thus making iterative optimization techniques a possible part of the design practice.

Recommendations for Future Study

The experience that resulted from this study indicates that there are several aspects of the terrain approximation problem that could be profitably investigated. The first three of these aspects are within the scope of this study but were excluded from the analysis because of time and resource constraints on the study. The last four are areas that lie outside of the bounds of the study.

Types of Numeric Surfaces—The polynomial surface is probably not the most general approximation to the terrain surface. If a more general surface (such as an improved Fourier or Spline surface) could be found, the NGI system would be able to make more efficient use of the measured terrain data. This would result in reduced data requirements for a given level of accuracy or increased accuracy from the same density of data.

Clustering Technique—The clustering technique used by the NGI system assumes that the most accurate results are obtained from a cluster formed from the points closest to the unknown point. This study did not investigate the generality of this assumption. If an algorithm that yields a cluster more representative of the terrain surrounding the unknown point is discovered, then the NGI system could make more efficient use of the measured terrain. For example, if discontinuities could be recognized, then the clustering process could take them into account.

Surface Fitting Technique—The least squares surface fitting technique is used by the NGI system because it is the optimum fitting procedure according to the conclusions resulting from this study. However, the weighted least squares fitting technique gave equally accurate results for the terrain samples available to this study. Other weight functions and other more extensive terrain samples might indicate that weighted least squares are in fact the most desirable. A minimax surface algorithm might also be developed for use by the system.

Terrain Roughness—If some method for quantitizing the terrain roughness were available, then the data density required over a given area for a specified level of accuracy could be predetermined. This information could also be used to estimate what an increase in data density would obtain in terms of increased accuracy for a particular set of terrain data. Other supplemental terrain data that might result in a more effective system might also be explored.

Throughput Rate Optimization—Once the NGI system has been made operational in an engineering environment, then pertinent throughput data can be collected. After these data are collected, the trade-offs between the roll-in of data from direct access storage, the amount of data resident in core, and surface fitting speed may be accomplished in order to optimize the throughput rate of the total system.

Analog Terrain Models—The possibility of using an analog model for approximating the terrain for use in a computer-aided design environment might also be investigated.

REFERENCES

1. Craig, W., and Burns, J. Digital Ground Models in Highway Location and Geometric Design—A Review of Types of Models and Studies of Accuracy of the Square Grid Type. British Road Research Laboratory, London, mimeographed, 1966.
2. Geissler, E. H. A Three-Dimensional Approach to Highway Alignment Design. Highway Research Record 232, 1968, pp. 16-28.
3. Godin, P., Deligny, J. L., Antoniotti, J. A., and Bernede, J. F. Visual Quality Studies in Highway Design. Highway Research Record 232, 1968, pp. 46-57.
4. Hamming, R. W. Numerical Methods for Scientists and Engineers. McGraw-Hill Book Co., New York, 1967.
5. Numerical Surface Techniques and Contour Map Plotting. International Business Machines Corp., White Plains, N. Y., 1964.
6. James, W. R. FORTRAN IV Program Using Double Fourier Series for Surface Fitting of Irregularly Spaced Data. In Computer Contribution 5 (Merriam, D. F., ed.), State Geological Survey, Univ. of Kansas, Lawrence, 1966.
7. James, W. R. The Fourier Series Model in Map Analysis. Northwestern Univ., Evanston, Ill., April 1966.
8. Krumbin, W. C. A Comparison of Polynomial and Fourier Models in Map Analysis. Northwestern Univ., Evanston, Ill., June 1966.
9. Kubart, B., et al. The Perspective Representation of Functions of Two Variables. Jour. of the Association for Computing Machinery, April 1968, pp. 193-204.

10. Maxwell, D. A., and Turpin, R. D. NGI Systems Design. Texas Transportation Institute, College Station, Research Rept. 120-1, 1968.
11. Miller, C. L. Digital Terrain Model Approach to Highway Earthwork Analysis. Photogrammetry Laboratory, M.I.T., Cambridge, Mass., 1957.
12. Miller, C. L. The Digital Terrain Model—Theory and Applications. Photogrammetry Laboratory, M.I.T., Cambridge, Mass., 1958.
13. Thieloult, A., and Deligny, J. L. Traces Electronic En Geometric Imposee; Suite 3—Interpolation Du Terrain. Special Service Des Autoroutes, Ministre de L'Equipment, Paris, 1966.

Highway Location and Design Utilizing Photogrammetric Terrain Data

CHARLES E. McNOLDY, Pennsylvania Department of Highways

This paper describes the current use of terrain data obtained through photogrammetric procedures for highway location and design. The equipment is described in some detail along with techniques and computer programs that are available. New approaches in determination of final pay quantities and an integrated design concept are discussed.

•THE PENNSYLVANIA Department of Highways is similar to most other state and private highway engineering establishments in that photogrammetry plays a most important role in the total highway program. Much has been written, presented, and published on the more common applications of photogrammetry. I will endeavor to keep this presentation free from the traditional uses and techniques of photogrammetry and hopefully share with you some practical procedures and techniques relative to the utilization of terrain data. In doing this, I hope to stimulate your thoughts and leave with you some useful information that will assist you in your own areas of operation.

The department, with its own forces and through contracts with photogrammetric engineering firms, produces and uses a great amount of large-scale topographic mapping. This mapping is normally accomplished at scales of 200, 100, and 50 ft to the inch. The 200-ft scale is utilized for design location studies in rural areas. The 100-ft scale is utilized for bridge site studies and design location studies involving urban areas. The 50-ft scale is normally utilized for the final design, except in highly urbanized areas where final design is accomplished from 25 ft to the inch mapping supplemented by field surveys.

The total internal photogrammetric capability of the department is located in Harrisburg and functions as an arm of the central office Bureau of Design. It is through this unit that all photogrammetric projects are either accomplished or contracted. If contracted, the photogrammetric work is inspected and approved for further engineering use. The Photogrammetry and Surveys Section is a service agency providing photogrammetric services to the 11 separate district engineering offices located throughout the state and to other central office bureaus, i.e., construction, traffic, materials.

In addition to the mapping, the department produces photogrammetric cross sections for (a) design location studies, (b) final design, and (c) construction payment (earthwork quantities).

Presently, the department obtains cross sections by the following 3 methods:

1. Conventional ground survey methods in the field,
2. Interpolation of contours from large-scale photogrammetric topographic maps, and
3. Direct automatic terrain recording from stereoscopic models.

This presentation is concerned with only the last method, that of obtaining cross sections from stereoscopic models.

Because of the volume of cross-section work in all 3 of these areas, and the limited amount of equipment available to accomplish terrain readout, priorities had to be

Paper sponsored by Committee on Photogrammetry and Aerial Surveys and presented at the 49th Annual Meeting.

established as to how this equipment would be utilized. Recognizing that even though assignment of the stereo-readout systems to final design and final earthwork surveys would greatly benefit the department, the most significant benefits would be derived through the use of these systems in the design location studies. Here the digital terrain model system is of primary importance to the department.

Accordingly, the greatest amount of cross-section readout work has been accomplished for design location study purposes. It is in this area that our major efforts have been directed and our phogrammetric cross-sectioning techniques and procedures most fully established.

DESIGN LOCATION STUDIES

Mapping Review and Corridor Refinement

Once the mapping at 200 ft to the inch for rural areas has been completed, it is sent to the requesting district engineering office for use in studying alternate roadway alignments.

At this point, the alignment of the proposed roadway has been defined as being within the band of mapping 7,000 ft in width (based on a 6-in. camera at a 6,000-ft altitude above mean terrain and 5-diameter magnification plotting instruments) as shown on the 200 scale map sheets. Subsequently, the task of the engineer is to determine the specific location of the roadway within the area mapped at 200 scale. There are many factors that are considered in making this determination. However, for the purpose of this presentation, the factor of topography, and more specifically how it is handled, will be considered. After a careful study and review of the corridor that has been mapped, a band of interest is selected within this corridor. This band of interest is rarely less than 3,000 ft or more than 7,000 ft in width, the only exception being occasional parallel flights resulting in mapping bands in excess of 7,000 ft. This band of interest is graphically shown on the cronaflex map sheets by limit lines drawn in pencil. This establishes that portion of the 200 scale mapping for which cross sections are desired.

In addition to establishing the limit lines of the band of interest, the engineer must determine a base line to which all cross sections are to be referenced. The location of this base line is normally through the center of the band of interest on the mapping. However, there is considerable flexibility in the positioning of this line. The only requirement is that it can be constructed on the map sheets.

Depending on the complexity and length of the band of interest, the computations for the horizontal geometry describing the base line are performed either manually or through direct teletype communications with the department's computer center in Harrisburg (Fig. 1) and the remote unit (Fig. 2) in the district engineering office. The following event sequence occurs when using the computer for the horizontal geometry.

Figure 1. The Pennsylvania Department of Highways utilizes 2 Burroughs B5500 computers in the central office Data Processing Center. A portion of the operation is shown here.

Figure 2. A remote unit to the Computer Center is in operation in each of the 11 district engineering offices.

The computer program requires the following input data:

1. The station value of the beginning point;
2. The north and east coordinates for the beginning point, all P.I. points, and the ending point; and
3. Either the radius or degree of curve desired at each P.I.

This program then computes the following:

1. P.I. to P.I. distances and bearings of tangent lines;
2. The curve data for each P.I.;
3. The station values of the P.I., P.C., and P.T. points;
4. The tangent length, curve length, and external distance for each curve; and
5. The north and east coordinates of all P.C. and P.T. points.

This information is received by the engineer on the remote teletype unit from the computer, and used to plot and construct the base line on the map sheets. This same output information is also stored on magnetic tape files for later use when the cross sections have been completed.

It is at this point that the work shifts from the engineer in the district engineering office to the Photogrammetry and Surveys Section in the central office.

Preparation for Terrain Readout

When a project arrives in the Photogrammetry and Surveys Section, it is reviewed to ensure proper preparation of the cronaflex map sheets and other materials necessary to reset the stereo models in the plotters.

The cronaflex map sheets must show the following information (Fig. 3):

1. Lines establishing the band of interest,

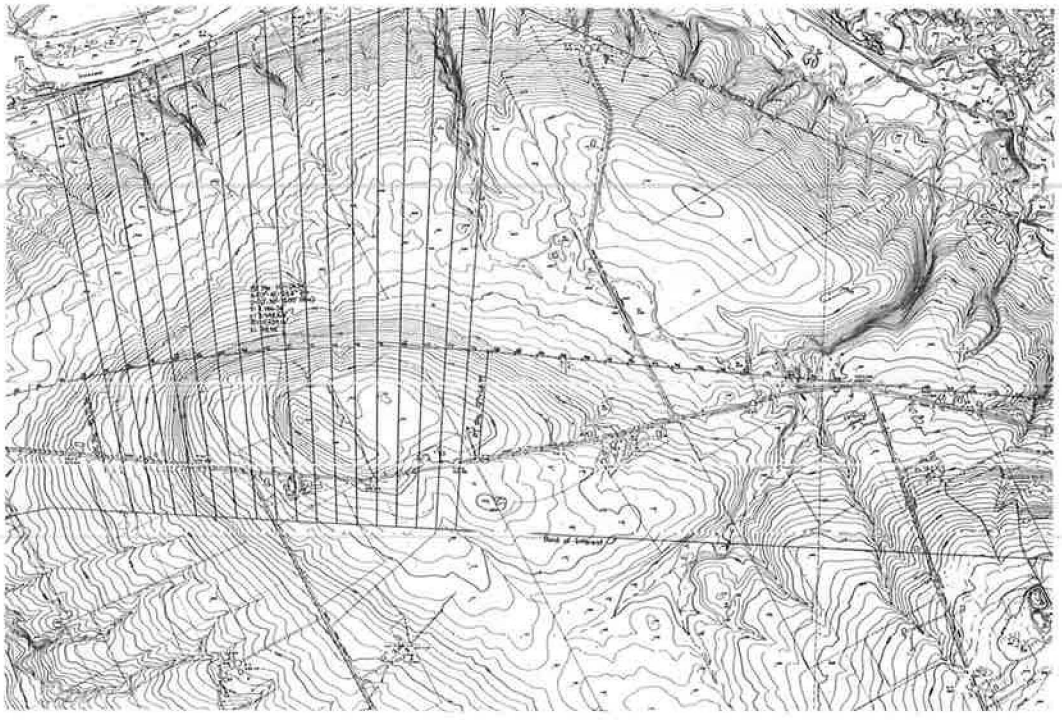

Figure 3. A topographic map showing the band of interest, base line, and curve data ready for the readout of terrain data.

2. A base line ticked at every 1-in. (200-ft) interval plus all P.C. and P.T. stations, and

3. All curve data in the conventional position adjacent to each P.C.

The cross-section interval is normally 1 in. (200 ft) at this scale. Cronaflex overlays aligned to the plotted base line are used extensively for cross-section orientation. This eliminates the need to draw every cross-section line on the map sheets (Fig. 4). For tangent sections, a master grid is used. This grid is 37 by 47 in. and has parallel lines 1 in. apart in one direction and parallel lines 5 in. apart and perpendicular to the other lines. At this map scale, the cross-section lines on the curves are usually drawn on the map sheets. Curve templates are used in some cases, but the most expedient procedure is usually drawing the lines through each 200 ft station and extending them a sufficient length to span the band of interest.

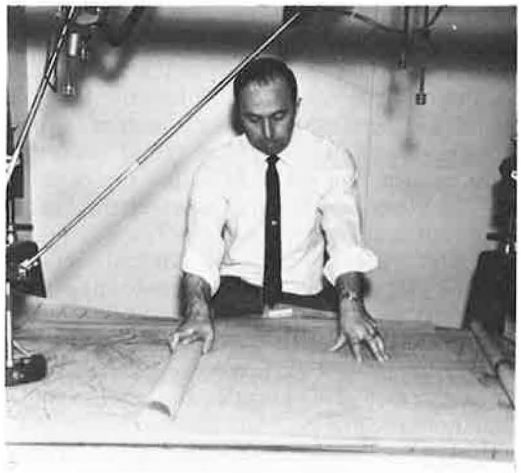

Figure 4. Cross-section grid being oriented over the base map for readout of terrain.

As these tanget and curve templates become worn through use, new ones are printed from the master scribed negatives constructed on the coordinatograph.

Description of Terrain Readout Equipment

The department is now operating 3 terrain readout units each attached to a standard 2-projector stereoplotter (Figs. 5 and 6). The oldest of the 3 units was installed in September 1965. The other 2 newer units were installed in September 1967. The older unit is presently undergoing major modification work to update and bring it to the same production capacity level of the 2 newer units. A brief description of the primary components and the functions they perform follows.

Horizontal Scaler Arm—This arm is placed on the plotter reference surface and oriented to track the cross section to be recorded. It is especially suited for the job it performs in that it has a usable linear distance of travel slightly more than 35 in. This special feature greatly facilitates reading of long cross sections as is the normal case in this application. The counting rate of the scaler is determined by the selection

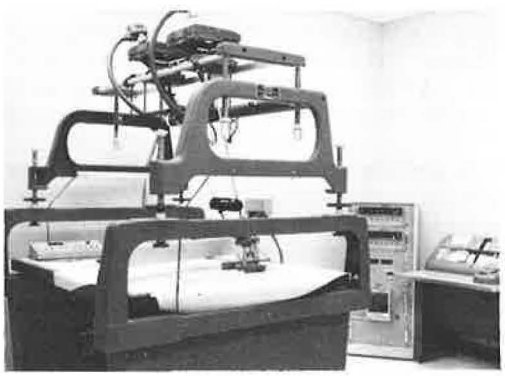

Figure 5. An overall view of the stereo instrument with terrain readout equipment attached.

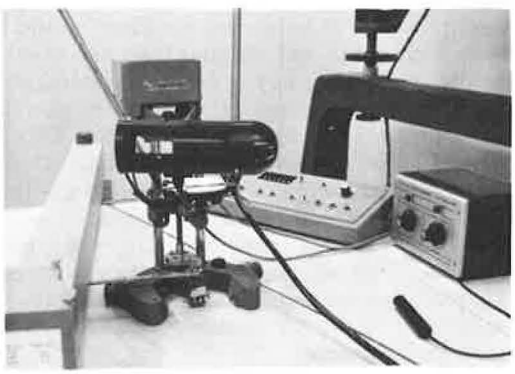

Figure 6. A close-up view of the horizontal scaler, operator control panel, and the stereo-image alternator system.

of gears in the gear box at one end of the arm. An optysyn (electronic, not magnetic) encoder attached to the main gear shaft transforms the revolutions of the gears into electrical pulse signals, which are displayed in numerals on the bidirectional counter in the control console. Thus, the horizontal distance through which the tracing table is moved is visible directly in feet on the control console display panel.

Vertical Scaler—The vertical scaler is an optysyn (electronic, not magnetic) encoder that is attached directly to the top of the Bausch and Lomb tracing table. It is driven by the elevation counter gear of the tracing table. This vertical scaler transforms the vertical displacement of the tracing table platen into electrical pulse signals. These signals are relayed to the control console where they are displayed. As with the horizontal distance, the elevation is displayed directly in feet. The tracing table with the vertical scaler is attached to an offset arm on the horizontal scaler by a removable pin. The combined horizontal scaling arm with the tracing table connected is conveniently portable to allow easy removal from the plotter surface during model setups. It is very easy to align to the cross-section lines, yet it has sufficient weight so the horizontal bar does not inadvertently shift off the cross-section line as the tracing table is moved from one end of the cross section to the other.

Control Console—The control console is the operational center of the entire system. It functions as it is directed according to the wiring in the patch panel on the lower front portion of the console. Besides the patch panel, the primary outward appearing features are 2 bidirectional counters of 6 digits each, one for the horizontal distance and one for the vertical elevation; an incremental 2-digit card counter; and a bank of 12 separate 10-position digital switches plus other control buttons and switches.

IBM 026 Card Punch—This is a standard card punch that operates under the command of the control console. When the record button is depressed, all preprogrammed constant data, the card number, the horizontal distance, and the elevation are automatically recorded on a punched card.

Readout Procedure

When setting up the stereo model prior to readout, the scaling arm, tracing table, and portable panel are placed on a table adjacent to the plotter. A second tracing table, free of the readout head and electrical cords, is used to perform the relative and absolute model orientation.

Once absolute model orientation has been attained, the appropriate grid is overlaid on the map sheet, and the horizontal scaling arm, the tracing table with scaler, and the portable panel are positioned on the plotter working surface. It is at this point that the operator initializes all switches and enters the appropriate information on the data switches on the control console and the portable panel.

The readout is accomplished in ascending station order for all cross sections in the neat stereo model. Each section is recorded by beginning with the point at the extreme left of the base line and ending with the point at the extreme right of base line. On a section 6,000 ft long, the readings would begin at -3,000 ft and end at +3,000 ft. Although the plus and minus signs are displayed on the bidirectional counter for the horizontal distance, they are not recorded on the cards. The computer works with the readings assuming a left to right scan sequence. A zero horizontal point, which is on the base line, is always recorded. This zero value tells the computer that the terrain points following are right of the base line.

The card format used to record the terrain is simple but compact. It is so arranged that 7 terrain points can be recorded on a single card in addition to the identifying station, the card number, the lane, the card type, and the rod or elevation format code (Fig. 7). These readout systems were designed and built taking into consideration the special requirements of the department. They have unique features, which add considerably to the efficient operation. There is an automatic error correction capability with the systems.

Should an operator prematurely activate the record button resulting in the punching of a terrain point that is in error in either location or elevation, he presses the error button on the portable panel. The following events occur automatically. The partially

PHOTOGRAMMETRIC CROSS SECTIONS

MERCER COUNTY LR 320 -LOCATION- 05/01/69

LANE	TY	F M	CD	STATION	DIST	ELEV	DIST	ELEV	DIST	ELEV	DIST	ELEV	DIST	ELEV	DIST	ELEV	DIST	ELEV
SL	02	E	09	0088+00.00	0602	1057.0	0670	1057.0	0812	1057.0	0958	1057.0	1085	1053.0	1199	1053.0	1267	1052.0
SL	02	E	10	0088+00.00	1306	1049.0	1369	1050.0										
SL	02	E	01	0090+00.00	2338	0912.0	2256	0917.0	2236	0917.0	2219	0912.0	2209	0911.0	2190	0924.0	2140	0926.0
SL	02	E	02	0090+00.00	2133	0923.0	2083	0925.0	2012	0927.0	1908	0931.0	1876	0929.0	1847	0932.0	1807	0942.0
SL	02	E	03	0090+00.00	1748	0945.0	1670	0949.0	1615	0948.0	1548	0951.0	1526	0948.0	1515	0954.0	1468	0957.0
SL	02	E	04	0090+00.00	1436	0951.0	1415	0959.0	1375	0960.0	1323	0967.0	1289	0973.0	1246	0978.0	1194	0984.0
SL	02	E	05	0090+00.00	1135	0990.0	1089	0998.0	1000	1007.0	0877	1015.0	0822	1018.0	0744	1021.0	0634	1021.0
SL	02	E	06	0090+00.00	0534	1023.0	0454	1025.0	0384	1026.0	0249	1025.0	0150	1026.0	0068	1028.0	0028	1030.0
SL	02	E	07	0090+00.00	0000	1031.0	0059	1035.0	0164	1046.0	0268	1054.0	0356	1064.0	0453	1071.0	0517	1073.0
SL	02	E	08	0090+00.00	0576	1076.0	0616	1073.0	0626	1070.0	0630	1073.0	0649	1072.0	0658	1071.0	0664	1074.0
SL	02	E	09	0090+00.00	0754	1073.0	0929	1072.0	1008	1070.0	1134	1068.0	1252	1065.0	1357	1064.0	1478	1062.0
SL	02	E	10	0090+00.00	1530	1059.0	1555	1057.0	1583	1059.0	1642	1060.0						
SL	02	E	01	0092+00.00	2376	0904.0	2348	0912.0	2273	0917.0	2231	0919.0	2219	0916.0	2209	0923.0	2174	0925.0
SL	02	E	02	0092+00.00	2159	0921.0	2129	0926.0	2106	0921.0	2037	0922.0	1997	0928.0	1971	0930.0	1956	0926.0
SL	02	E	03	0092+00.00	1933	0930.0	1894	0945.0	1844	0946.0	1793	0943.0	1749	0950.0	1703	0952.0	1629	0957.0
SL	02	E	04	0092+00.00	1551	0962.0	1510	0966.0	1464	0969.0	1424	0969.0	1382	0974.0	1343	0977.0	1298	0987.0
SL	02	E	05	0092+00.00	1248	0994.0	1197	0997.0	1134	1005.0	1051	1011.0	0964	1018.0	0883	1021.0	0815	1025.0
SL	02	E	06	0092+00.00	0722	1026.0	0669	1028.0	0583	1028.0	0431	1030.0	0334	1032.0	0194	1034.0	0098	1037.0
SL	02	E	07	0092+00.00	0030	1041.0	0000	1043.0	0063	1051.0	0132	1058.0	0201	1064.0	0279	1071.0	0367	1076.0
SL	02	E	08	0092+00.00	0505	1080.0	0595	1081.0	0677	1081.0	0692	1078.0	0699	1082.0	0714	1080.0	0722	1078.0
SL	02	E	09	0092+00.00	0729	1081.0	0845	1081.0	0979	1080.0	1109	1078.0	1200	1077.0				
SL	02	E	01	0094+00.00	2416	0911.0	2356	0913.0	2295	0916.0	2270	0918.0	2257	0917.0	2242	0921.0	2201	0921.0
SL	02	E	02	0094+00.00	2150	0922.0	2099	0918.0	2057	0920.0	1978	0924.0	1912	0927.0	1888	0930.0	1874	0940.0
SL	02	E	03	0094+00.00	1827	0943.0	1764	0942.0	1713	0946.0	1690	0947.0	1670	0948.0	1618	0951.0	1581	0960.0
SL	02	E	04	0094+00.00	1556	0967.0	1511	0971.0	1467	0976.0	1435	0981.0	1392	0990.0	1370	0993.0	1267	1002.0
SL	02	E	05	0094+00.00	1166	1011.0	1059	1018.0	0981	1020.0	0945	1022.0	0909	1023.0	0893	1022.0	0874	1025.0
SL	02	E	06	0094+00.00	0792	1025.0	0680	1029.0	0580	1030.0	0467	1032.0	0342	1036.0	0246	1038.0	0143	1046.0
SL	02	E	07	0094+00.00	0078	1052.0	0018	1058.0	0000	1059.0	0039	1066.0	0089	1071.0	0150	1073.0	0186	1078.0
SL	02	E	08	0094+00.00	0240	1082.0	0334	1085.0	0414	1086.0	0513	1087.0	0569	1090.0	0636	1090.0	0664	1088.0
SL	02	E	09	0094+00.00	0694	1090.0	0742	1090.0	0752	1087.0	0755	1089.0	0773	1089.0	0781	1087.0	0787	1090.0
SL	02	E	10	0094+00.00	0853	1088.0	0937	1088.0	1038	1087.0	1136	1086.0	1244	1085.0	1366	1084.0	1449	1082.0
SL	02	E	01	0096+00.00	2464	0910.0	2431	0913.0	2379	0912.0	2336	0906.0	2306	0906.0	2286	0912.0	2271	0919.0
SL	02	E	02	0096+00.00	2234	0920.0	2204	0912.0	2157	0913.0	2120	0917.0	2069	0918.0	2043	0923.0	2019	0921.0
SL	02	E	03	0096+00.00	1998	0925.0	1961	0934.0	1912	0941.0	1858	0947.0	1793	0957.0	1734	0962.0	1673	0967.0
SL	02	E	04	0096+00.00	1624	0974.0	1555	0983.0	1506	0988.0	1446	0993.0	1415	0995.0	1381	0999.0	1287	1010.0

Figure 7. A terrain listing indicates the station and the distance and elevation of the points selected during readout operations.

completed card in the keypunch is released with a single 12 punch being entered in column 80. As this card passes the read head of the keypunch, a duplication cycle begins on the following card that is passing by the punch head. The duplication continues to a point on the card that is one terrain point short of the original card, for example, if an operator has 5 good terrain points on a card and makes a bad reading on the sixth point. The card is automatically duplicated up to and including the fifth terrain point and then it stops. The operator then makes the correct point observation and continues to read on. Even the card number is held from its normal automatic advancing during this reject and duplication, so there is no loss of card number sequence. The operator remains at the plotter throughout the operation and does not have to manually remove the error card or in any way manipulate the keypunch. During a later card edit on a card collator, the error cards are automatically sorted out of the card decks and discarded.

The most frequently used buttons, which control record, card release, and card counter reset, are located in numerous locations, such as the operator's hand-held switch, the portable panel, and the control console. This facilitates the initializing of the system prior to and during readout. The operator accomplishing the terrain readout completes the model set-up sheets as well as a log sheet where he checks off the stations completed and notes any difficulties encountered. These sheets provide quick answers to most questions that may arise later.

Of the total 200 scale mapping produced, about 20 percent is accomplished by department forces and the remaining 80 percent by contract. Thus, about 4 of every 5 terrain readout jobs performed involve resetting of models previously compiled by photogrammetric engineering firms. This has been an excellent monitoring system for the quality of work being done under contract.

Preliminary Terrain Card Edit

Once completed, all cards on a project are submitted to the Data Processing Center for a preliminary card edit. This preliminary edit is performed on an IBM 407. It checks, for proper card sequence, blank colums that should have been punched, double punches, and reject or 12 punches in column 80. Any cards that are sorted out due to these conditions being present are kept separate and listed on the last sheet of the printout. Corrections are made, and the cards permanently turned over to the computer center.

Data Processing

All processing is accomplished on one of the department's 2 Burroughs B5500 computers. These separate programs are utilized in the analysis of the terrain information. A look in depth and detail at the inner workings of these programs is beyond the scope of this presentation. Only the major aspects will be covered to show how the terrain data are used.

Terrain Edit and Merge—The first of the 3 programs is the terrain edit and merge program. This program edits the terrain cross sections and creates a tape with original ground cross-section information for use in subsequent programs. It searches for and notes the following: Error 1—negative elevations; Error 2—missing or duplicate card numbers; Error 3—station numbers not ascending; and Error 4—horizontal distances not in ascending order.

Using as a criteria the controlling parameters established by the engineer, the program checks for the following:

1. The minimum terrain distance left and right,
2. Distance between stations,
3. Longitudinal slope,
4. Transverse slope,
5. Terrain card out of sequence, and
6. Missing terrain point on the base line.

The checking of these criteria is essential to ensure smooth program operation later on. The merge phase of the program enables the addition and deletion of terrain points or complete cross sections without rerunning the terrain edit phase.

Alignment Design—The second program, which is the alignment design program, computes the horizontal curve data and station values for a given roadway horizontal alignment. It uses data from the terrain edit and merge program. The horizontal alignment may take any one of the following 3 types:

1. One line where the survey base line and construction centerline coincide;
2. Two lines where the survey base line and construction centerline do not coincide but have a determinable geometric relationship; and
3. Three lines where you have the survey base line and 2 independent construction centerlines such as a left and right roadway. No two of the lines are coincident, but they all have a determinable geometric relationship.

Before this program can be run, the engineer must define the alignment of the line on which he desires the horizontal geometry to be computed. This he does by providing the computer with north and east coordinates for the 2 terminal points and any P.I. points as well as the degree, or radius, of curves where required.

For every run on the computer, each with a separate alignment, the engineer receives a tabulation of survey line stations and equivalent secondary alignment stations. Also computed are offset distances between the survey line and the secondary line and the angle between the perpendicular offset and the secondary alignment. Once the terrain is in the computer, multiple trial runs for different alignments can be obtained with relative ease.

Roadway Design—As the engineer reviews the horizontal alignment resulting from each computer run, he decides which alignments he wants to take through the third and last computer program, which is the roadway design program.

The roadway design program utilizes as input data information from both the terrain edit and alignment design programs previously discussed.

The program computes the vertical geometry consisting of the following:

1. The profile grade,
2. The vertical curve data for each vertical P.I.,
3. The template shape for each terrain station,
4. The points of slope intersect with the terrain, and
5. The earthwork areas and volumes between every 2 consecutive stations plus subtotals every 1,000 ft and the final totals for the entire job.

The use of this program series on a selective basis enables the engineer to make a comparison of the various possible alignments and greatly assists in the selection of the alignment to be recommended at the public hearing, before going into the final design phase.

FINAL DESIGN

After an alignment has been tentatively approved by all parties concerned, topographic mapping at a scale of 50 ft to the inch in rural areas and 20 ft to the inch in highly urbanized areas is produced on the alignment. The mapping width at these scales is normally between 600 and 1,200 ft. The procedures for producing photogrammetric cross sections for final design are very similar to those previously described for the design location study. One minor change is made in the wiring of the patch panel on the control console to permit elevation reading and recording to the tenth of a foot.

Upon completion of the cross-section readout, the card deck is submitted to the Data Processing Center for a preliminary card edit as was the case in the design location study. After edit, the terrain cards and supporting material are returned to the district office for study, analysis, and preparation of additional information. All required data are then forwarded to the Data Processing Center for the purpose of computing the final design geometry. The computer final design programs produce grade profile data, generate templates, compute cut and fill earthwork quantities, and produce tapes for the plotting of data on an automatic line plotter.

The department has entered into an agreement with Swindell-Dressler Company, a consulting engineer firm, for the design of a project utilizing a computer-oriented design concept with computer graphics. Here, again, the terrain data are generated through readout from the stereo models.

The total system involves 8 programs as follows:

1. Input—load terrain data and horizontal geometry and establish parameters and limitations in accordance with design criteria;
2. End areas—calculate end areas, slope stakes, and ditches according to template parameters (an example is shown in Fig. 8);

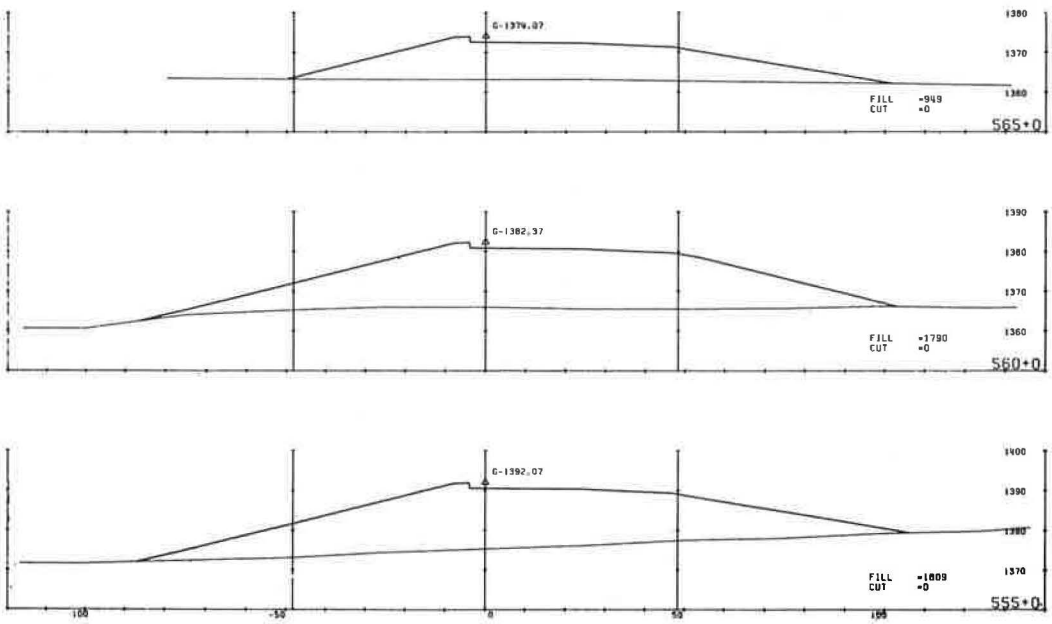

Figure 8. Cross sections plotted by a data plotter as a result of the computer operations.

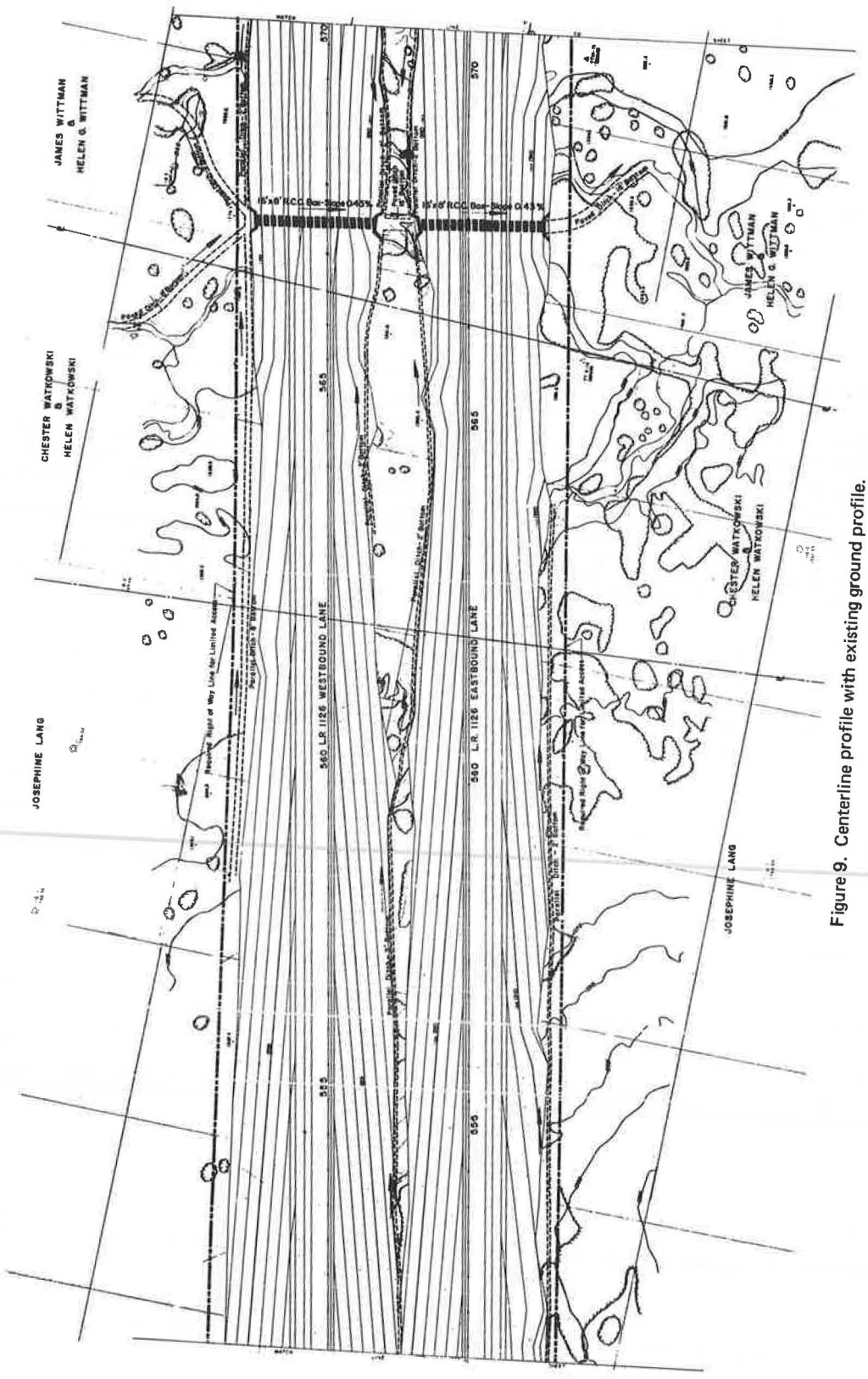

Figure 9. Centerline profile with existing ground profile.

3. Centerline profile—establish grades, vertical curves, and original ground and profile elevations;
4. Mass haul diagram;
5. Topo plan;
6. Contour map—a plot depicting the contours of the finished roadway;
7. Vertical plot—graphics indicating the grade lines for the roadway, ditches, and intercepts with original ground; and
8. Perspectives—perspective views of the design from a station and elevation selected by the design engineer.

The Swindell-Dressler Company utilized an IBM 360 Model 44 (64K) computer and a CalComp plotter for our project. The required computer programs are written in FORTRAN IV language. For further information, it is suggested that Mr. George Kisak of Swindell-Dressler Company's Computer Division be contacted by writing 441 Smithfield Street, Pittsburgh, Pennsylvania 15222. In still another evaluation, the department is considering the elimination of cross sections through the use of a contour grading plan. The construction plan, in this case, will consist of the design with original ground contours and "to-be-built" contours included on a plan sheet (Fig. 9). In this procedure, the basis for the construction plan will be the topographic map prepared by photogrammetric methods.

CONSTRUCTION PAYMENT (EARTHWORK QUANTITIES)

We are presently engaged in the readout of as-built cross sections utilizing color aerial photography. All previous projects were accomplished using panchromatic film.

Research conducted by the department during 1966-67 indicated there was less than one percent difference between volumes determined by photogrammetric methods as opposed to conventional field surveys. The research was conducted with black and white photography.

The main problems encountered were the difficulties in obtaining accurate elevation readings on the concrete pavements and the inability to see ditch slopes. These problems should be overcome through the use of color aerial photography.

The project presently being accomplished with color photography is 5.6 miles in length in moderately rolling terrain. Although this is a production project, we are also using it to research certain techniques relative to color versus panchromatic film, required density of panels, and control points for stereo model orientation.

CONCLUSIONS

No matter what procedure may be accepted in the future as a standard, photogrammetric data will continue to be very much in demand as the basic source material.

With the ability to place terrain data directly onto punch cards or tape, the photogrammetric engineer will find his services increasingly required as the computer systems and graphics are refined and as the young design engineer is trained to use computer-oriented procedures. Our workload will again increase as we gain acceptance from the construction contractor for pay quantities determined from photogrammetric data.

REFERENCES

1. Smith, B. L., and Yotter, E. E. Computer Graphics and Visual Highway Design. Highway Research Record 270, 1969, pp. 49-64.
2. Merrell, R. L. Determination of Accuracies in Earthwork Quantities From Photogrammetrically-Made Surveys. Texas Highway Department, Research Rept. 38-1F, 1968.

Use of Color Aerial Photography for Pavement Evaluation Studies

E. G. STOECKELER, Maine State Highway Commission

Many interlocking factors contribute to the amount of information on pavement distress features that can be gleaned from aerial photographs. Twenty-two different air-photo coverages of a short section of a 4-lane highway near Bangor, Maine, were taken over a 1-year period using 3 types of color film and 2 types of black and white film at photo scales varying from 1 in. = 100 ft to 1 in. = 1,000 ft. Variables to contend with included the (a) appearance of pavement, (b) background of the observer, (c) sky conditions, (d) resolution characteristics of the type of paper print or transparency, and (e) the type of viewing equipment. A technique for comparing the relative amount of detail discernible on the different photo coverages was developed. Based on the comparisons of several hundred crack pattern records made by 3 different observers, it was concluded that the maximum amount of information on flexible pavement distress features can be extracted from infrared color transparencies. For extensive general pavement performance studies requiring less detailed information, panchromatic glossy prints are adequate. The minimum photo-scale requirement is contingent on pavement conditions (principally whether the cracks are sealed or unsealed) and the type of information required for both intensive and extensive pavement evaluation studies. For reconnaissance surveys, a photo scale of 1 in. = 500 ft is adequate; and for more detailed studies, photography having a scale of 1 in. = 200 ft or larger is suggested. For both types of studies, stereo coverage is highly recommended.

•PAVEMENT OVERLAY PROJECTS along portions of a 4-lane highway between Augusta and Bangor, Maine, were scheduled for the 1967 and 1968 construction seasons. A number of different designs were proposed for various sections of this extensive research study. It was anticipated that reflection cracks would develop in the rebuilt pavements and that the amount and rate of the development would vary with the different types of overlay designs, original embankment design, terrain characteristics, average daily traffic, microclimate, construction practices, and a host of other contributing influences.

It was felt that a detailed record of the condition of the flexible pavement prior to the placement of the overlay would be a valuable tool in future performance evaluations of different overlay designs.

A feasible and economical method of securing a record of the crack pattern in the highway scheduled for repavement was by means of aerial photography.

The most suitable type of photography necessary for this particular purpose was not known. Therefore, in February and March 1967, a number of photo coverages of a short section of a highway near Bangor were taken with panchromatic film at scales ranging from 1 in. = 100 ft to 1 in. = 400 ft, at shutter speeds varying from $^1/_{150}$ to $^1/_{600}$ second, and under different sky conditions from light overcast to clear. This photography was

Paper sponsored by Committee on Photogrammetry and Aerial Surveys and Committee on Pavement Condition Evaluation and presented at the 49th Annual Meeting.

taken by a local private aerial photography firm at no cost to the Maine State Highway Commission other than the nominal charge for paper prints. Based on a rapid evaluation of 8 different coverages, it was decided to secure photography of the reconstruction projects slated for the 1967 construction season. Photo specifications were as follows: (a) panchromatic film with a minus blue filter, (b) minimum shutter speed of $^1/_{300}$ second, (c) scale of 1 in. = 150 ft, and (d) very high overcast with no breaks, if possible, or no clouds. This photography is being used currently to record the location of cracks developed in the overlay section during the past 2 years. The photography is considered adequate for the purpose intended. A sample of the employment of this photography as an effective tool for overlay performance studies is contained in the Appendix of this paper.

It was recognized that color photography might be more useful for detecting various types of flexible pavement distress features. Stallard (5) used several types of color and black and white photographic materials to identify staining associated with deterioration of rigid pavements in Kansas. He concluded that color prints at a scale of 1 in. = 100 ft were necessary for detecting initial stage staining, but black and white prints were adequate for recording the areal extent of more advanced staining. However, the photo specifications recommended for the identification of stains on a light-toned concrete surface might not necessarily be most suitable for the detection of features associated with failures in a dark bituminous pavement.

The scope of this paper is to determine the optimum film type and scale combination from which adequate information can be gleaned for flexible pavement evaluation studies. The study was cosponsored by the U.S. Department of Transportation, Federal Highway Administration, Bureau of Public Roads, and the Maine State Highway Commission. Methodology and evaluation techniques used in the course of this study are more fully described in a limited distribution report prepared by the author (6).

PROCEDURE

Interpreters have long recognized that the photo image of many natural or man-made objects may vary considerably even if the photography is taken with the same type of film and at the same scale. The photo tone of a given soil type may vary from practically white to dark gray, depending on the moisture content. The photo pattern of a deciduous forest in winter is very different from that in spring, summer, or fall. The general appearance of a bituminous pavement also may vary considerably under different situations. At the onset of this study it was realized that the definition of the photo images of various types of pavement distress features is dependent, to a large degree, on the contrast between the pavement surface and the particular type of deformation. One of the aims of this study was to ascertain the most advantageous conditions that would result in the best quality photography for the identification of these features.

To conduct a constant surveillance of pavement conditions and changes in surficial characteristics that might be recorded on film, the study area was conveniently located in the immediate vicinity of the writer's office. The 5-mile section of the study area just north of Bangor selected for multiple photo coverage was constructed in 1960 and 1961. The southern portion of the area was repaved with one course of binder in the fall of 1967; consequently, both fresh and weathered pavements were included in the study area. It was anticipated that reflection cracks would develop in the pavement overlay and that additional photo coverages would be obtained in the winter and spring of 1968 in connection with a reflection crack study being conducted currently by the Maine State Highway Commission.

Nine coverages, taken on June 1, 1967, are used as a basis for the film type evaluation phase of this study. Three film types, namely Panchromatic, Ektachrome MS Aerographic, and Ektachrome Infrared Aero, were taken of the same area within a 2-hour period; consequently, pavement conditions were identical for all 9 coverages. Figure 1 shows a sample of each of the coverages. For each film type, coverages taken at 3 different altitudes were on the same roll of film and processed in the same manner. Sky conditions were clear for all coverages. In other words, every attempt was made to eliminate all variables except scale and film type so that valid comparisons

The color plates of Figures 1, 4, and 5 on the following pages were provided by the author through the courtesy of the Maine State Highway Commission.

Figure 1. Nine vertical aerial photographs of the same area taken with three different film types at approximate photo scales of 1″=1000′, 1″=500′ and 1″=200′. The black and white photos were made from a panchromatic negative, the natural color prints (left opposite) from Ektachrome MS Aerographic negatives and the false color prints (right opposite) from Ektachrome Infrared Aero positive transparencies. All nine photos were taken with the same camera within a two-hour period. Below is a low altitude oblique of the interchange area showing pavement condition a few days prior to the date that the verticals were taken.

Panchromatic

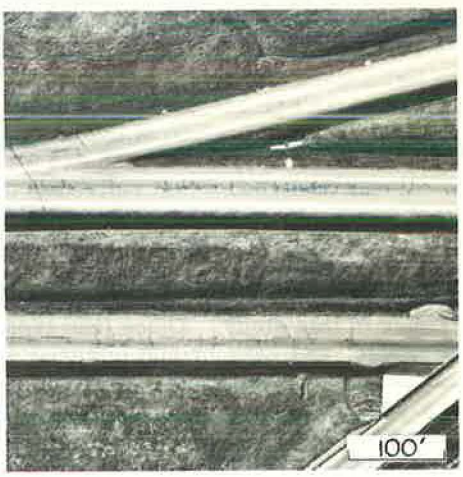

Ektachrome MS Aerographic

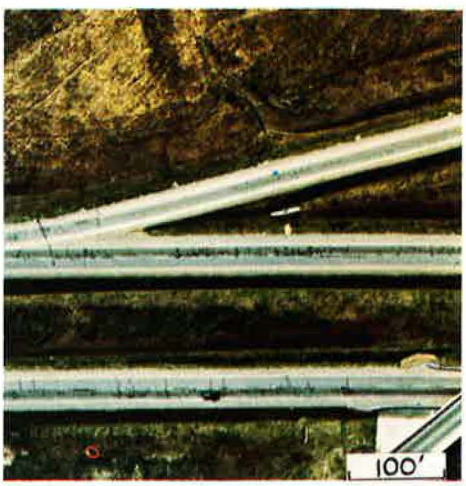

Ektachrome Infrared Aero

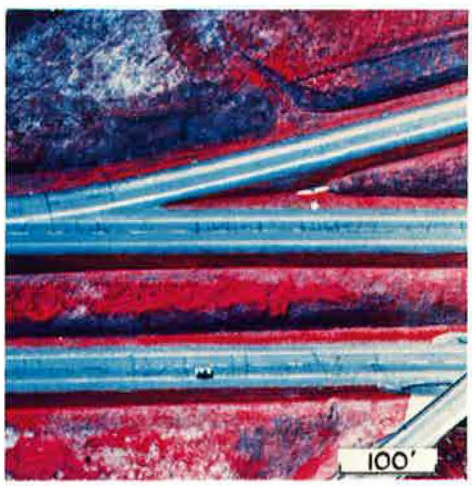

Original Scale 1″=1000′

Original Scale 1″=500′

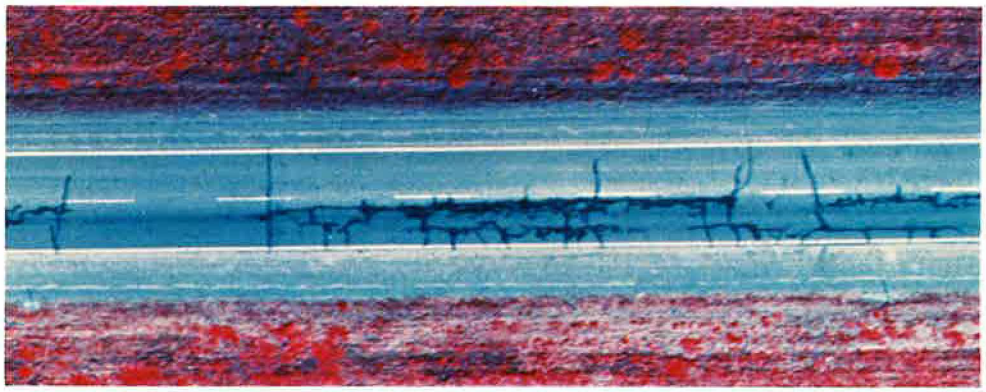

Original Scale 1″=200′

Figure 4. The relative amount of pavement cracking visible on vertical airphotos taken at three different altitudes with Ektachrome Infrared Aero film. Each transparency was enlarged about four diameters to simulate the magnification obtained with a pocket stereoscope. The photos were taken two weeks after the sealant was applied.

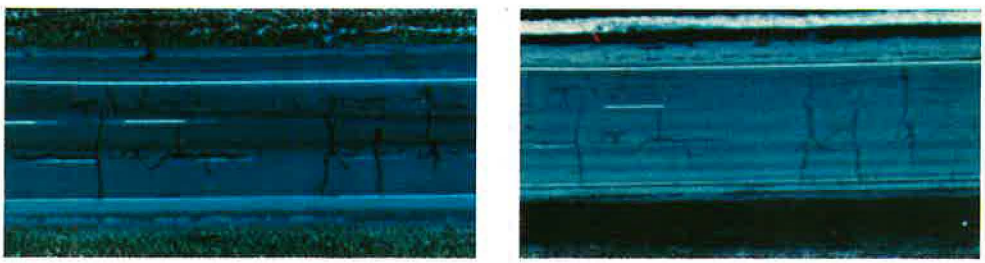

Figure 5. After being subjected to over six months of summer and fall traffic, the contrast between the crack sealant and the adjacent pavement is pronounced in the photo on the left taken on December 1. After exposure to repeated salt and sand applications the sealed cracks are less distinct, as shown in the March 11 photo on the right. Both photos were taken with Ektachrome Infrared Aero film at a scale of 1″=200′ and enlarged four diameters.

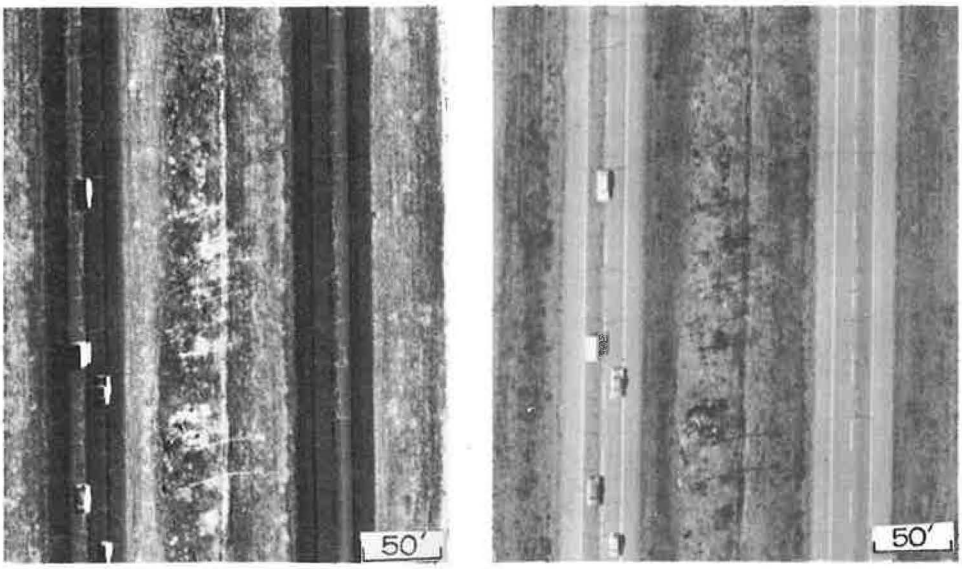

Figure 2. Two types of black and white enlargements made from Ektachrome Infrared Aero color film having an original photo scale of 1''=500'. The illustration on the left, made directly from the positive transparency film is a negative print, i. e., black appears white and vice versa. The normal print on the right was made from an internegative of the original positive transparency. Color prints (see middle photo of Figure 4) can be made from the same internegative.

Figure 3. An oblique depicting pavement conditions in the later part of May 1967, a few days prior to the date of the multiple vertical coverages shown in Figure 1. The width of the sealant stripe is indicative, to a degree, of the severity of the pavement failure.

among the coverages could be made to determine the relative amount of detail visible on each scale and film type combination. Thirteen additional coverages taken between February 1967 and May 1968 were used to evaluate other contributing factors pertaining to the seasonal aspect, sky conditions, and, above all, pavement conditions at the time of photography. (Photo coverages taken on the following dates were provided gratis by the James W. Sewall Company, Old Town, Maine: February 17, June 14, June 27, December 1 and December 2, 1967, and May 8, 1968.)

It should be noted that a considerable amount of photo detail is lost or subdued in the process of reproducing the illustrations used in this report. This is especially true of color prints made from Ektachrome Infrared Aero and Ektachrome Aero positive transparencies. To prepare a color reproduction from these original films, it is necessary to make an internegative from the positive transparency, a color print from the internegative, a 4-color negative plate from the color print and, finally, a printed color illustration from the color negative.

A number of black and white illustrations used in this report were made from color film originals. Normal black and white, as well as color prints, can be made from internegatives of Ektachrome Aero and Ektachrome Infrared films. Negative prints can be made directly from these films as shown in Figure 2. For the reader unaccustomed to viewing this type of print, the tone reversals are somewhat confusing. The definition, or the degree of sharpness, of photo images of minute pavement features on the negative print is better than on the print made from the internegative. Furthermore, an internegative of each 9- by 9-in. aerial film frame costs about $10, which is more than the cost of the original color transparency including film, processing, and aircraft charges.

Variations of Pavement Features Affecting Photogenic Qualities and Image Definition

The ability of an interpreter to detect a very small object on an air photo is dependent on the definition or clarity of the photo image. Apart from the equipment and materials used to produce and view the photo, the difference in the reflective characteristics of an object and the surrounding area is of paramount importance. For example, a sand-filled one-quarter inch crack formed in a solid-black fresh bituminous pavement is more readily discernible than an inch-wide sand-filled crack in a light-colored pavement partially covered with the same type of sand.

Following are a number of pavement condition variations that may affect the contrast between the pavement surface and cracks or other surficial deformations. The degree of this contrast is revealed by the relative definition of the image appearing on a film. In the ensuing discussion, the photo scale of photography referred to is as follows: large—1 in. = 200 ft, medium—1 in. = 500 ft, and small—1 in. = 1,000 ft.

Sealed Cracks—The most important single feature affecting the recognition of pavement cracks on an air photo is whether or not the crack has been filled with a sealant. The sealant is placed in a strip varying in width from an inch to a band over a foot wide where a number of closely spaced parallel cracks occur, especially in rutted wheelpaths. The viewer, in effect, sees the photo image of the sealant rather than the crack itself. A low altitude oblique depicting the general condition of the pavement in the study area is shown in Figure 3.

Freshly placed crack sealant is jet black, much darker than a weathered bituminous pavement exposed to the elements for a few years. The image of a fresh sealant stripe, 3 in. or more wide, on a light-toned weathered pavement is very distinct and is discernible on small-scale color photography (Fig. 4). Against a medium to dark gray pavement background the sealant image has a fuzzy appearance and is not readily discernible on small-scale photos but usually fairly well defined on medium-scale photos.

In Maine, cracks are usually sealed in late spring or early summer. Until the advent of salt and sanding operations in late fall, the sealant retains a very dark gray to nearly black tone, and the weathered pavement surface generally has a light to medium gray appearance.

After repeated salt and sand applications (Fig. 5), the sealant has a medium gray tone, and the contrast between the sealant and the adjacent surface is materially subdued.

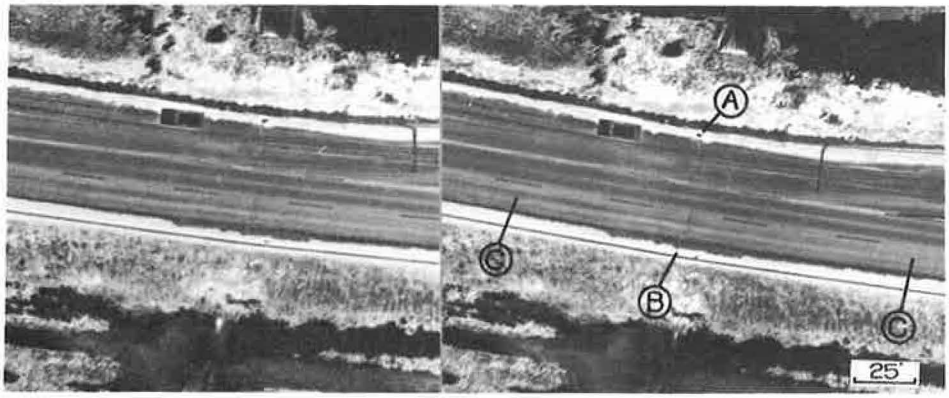

Figure 6. Stereopair of an unsealed transverse reflection crack and associated frost heave developed over a culvert in a recently placed pavement overlay. The crack was about 1'' wide and the heave was a little over ½'' high and 18'' wide on March 11, 1968 when the photo was taken. The crack extends from the man standing on the ramp shoulder at A to the passing lane shoulder at B. The ripple or washboard pattern C is distinct in the passing lane but not in the travel lane. The stereogram is constructed with negative black and white enlargements made from Ektachrome Infrared Aero positive transparencies having an original scale of about 1''=200'

Under these conditions, even stripes a foot wide are difficult to detect on small-scale photos. On medium-scale photos, the sealant is much easier to detect. After 2 years of exposure to traffic and the elements, most of the sealant has been worn off and is practically the same color as the surrounding weathered surface. With these conditions, photography having a scale of 1 in. = 200 ft or larger is necessary.

Unsealed Cracks—In Maine, transverse temperature cracks are generally best developed during the latter part of February at the time of deepest frost penetration. Cracks formed at the crests of differential frost heaves are also widest at this time of the year. Very few are over one inch wide at the pavement surface even at the period of maximum crack development. In the pavement overlay section included in the study area, it is estimated that over 90 percent of the reflection cracks were less than one-half inch wide. On low altitude photography having a scale of 1 in. = 200 ft, the image of a half-inch crack is $^{1}/_{5,000}$ in. wide. Unless there is a definite contrast between the crack and the adjacent surface, it would be practically impossible to see an image this small even on film having excellent resolution and edge-sharpness characteristics.

Occasionally, unsealed cracks less than one-eighth inch wide are discernible on coverages having a scale of 1 in. = 500 ft. In this particular case, the photo image of the crack is about $^{1}/_{50,000}$ in. wide. Quite often there is a discoloration on the pavement surface immediately adjacent to the crack, creating a "halo," which, in effect, increases the size of the photo image of the approximate crack location. Frequently a very slight ridge less than one-half inch high and a few inches to over one foot wide is associated with a transverse crack (Fig. 6). In the process of snow removal, bituminous coating is scraped off the aggregate along the low ridge centered on the crack, resulting in a light-colored band across the dark gray to black background of fresh pavement. These discolorations, which are readily discernible on large-scale photos, are often barely perceptible in the field.

Longitudinal cracks developed along centerline and pavement edge construction joints are usually difficult to identify. If the construction joint crack is located near the edge of the centerline or delineator paint stripe, it is practically impossible to detect cracks, even those over an inch wide. Unsealed cracks formed in a straight line along the

quarter point can usually be spotted on large-scale photos provided that the cracks, generally less than one-quarter inch wide, are filled with a material that is lighter colored than the surrounding pavement.

Longitudinal cracks formed along the wheelpaths are very difficult to detect because of the lack of contrast between the unsealed crack and the pavement. Unsealed cracks, then, are not readily discernible unless pavement conditions are such that there is a definite tonal contrast between the crack and the adjacent surface. After the frost-melting period, the pavement subsides, and many cracks that were over half an inch wide in midwinter "close up" to a hairline size. Many smaller cracks completely disappear by late spring, especially in the travel lane. Even on the very best large-scale photography, only a small percentage of small unsealed cracks of this type can be identified.

Rutting—Troughs developed along the wheelpaths are generally associated with long continuous longitudinal cracks (Fig. 7). In more advanced stages of pavement deterioration, closely spaced parallel longitudinal and connecting lateral cracks form a coarse alligator pattern and severe rutting. The application of sealant on the multiple cracks results in a very conspicuous dark-toned band often extending continuously for hundreds of feet along the wheelpaths. The width of the sealant band is indicative, to a degree, of the number of parallel cracks and the severity of pavement disintegration. Rutting in this advanced stage can be seen on color or black and white photos having a scale of 1 in. = 500 ft.

At the initial stages of rutting, longitudinal cracks are discontinuous or absent; nevertheless, a definite trough may be present. To detect a deformation of this type it is definitely necessary to view the photographs stereoscopically. Persons with normal binocular vision and only a casual knowledge of air photos can identify ruts only one-quarter inch deep on photography having a scale of 1 in. = 200 ft.

The pavement surface along the wheelpaths appears lighter because the bituminous coatings have been worn off, exposing the light-colored bare aggregate. The pavement between the wheelpaths, or along the quarter point, is darkened by exhaust fumes and oil. This creates an air-photo pattern that could be mistaken for rutting if viewed on a single photograph. This pattern is less pronounced on the passing lane where the traffic is lighter. A misinterpretation of this type can be avoided by using a stereoscope.

Pavement Ripples—Low parallel transverse ridges, fairly regularly spaced at 2- to 8-ft intervals, were observed on both fresh and weathered pavements. The gentle undulations, usually only a few tenths of an inch high, were apparently formed during the paving operation. At least in the study area, pavement ruptures were usually not associated with this type of surficial disfiguration. The crests of the ripples have a slightly lighter tone, like the low ridges associated with transverse temperature cracks described previously. The photo image of an individual ripple is very similar to that of an unsealed transverse crack. However, the ripples occur in a series of closely spaced ridges forming a "washboard" pattern, unlike more widely spaced temperature cracks (Fig. 8). Because of this, it is usually possible to differentiate between the two similar photo patterns. Although the ripple pattern is quite distinct on large-scale photos, it is very difficult to detect in the field, especially when the pavement surface is dry.

Frost Heaves—The period of severe pavement instability varies from 2 to 5 weeks in length depending on the severity of the winter, local soils and drainage conditions in the embankment, type of spring weather, amount and type of traffic, and other contributing factors. Due to variations in the local environment, differential subsidences may develop at one part of the highway during the early part of March and at another spot, not too distant, several weeks later. It is obvious that only a portion of deformations due to frost action would be recorded on any single photo coverage. This is especially true of the severe pothole variety that often develops during a short period of a few days. This type of deformation is generally confined to an area of a few hundred square feet or less.

For studies stressing pavement deformation due to frost action, several photo coverages should be obtained when frost conditions in the embankment are as follows: (a) at the anticipated date of maximum frost penetration and accompanying vertical movement, (b) on the date when the base is thawed and the subgrade is still frozen, and (c) when frost has melted below the center of the highway but is still present in the subgrade under the shoulders. Photography for detailed frost-action studies should have a scale of 1 in. = 200 ft or larger. With the 3 coverages described, it is probable that most,

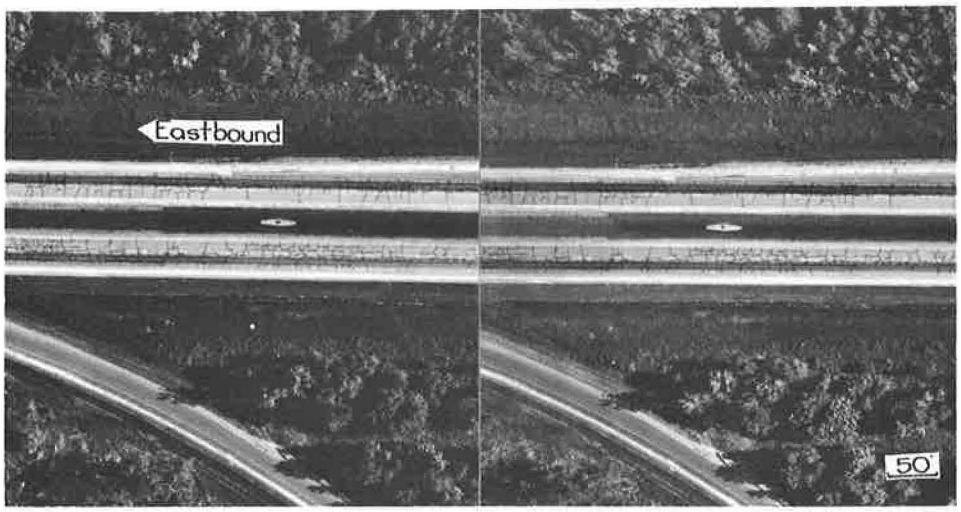

Figure 7. Stereopair of severe rutting. Longitudinal cracks are practically continuous along the wheel paths and are interconnected with laterals. At sections along the wheel paths where the sealant stripe is wide, two or three parallel longitudinal cracks have formed in the trough.

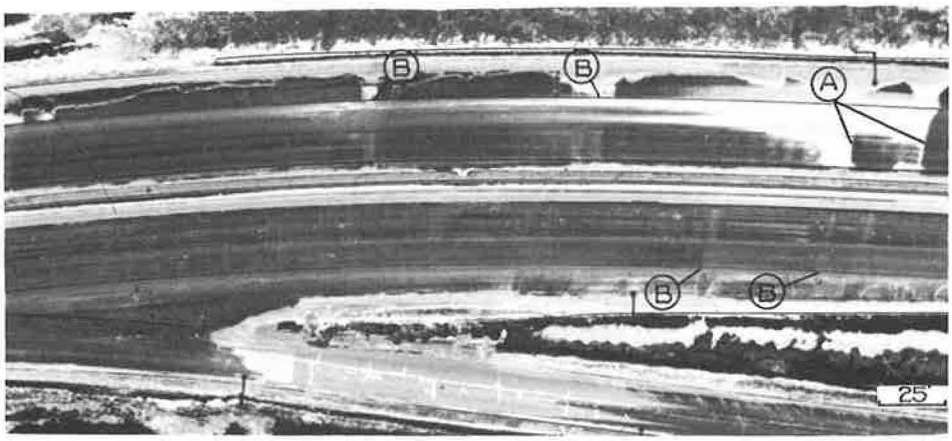

Figure 8. Vertical view of pavement ripples a few tenths of an inch high visible on the binder course of a recently placed overlay. The illustration is a black and white negative print made from an Ektachrome Infrared Aero transparency taken March 11, 1968. The white pattern along the northbound lane is formed by melt water carried by wind action along the travel lane and for shorter distances along the passing lane immediately ahead of the two transverse cracks (A). Transverse cracks also occurred at locations indicated by the letter B. All other more or less uniformly spaced, transverse pavement discolorations are ripples and are not associated with pavement cracks.

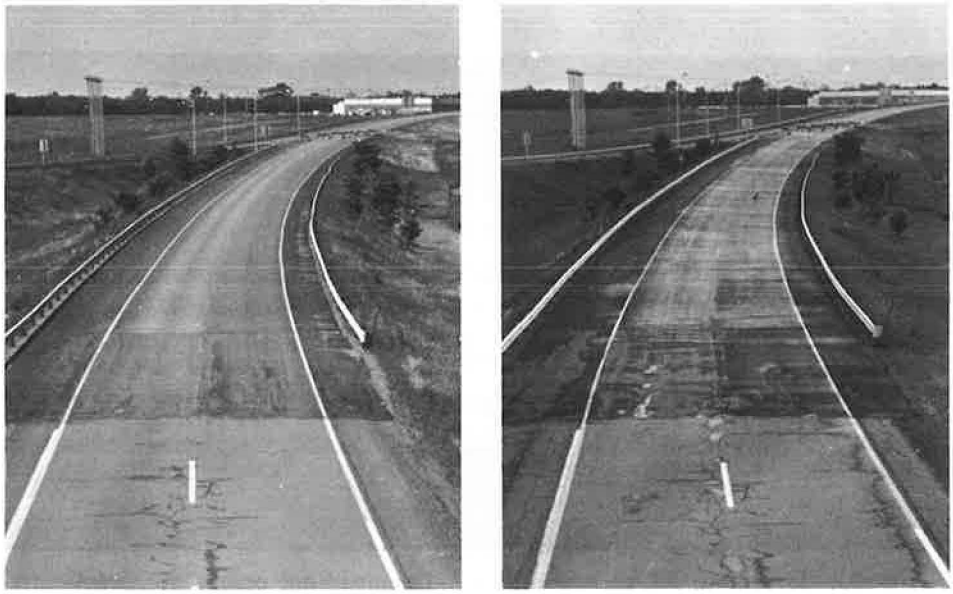

Figure 9. Two views of a pavement overlay in a wet and dry condition. Most of the 16 reflection cracks developed between the end of the taper and the off-ramp barricade could be seen when the pavement was wet but practically none when it was dry.

although not all, depressions and heaves could be identified and accurately located by photo-interpretation methods.

Other Considerations Affecting Definition of Photo Images of Pavement Distress Features

Water, Sand, and Salt—Unsealed cracks and minor irregularities in a roadway surface are easiest to see when the pavement is wet. Ripples, frost heaves, and cracks that may be imperceptible on a dry pavement are often quite distinct when the surface is wet (Fig. 9).

This might suggest that it would be ideal to obtain photography when the pavement is wet. However, it is very difficult to obtain photography when moisture conditions are uniform. In windy weather, more exposed sections of a highway may have a dry surface while other portions are wet. Frequently, the travel lane is dry and the passing lane may be wet. Variegated pavement conditions sometimes result in very complex photo patterns that often are difficult to interpret.

Immediately following snow removal and sanding operations, the appearance of the roadway surface is also extremely variable. After a heavy salt application, the photo tone of the pavement ranges from a very light gray salt-crusted surface on the travel lane to a nearly black, slush-covered, snow-streaked passing lane. Especially in late winter or spring, it is very important to schedule the photo flight at a time when the least amount of these undesirable pavement appearance features are present.

Shadows—Rather rigid light requirements for color film generally necessitate taking the photos under clear-sky conditions. In the northern latitudes during the winter months, aerial photography for most purposes is usually limited to a 3- or 4-hour period around noon. However, acceptable color photography can be obtained under adverse sky conditions for pavement evaluation purposes because color fidelity is not absolutely essential. A number of illustrations in this report were made from Ektachrome Infrared

Aero film taken between 10:30 and 11:45 a.m. on March 11, 1968. For this coverage, the aircraft was flown about 300 ft below a light overcast. An F5.6 aperture and a 1/200 second shutter speed were the exposure. Light conditions varied somewhat because of variable density of the overcast. The image motion resulting from the relatively slow shutter speed was considerably in excess of the recommended tolerance (1). Nevertheless this particular coverage proved to be the best of all of the 22 coverages available for this study for detecting minute pavement deformations such as ripples, small frost heaves, and very narrow unsealed reflection cracks in a fresh pavement overlay.

One obvious reason for taking photos under an overcast is the absence of shadows. This is an important factor to consider when writing specifications for photography to be used essentially for roadway performance studies especially in northern latitudes where the sun angle is low during the winter season. Shadows can be a definite problem in photographing roads located in mountainous terrain, urban areas with high flanking buildings, and routes having narrow rights-of-way. Roadways lined with deciduous trees should be photographed in winter or early spring before leaves are developed (Fig. 10).

For special frost-action studies involving local variations in microclimate due to shadows in the vicinity of bridges, deep cuts, and the like, photography should be taken under an overcast because the local area of interest might be in a shadow and much of the pavement detail would not be visible or only faintly discernible, as shown in Figure 11. It should be pointed out that shadows in infrared color film are very dense, obliterating practically all detail.

Traffic—On vertical air photos, it is obvious that the pavement surface cannot be seen under a car and much detail is lost or only partially visible in the shadow of a vehicle. Highways in the vicinity of large metropolitan areas, especially during rush-hour periods, have much of the pavement surface completely masked.

In the section of the highway used for this study, the average daily traffic during the winter months is about 6,000. The number of vehicles averaged about ten per mile in all of the different coverages used for this study, so only a very small percentage of the roadway was masked by cars.

Stereoscopic coverage was obtained for all photography used in this study. With a small volume of traffic the chances of having the same spot on the highway occupied by different cars in the 2 end-lapping photographs are remote. However, in the process of comparing the amount of pavement detail visible on 9 different coverages, it was difficult to select a 300- to 500-ft section of the highway that did not have any cars in the same short stretch selected in all of the coverages. Only in a few of the cases was it necessary to discard a preselected study section because the same portion of the pavement was masked by 2 different vehicles appearing in adjacent frames. In stereo coverage of a highway having vehicles spaced less than 100 ft apart, the chances of having some parts of the pavement covered by vehicles on both adjoining photos are relatively high. Photography should be obtained, if possible, when the least amount of traffic is expected.

Resolution Variations in Different Types of Prints and Transparencies

A variety of different types of reproductions can be made from different film types. For example, from the original Ektachrome MS negative, both color and black and white opaque prints or positive transparencies can be made. The Ektachrome Infrared Aero and Ektachrome Aero types were processed to produce a positive transparency. By using an internegative of these transparencies, it is possible to reproduce either black and white or color prints. Negative black and white prints can be made from color transparencies. It would have been desirable to have both prints and transparencies of each of the color film coverages, however, this would have been very costly.

The resolution of the final print or transparency viewed by the interpreter is all important. A certain amount of resolution is lost in every additional step required to make a positive print. The Ektachrome Infrared Aero and Ektachrome Aero types are reversal films that produce a positive transparency, so no additional processing steps are required. It is generally recognized that a greater amount of detail can be seen on

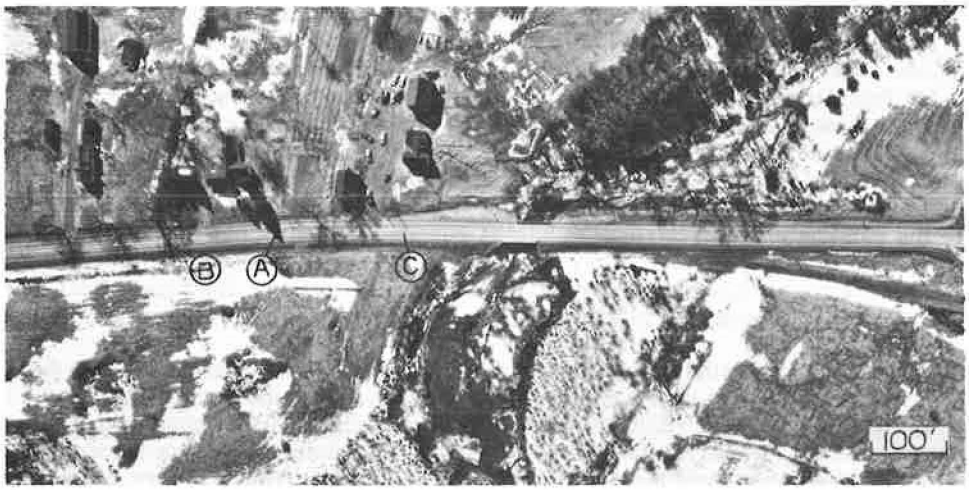

Figure 10. Solid conifer (A) shadow cast across this secondary roadway practically obliterates pavement detail. Sealed cracks are very difficult to detect in the maze of narrow shadows of leafless hardwood limbs (B). Utility pole (C) shadows also might be mistaken for a sealed crack. This photo was taken in late March before deciduous foliage was developed. Photography should be taken under an overcast for situations of this type.

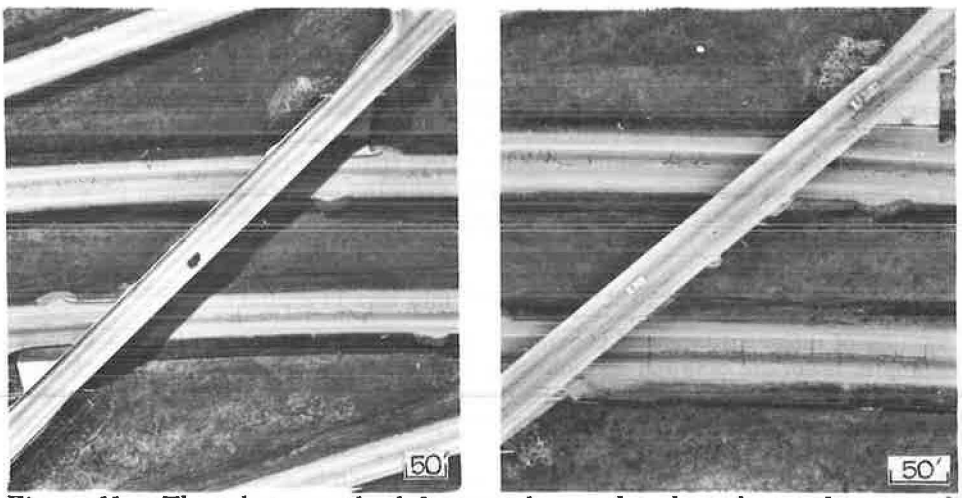

Figure 11. The photo on the left was taken under clear sky conditions and the one on the right under a light overcast. Pavement detail in the bridge shadow is very faint. Both photos were taken with panchromatic film.

transparencies viewed by transmitted light than on opaque prints (4). Consequently, it was expected that image resolution should be better on the transparencies than on opaque prints.

Comparisons on the amount of detail visible on different types of prints and transparencies reproduced from the same negative were made using a variety of viewing instruments. Positive transparencies and negatives were viewed with a scanning stereoscope having 1.5X and 4.5X magnification. Opaque prints were viewed with pocket and scanning stereoscopes. A 10-30 power monocular zoom macroscope was used for a few comparison resolution tests also. Each observer used the same viewing equipment and illumination source for any particular set of comparison tests.

It was noted quite often that the photo image of a pavement deformation on one photo might be readily identifiable but very faint or absent on the adjacent end-lapping photo. Flaws in a print caused by dust or lint could be mistaken for a pavement deformation if only that particular single print were viewed. The advantage of using stereopairs as a standard procedure is obvious.

Evaluation Techniques

Information Required for Pavement Evaluations—The initial step in the analysis was to itemize surficial features associated with bituminous pavement deterioration and deformations used in the preparation of different types of pavement performance studies, condition surveys, and highway sufficiency ratings. Hveem (2) pointed out that there is a conspicuous lack of agreement on pavement failure terminology on a nationwide basis. There is also a definite lack of agreement among engineers on the comparative seriousness of a particular type of deformation and the underlying cause, or causes, of a specific type of pavement deterioration. It is not the purpose of this paper to delve into causes of failures but to detect manifestations that might indicate the relative degree of distress or degradation of a pavement.

To illustrate the type and amount of detail visible on different types of photography to a group of engineers interested in pavement evaluation studies, but not versed in photo-interpretation techniques, several methods of projection and sketch-preparation procedures were devised.

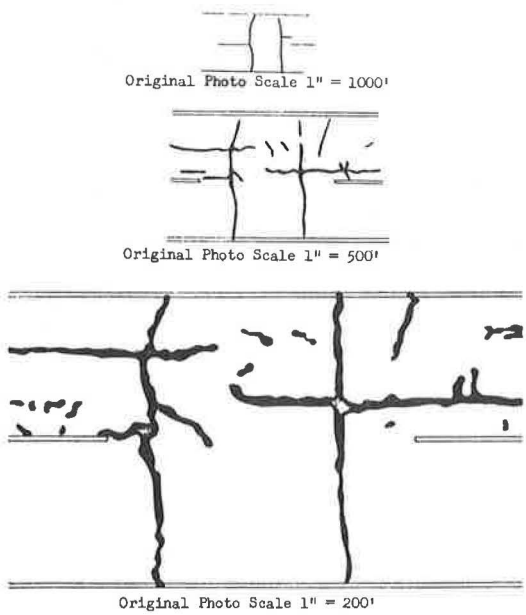

Figure 12. The relative amount of sealed crack detail visible on photos taken at different altitudes. These sketches were produced by tracing the image made by a microfilm projector.

Standard overhead opaque and transparency projectors capable of handling a 9- by 9-in. photo format were used to demonstrate the relative amount of pavement detail discernible by film type and photo scale. Projections resulting in 5 to 30 diameter enlargements of the original photo were made to show differences in image definitions for different types of coverages.

Another approach to illustrate resolution of photo images visible on different coverages was accomplished with the use of microviewers, for both transparent and opaque materials. A variety of commercial viewers having fixed magnifications ranging from 15X to 24X were employed for this demonstration technique. A sample of sketches made by tracing outlines of pavement features visible on projections made from panchromatic glossy prints at 3 different photo scales is shown in Figure 12.

The paramount object of these demonstrations was to draw out opinions on

the degree of sophistication necessary to provide an adequate amount of information for making both extensive and intensive pavement performance studies. Based on discussions resulting from these presentations, the following simplified list of surficial distress features was considered to be sufficient for detailed pavement evaluation studies in Maine:

1. Transverse cracks: (a) sealed and unsealed; (b) length, more than 10 ft, 2 to 10 ft, less than 2 ft; and (c) single or multiple with laterals.
2. Longitudinal cracks: (a) sealed and unsealed; (b) length, more than 10 ft, 5 to 10 ft, less than 5 ft; and (c) single or multiple with laterals.
3. Vertical deformations: (a) rutting (longitudinal); heaves (transverse); and (c) ripples.

For studies requiring less detailed information, such as for a statewide highway sufficiency rating report, data on unsealed cracks were not considered to be essential.

Methodology for Comparing Coverages—To compare numerous coverages, using projections, or sketches made from projections, was not practical. To use all of these features for making a quantitative evaluation of some 20 different coverages was not feasible. Consequently, for the purpose of determining the optimum scale-film type combination, the 9 coverages taken on June 1, 1967, were used for the initial set of comparisons. To simplify the analysis process, only sealed transverse cracks occurring in the passing lane were employed.

Several sections of roadway, ranging from 250 to 500 ft in length, were selected for this phase of the study. Three observers, other than the writer, were engaged to identify transverse cracks visible on each of the 9 coverages. Backgrounds of the observers are as follows: (a) a photo interpreter with over 10 years of experience in terrain analyses but with no training in pavement-performance studies, (b) an observer well versed in pavement evaluation studies and rather familiar with photo-interpretation techniques, and (c) a draftsman having practically no experience in either photo interpretation or pavement evaluation.

It was recognized that the process of comparing the amount of detail visible on different coverages involved numerous complex, interlocking variables. Following is a list of variables that could, to one degree or another, affect the definition or appearance of pavement features on different types of aerial photography: (a) pavement condition, (b) photo scale, (c) film type, (d) sky condition, (e) viewing equipment, (f) type of photo print, negative or positive transparency, and (g) capability of the observer. Photographic equipment, exposure, lab processing procedures, and other technical aspects pertaining to the photography used for these analyses are all important; however, an evaluation of these considerations is beyond the scope of this study.

In each of the 7 major categories of variables listed in the previous paragraph there are many possible subdivisions. Consequently, the number of possible combinations of variables to evaluate could run into the thousands. For a study of this type, it would be ideal to obtain simultaneous exposures of 5 or 6 different types of film, using identical camera equipment, taken at 3 or 4 different altitudes and each film type processed identically. This would automatically eliminate many variables. The 9 coverages, 3 film types, and 3 different scales, obtained within a 2-hour period described previously (Fig. 1), are considered to be as close to the "ideal" as possible utilizing the photographic equipment available.

After a tedious trial and error period, the following method of collecting and recording comparison data was devised.

1. Two 500-ft-long sections of the roadway having a variety of sealed cracks in the passing lane were located on each of the 9 coverages. In the study sections selected, all cracks were sealed 2 weeks prior to the date of the photography. The width of the sealant stripe varied from 1 to 8 in., and the lengths ranged from a few inches to transverse cracks completely across the 12-ft lane.
2. Painted centerline stripes used as reference points were indicated on the photos for orientation purposes. Stereopairs were set up by the writer for independent viewing by each of the observers. Small-scale coverages (1 in. = 1,000 ft) for each of the

3 film types were used first, then progressing to the 1 in. = 500 ft coverages and finally the 1 in. = 200 ft photography.

3. The writer, acting as a note keeper, recorded the location and configuration of each crack as described by the observer on a form having numbered centerline stripes corresponding to the stripes indicated on the photo. It was found that it was difficult for the observer to locate a particular crack on the photo and then sketch the crack on the record form. This involved looking up from the stereoscope, plotting the crack, and then reorienting himself on the photo to locate and record the next crack. Using this procedure proved to be very tiring and confusing to the observer. The most satisfactory technique was to have the observer verbally describe the location and configuration of each crack while keeping his eyes "glued" on the photos. With practice, the recorder could interpret the observer's verbal description and make a reasonably accurate facsimile of the location, configuration, and size of a particular crack.

Shown in Figure 13 is a record of crack detail, as described by one observer, visible on each of the 9 coverages along with a field check. By using an overlay of records made by the same observer, a valid comparison of the relative accuracy and amount of detail visible on each of the coverages can be made to determine which scale-film type combinations are adequate to provide information for a particular type of pavement evaluation study made by an individual having a comparable background.

The same procedure can be used to compare the accuracy of data recorded by different observers as shown in Figure 14. On coverages where the definition of the photo image is very faint and not easily identified, the background factor is very important. In this particular illustration the images of very narrow unsealed reflection cracks were not only industinct but were quite similar to photo patterns produced by pavement discolorations, which resulted in many interpretation errors, especially for an observer having practically no experience in pavement evaluation studies or photo interpretation.

Numerous comparisons of records were made in an attempt to evaluate photographic materials used, including negatives, glossy and semimatte bromide paper prints, negative black and white paper prints made from color positive transparencies, ESTAR Base prints, color prints, and positive color transparencies. Photo scale, film type, pavement condition, and other variables discussed previously were evaluated by means of the record comparison method.

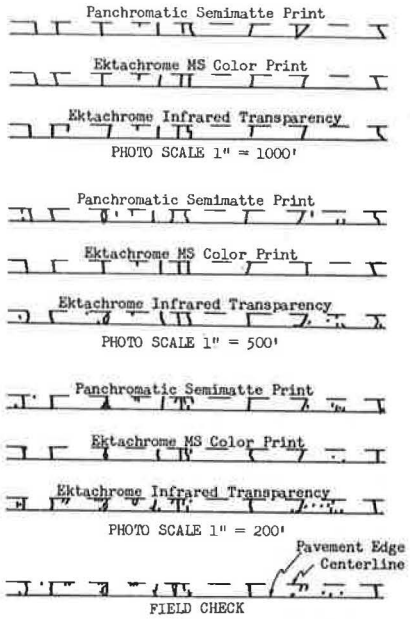

Figure 13. A schematic presentation of the relative amount of pavement surface detail seen by the same observer on 3 film types taken at 3 different scales. A comparison of the records made from different types of photography with the field sketch reveals that the most accurate information was obtained from the Ektachrome Infrared transparency taken at a scale of 1 in. = 200 ft.

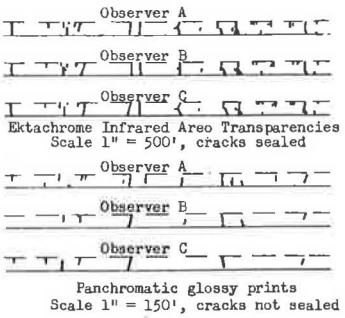

Figure 14. A comparison of crack location records prepared by 3 different observers. The upper set was prepared from photos in which the crack pattern was very distinct and the resultant records of the 3 observers were practically identical. The lower set was made from photos on which the crack pattern was considerably less discernible and the records are quite dissimilar. When using the upper set of photography, all 3 observers exhibited confidence in their analyses, and just the opposite for the lower set. This is an indication of the adequacy of the photography for the purpose intended.

CONCLUSIONS AND RECOMMENDATIONS

No single scale-film type combination can be recommended for pavement evaluation studies because of the numerous complex factors discussed in the previous pages. On a nationwide basis it is doubtful that many states would have, simultaneously, identical situations in all of the following considerations: (a) personnel with backgrounds and experience in the fields of both pavement evaluation and photo interpretation, (b) amount and type of pavement detail criteria requested by engineers for pavement distress analyses that are tailored to local conditions, (c) climate and environment, and (d) available photographic and viewing equipment. All of these factors contribute, to one degree or another, to the type of photography necessary for flexible pavement evaluation studies. The following observations are applicable specifically to the overall situation as it exists in the state of Maine. However, many of the considerations and recommendations should be applicable nationally.

Paramount Significance of Pavement Condition

It is the opinion of the writer that the condition or appearance of the pavement at the time of photography is the most important single factor influencing the amount of information that can be gleaned from any particular photographic coverage. Photography should be taken, if possible, when the contrast between the deformation feature, such as a crack, rut, or bump, and adjacent pavement surface is most distinct. Following is a list of "ideal" pavement conditions and other considerations that will affect the quality of the photo image of minute pavement features.

1. All cracks should be filled with black sealant. For coverages of fresh pavements having unsealed cracks, the photography should be taken when the cracks are widest, generally at the period of maximum frost penetration.
2. Pavement should not be discolored by crusted salt, winter sand cover, snow, or slush.
3. For older pavements, coverage should be taken during the frost-melting period when microrelief, especially rutting, is most pronounced.
4. Photography should be taken under a light overcast when shadows are very faint or absent.
5. Pavement surface should be uniformly damp to wet.
6. Volume of traffic should be minimal at the time of photography.

If the photography is obtained when conditions differ from those given above, pavement microfeatures will be more difficult to detect, regardless of the film-scale combination used for the particular coverage.

Observers should be in the field during the photo flight to record ground truth data, including measurements of crack widths, rutting depths, and heights of heaves. Black and white and color ground photos, preferably in stereo, should be taken of pavement distress features and also of any discolorations or markings that might produce photo images that could be mistaken for pavement failures. If the photography is taken immediately after a rain, the relative degree of wetness of the pavement should be noted along the flight line, especially differences in the appearance between the travel and passing lanes. Information of this type is useful to the photo interpreter in the process of developing methods of identifying pavement deformation photo patterns.

Photo-Scale Requirements

For studies requiring information on pavement microrelief, unsealed cracks, and identification of small objects having indistinct photo images, photo scales of 1 in. = 200 ft or larger are recommended. Photography having a scale of 1 in. = 500 ft is adequate for general, extensive studies that do not require information on unsealed cracks or pavement relief.

Suggested Film and Reproduction Types

The definition of minute pavement distress features was best on Ektachrome Infrared Aero positive transparencies. Resolution, contrast, and edge sharpness appeared to be

better on this film type than on panchromatic and Ektachrome MS Aerographic negatives. The resolution of panchromatic glossy prints was superior to that of Ektacolor paper prints. Detail on Ektachrome Infrared Aero transparencies was more readily discernible than on the other film types. When viewed through a monocular zoom lens, Ektachrome MS color prints were very fuzzy at a 10X magnification and panchromatic semimatte prints at the same magnification were also indistinct. On glossy panchromatic prints, excessive granularity and loss of edge sharpness was very evident at a 15X enlargement. Definition of images was fairly good on both Ektachrome MS Aerographic and panchromatic negatives at a 15X magnification. Photo images were sharp at magnification in excess of 20X on the Ektachrome Infrared Aero and Ektachrome Aero positive transparencies.

For intensive pavement evaluation studies requiring the maximum amount of detail on minute features, Ektachrome Infrared Aero film is recommended. Panchromatic prints with a glossy finish are adequate for studies requiring less exacting information. It is possible that multispectral photography and other types of remote sensors might prove useful for pavement evaluation studies (3).

ACKNOWLEDGMENTS

The author is grateful to various members of the Materials and Research Division for their critical reviews of the manuscript. Thanks are extended to Messrs. Wilbur Tidd, Raymond Woodman, Jr., and Donald Madden, who acted as observers for the numerous, tedious comparison experiments conducted in the course of this study. Mr. Ralph Dunbar, Division Engineer, kindly arranged to have sealant placed on the pavement cracks along portions of the study area just prior to the date that multiple photo coverages were obtained. Many different photo coverages were flown free of charge by the James W. Sewall Company, Old Town, Maine. To all, the writer is deeply appreciative.

REFERENCES

1. Manual of Color Aerial Photography. American Society of Photogrammetry, Falls Church, Va., 1968.
2. Hveem, F. N. Types and Causes of Failure in Highway Pavements. HRB Bull. 187, 1958, pp. 1-52.
3. Rib, Harold T. Remote Sensing Applications to Highway Engineering. Public Roads, Vol. 35, No. 2, 1968.
4. Welch, R. Film Transparencies vs. Paper Prints. Photogrammetric Engineering, Vol. 34, No. 5, 1968.
5. Stallard, Alvis H. An Evaluation of Color Aerial Photography for Engineering Purposes. State Highway Commission of Kansas, Spec. Rept. 1, 1965.
6. Stoeckeler, E. G. Use of Color Aerial Photography for Pavement Evaluation Studies in Maine. Mats. and Res. Tech. Paper 68-6R, Nov. 1968.

Appendix

REFLECTION CRACK STUDY

Four sections of a highway between Augusta and Bangor, totaling approximately 17 linear miles, were repaved during the 1967 and 1968 construction season. A number of different overlay designs and construction procedures were used at each of 4 separate localities included in the repavement program.

Local conditions at the 4 sections varied considerably with respect to terrain, traffic count, original embankment design, construction practices, age of pavement, source of materials, and a host of other factors that could contribute to the deterioration of the pavement.

Because of many variations in local conditions along the 17 miles of roadway, it is understandable that the amount and type of cracking in the old pavement varied considerably at sections having different overlay designs. To determine the effectiveness of the various designs, it was necessary to obtain a record of the crack pattern of the old pavement prior to placement of the overlay. The most feasible and economical method of obtaining this record was by means of aerial photography.

In the Bangor area most cracks were filled with sealant a few weeks prior to the date the aerial photography was flown. However, at the other 3 locations only a portion of the cracks were freshly sealed. In some sections the smaller cracks, especially in the passing lane, had never been sealed. Pavement conditions in the Bangor area were ideal for photography because of the high contrast between the fresh black sealant and the light-toned weathered pavement. At the other areas the sealant, exposed to 1 or 2 years of oxidation, wear, and sand and salt applications, was just a little darker toned than the adjacent pavement surface. Under these pavement conditions the sealant photo image is less distinct and more difficult for an untrained observer to identify. Because of the adverse pavement photography conditions at portions of the project, it was necessary to secure large-scale photography in order to detect microfeatures such as narrow unsealed cracks. The coverage was taken with panchromatic film at an average scale of 1 in. = 150 ft. Based on several rapid field checks, in sections of the highway at Waterville and Augusta where small unsealed cracks occurred, it is estimated that about one-fifth of the cracks in this condition could not be detected on the coverage taken for this study.

A constant surveillance of the overlay sections was initiated at the end of the 1967 construction season. Very few cracks reappeared prior to the first week in January 1968. After a 2-week period of subzero temperatures, cracks developed at a rapid rate especially in a design section in the Bangor area having a hot bituminous binder course only $1\frac{3}{4}$ in. thick.

By comparing the location, configuration, and dimensions of the new cracks with the pattern visible on the photography taken prior to repavement, it was obvious that the recently developed ruptures were directly associated with cracks existing in the underlying weathered pavement. By making a number of measurements from reference points readily identifiable on the photos to points along newly developed cracks, it was

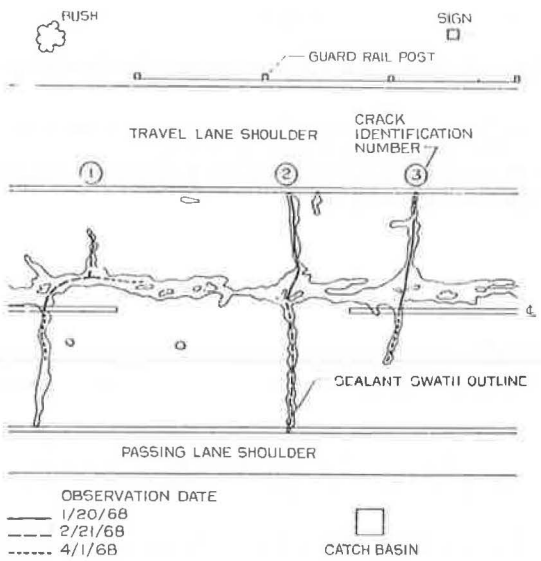

Figure 15. Sketch showing crack pattern in an old weathered pavement and the extent of reflection cracks observed on 3 different dates. The sketch was prepared by tracing detail from a microfilm viewer projection of a panchromatic print.

REFLECTION CRACK RECORD

LOCATION Project 801-3(2) Sta. 102+19 to 210+00

Date of Observation — Pavement Condition — Overlay Design A-2

1/20/68 Dry — Observer Smith

2/21/68 Wet — Lane NB

4/1/68 Wet — Photo 21-9

Crack No.	Travel Lane				Passing Lane			
	Joint	OWP	1/4PT IWP	E IWP	1/4PT IWP	OWP	Joint
1							
2							
3							

REMARKS Crack No. 1 - 13 foot lateral along Travel Wheel Path on 4/1/68

Figure 16. Reflection crack record. Cracks are grouped into 3-ft-length classes. For convenience the 24-ft roadway section is subdivided by 8 equidistant reference points. The 3 cracks schematically shown in this example are presented pictorially in Figure 15.

TABLE 1

RELATIONSHIP OF TRANSVERSE REFLECTION CRACKING BY OVERLAY DESIGN, LANE, AND DATE

Binder Course (in.)	Cover or Tack Coat	Total Length Transverse Reflection Cracks (ft/mi)					
		Jan. 19, 1968		Feb. 21, 1968		April 15, 1968	
		Trav.	Pass.	Trav.	Pass.	Trav.	Pass.
1¾	Emul. Asphalt	812	942	1,179	1,254	1,700	1,528
1¾	Chips	138	249	351	774	418	925
2¼	Emul. Asphalt	484	492	784	886	1,118	1,068
2¼	Chips	116	247	270	603	350	701
2½	Emul. Asphalt	199	303	438	531	505	662
2½	Chips	96	112	186	318	231	381

Note: Hot bituminous binder course placed October 1967; no wearing course.

TABLE 2

RELATIONSHIP OF THE AMOUNT OF CRACKS IN THE OLD PAVEMENT WITH THE AMOUNT OF REFLECTION CRACKS BY DESIGN, LANE, AND DATE

Lane	Total Length Cracks per 1,000 Feet				
	Old Pavement July 1, 1967 (ft)	Reflection Cracks in Overlay			
		Jan. 20, 1968		Feb. 21, 1968	
		Feet	Percent	Feet	Percent
Northbound Lane[a]					
Travel	493	99	20.1	141	28.6
Passing	309	180	58.3	252	81.6
Southbound Lane[b]					
Travel	1,434	0	0	24	1.7
Passing	435	24	5.5	202	46.4

[a] 1¾ in. hot bituminous mix, emulsified asphalt tack coat.

[b] 1¾ in. hot bituminous mix, stone chip cover coat.

determined that they were located within a few inches of the old cracks. Reference points such as guardrail posts, catch basins, signs, ornamental bushes, and other objects close to a new crack were used to establish its exact location on the photo. A large-scale sketch illustrating plotting procedures is shown in Figure 15. Each newly developed crack was assigned an identification number, which was annotated on the photo. In addition, a method was devised to record the length of each crack on each of the 3 observation dates. A sample of the form is shown in Figure 16.

The lengths of the reflection cracks were not actually measured in the field because of the time involved and also because of safety requirements. By using construction joints, wheelpaths, and quarter points as references, an observer can estimate crack lengths to the nearest foot. It required 4 to 5 days to record cracks developed in the 17 linear miles of a 4-lane highway included in the 2-year reconstruction program. These data will be the basis for the determination of the rate and amount of reflection crack development for each overlay design. Table 1 gives an example of the relationship of amount of reflection cracking by design, lane, and date. Table 2 gives the percentage of reflection cracks developed in a 1,000-ft portion of a partially completed overlay design section in the Bangor area. These samples are only two of many comparisons that can be made with the existing data.

Multispectral Data Interpretation for Engineering Soils Mapping

MARC G. TANGUAY, Ecole Polytechnic, Montreal; and
ROBERT D. MILES, Purdue University

The application of multispectral remote sensing to engineering soils mapping was investigated along a 60-mile test flight in Indiana. The multispectral data included 15-channel imagery and 4 types of aerial photographs (black and white, infrared black and white, color, and color infrared). The study showed the color film to be the best for mapping soils and soil conditions. A cost analysis showed the color film to be the most economical because the interpretation time was less and the results more reliable. The multispectral data were analyzed by visual methods, by densitometry, and by use of a computer. The computer analysis proved to be efficient and practical. The spectral response of some engineering soils are discussed, and digital computer maps are shown as examples of automatic classification for the multispectral data. A special feature in the computer analysis assists in selecting the optimum combinations of channels. Options in the computer programs permit development of separate map displays showing various soils and soil conditions of interest to the engineer. The spectral response concept is valid for soils mapping, but adequate ground control is necessary to assist in the automatic analysis. Vegetative cover is a limiting factor.

•THE EVALUATION of remote sensing methods and types of aerial films as a source of data for civil engineering purposes has been investigated only in the last few years. This paper describes the results of research conducted on the evaluation of these techniques in order to produce engineering soils maps for site selection studies. The research project was cosponsored by the U.S. Department of Transportation, Federal Highway Administration, Bureau of Public Roads, and the Indiana State Highway Commission. The work was executed at the Airphoto Interpretation and Photogrammetry Laboratory of the School of Civil Engineering, Purdue University (14). The automatic analysis of multispectral data on computer was done at the Laboratory for Applications of Remote Sensing (LARS), Purdue University. This research is an extension of the work initiated in 1965 by Harold T. Rib and R. D. Miles (5, 6).

DATA COLLECTION

A test site was selected early in 1967 in south central Indiana along state Route 37. The area was selected on the basis of variability of earth materials and land forms. Figure 1 shows the route selected. It is a 70-mile section of a proposed highway from Indianapolis to Bedford, Indiana.

Intermediate scale aerial coverage with black and white Kodak Plus-X panchromatic film was obtained April 11, 1967, by personnel of the Indiana State Highway Commission (ISHC) plane. This produced 1:12,000 scale photography of the entire route for planning data collection procedures and the multichannel flights.

Paper sponsored by Committee on Photogrammetry and Aerial Surveys and presented at the 49th Annual Meeting.

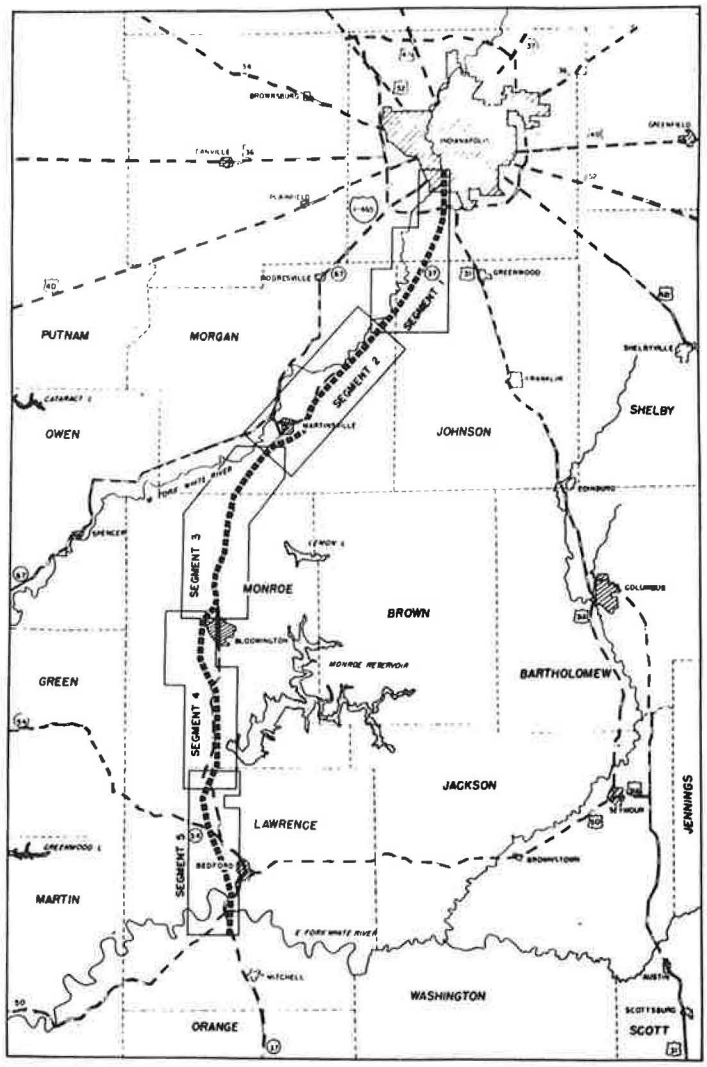

Figure 1. Mosaic areas along study route.

The multispectral imagery was obtained on contract by personnel of Willow Run Laboratories, University of Michigan. Permission was obtained from the Office of Naval Research and the Army Electronics Command to use the Project Michigan M-5 scanner. The multichannel data collection flight took place on April 28, 1967. The aircraft, operated by personnel of the Willow Run Laboratories, flew over the designated area collecting information in 15 different bands of the electromagnetic spectrum as given in Table 1.

Personnel of the Indiana State Highway Commission obtained the aerial photography for this project. They used a 6-in. focal length Wild RC-8 aerial camera mounted in a single engine aircraft. Table 2 gives the series of flights, films, filters, and other conditions pertinent to the photography and imagery.

Prior to aerial flights, several days were spent in the field collecting data concerning (a) moisture conditions of soils, (b) direct temperature readings on soils, and (c) apparent temperature of soils and rocks by means of an infrared radiometer. The

maximum information obtained in one day was on April 28, 1967, when the scanner was used to collect the multispectral imagery at 2 different altitudes. Also, ISHC personnel obtained 3 rolls of Ektachrome MS aerographic film.

A regional engineering soil map was prepared at a scale of 1:20,000 using USDA aerial photographs. This mosaic provided information on regional distribution of land forms and parent materials. After receiving the prints, films, and imagery, mosaics were assembled and engineering soil maps were prepared. Nineteen different photo-maps were prepared by interpretation of black and white, color, or color infrared films and prints.

TABLE 1

SPECTRAL BANDS FOR IMAGERY OF INDIANA PROJECT

Spectrum	Band Number	Band Width (microns)
Ultraviolet	UV	0.32-0.40
Visible (violet)	1	0.40-0.44
Visible (blue)	2	0.44-0.46
Visible	3	0.46-0.48
Visible (blue-green)	4	0.48-0.50
Visible	5	0.50-0.52
Visible (green)	6	0.52-0.55
Visible	7	0.55-0.58
Visible (yellow)	8	0.58-0.62
Visible (red)	9	0.62-0.66
Visible (red)	10	0.66-0.72
Near infrared[a]	11	0.72-0.80
Near infrared	12	0.80-1.00
Middle infrared	IR4	4.50-5.50
Far infrared	IR8	8.00-13.5

[a]The near infrared up to approximately 1.5 microns is also called reflective infrared.

ENGINEERING SOILS MAPS FROM AERIAL PHOTOGRAPHS

This investigation involved the evaluation of the incremental information obtained by use of different aerial photos and sensor data. The first set of maps was produced from the 1:20,000 scale aerial photographs by standard photo-interpretation techniques and show land form-parent material distribution. The maps portray an area about 3 to 5 miles wide by 70 miles long and were reproduced as photo-maps as shown in Figure 2. These maps show land forms, and profiles, test holes, the location of special large scale maps (example: map 2.2.2), and the areas studied by the use of the LARS computer approach (example: area 5).

The tentative route is indicated by a black and white, narrow dashed strip. The special maps are indicated by white brackets, the computer-interpreted areas by

TABLE 2

PHOTOGRAPHY AND IMAGERY DATA SHEET

Date and Instruments	Alt. (ft)	Time Start	Time End	Speed	F-Stop	Mean Terrain (ft)	Approx. Scale	Film Types
April 11, 1967 RC-8 (6 in.)	6,700	—	—	—	—	700	1:12,000	Plus-X pan (1 roll)[d]
April 28, 1967 Scanner[a]	3,200	10:55[b]	11:38[b]	—	Cone	700	1:28,800	Multispectral
April 28, 1967 Scanner[a]	1,600	11:48[c]	12:35[c]	—	Cone	700	1:14,400	Multispectral
April 28, 1967 RC-8 (6 in.)	2,400	9:55	12:18	200	6.8	700	1:6,000	No. SO-151 (3 rolls) No filter
May 18, 1967 RC-8 (6 in.)	2,400	9:50	12:35	200	8.0	700	1:6,000	Plus-X (1 roll) No. 8442 (blank) No filter
May 19, 1967 RC-8 (6 in.)	2,400	9:40	12:00	200	6.8	700	1:6,000	No. 8442 (3 rolls) No filter
May 22, 1967 RC-8 (6 in.)	2,400	12:40	13:06	200	6.8	700	1:6,000	No. 8443 (2 rolls)[d] Antivignetting
May 24, 1967 RC-8 (6 in.)	2,400 2,400	10:05 11:35	10:32 13:42	— —	8.0 8.0	700	1:6,000	No. 8443 (2 rolls)[d] Infrared BW (4 rolls)
May 25, 1967 RC-8 (6 in.)	2,400	11:00	11:30	—	8.0	700	1:6,000	Plus-X (1 roll)[d] (rerun)

[a]Multispectral scanner M-5, Project Michigan, Willow Run Laboratories, University of Michigan.
[b]Going north.
[c]Going south.
[d]Exposed with an antivignetting filter.

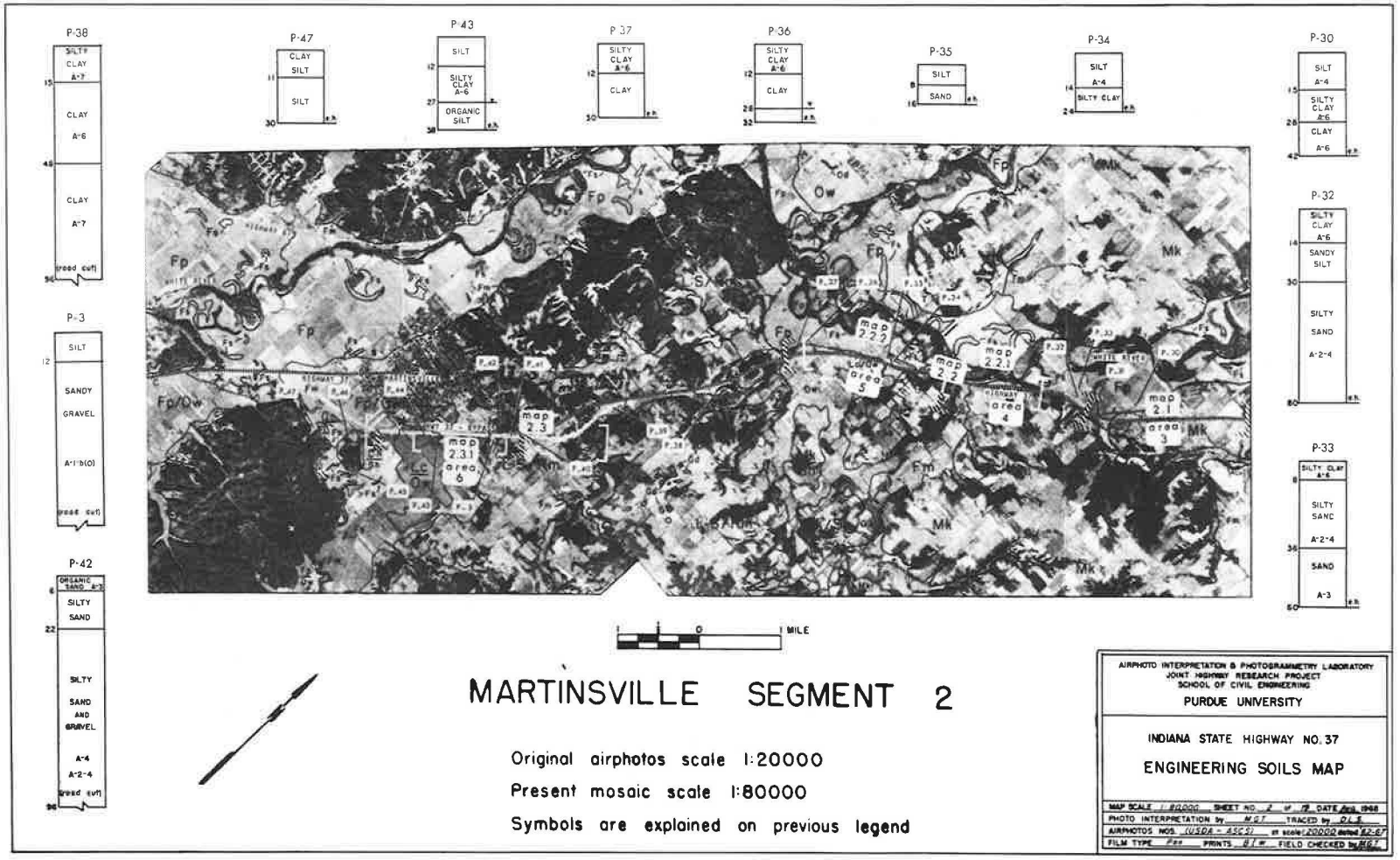

Figure 2. Example of regional engineering soils map.

hatched brackets, and the test holes and soil profiles by white labels designated P followed by a number. The land forms are marked by continuous black lines and labeled with black symbols. The range and township lines, section corners, and section numbers are indicated in white numbers and letters.

The symbols used on all the photo-maps are shown in Figure 3 (1, 2). The symbols are divided into 5 different parts to indicate land form, soil textural class, drainage class, depth to bedrock class, and slope class. Examples are given in the legend shown in Figure 3.

The land form-parent material maps were developed to provide a regional concept of physiography and materials distribution. These maps assist in the preparation of

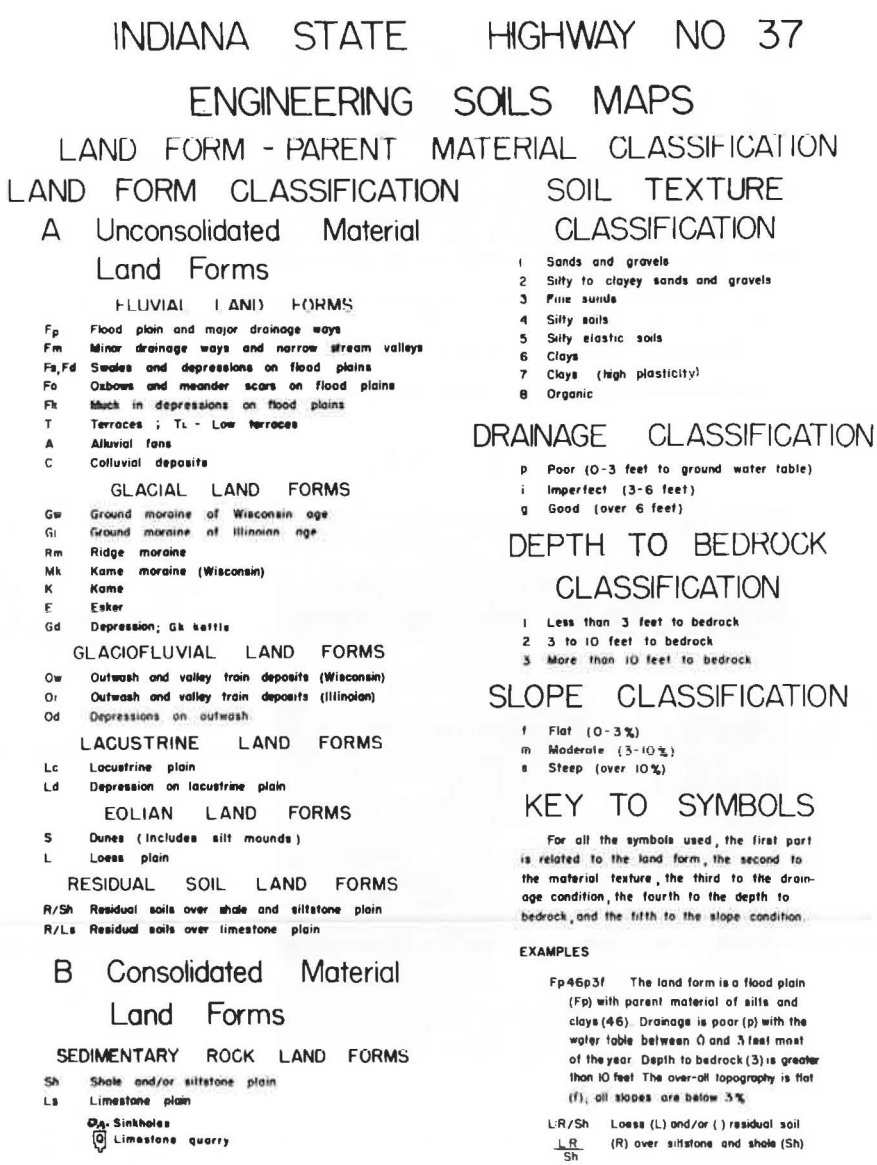

Figure 3. Legend for photo-maps.

detailed, large-scale engineering soil maps. The regional map is required unless county engineering soil maps are available.

A series of detailed engineering soils maps were prepared on various photo-mosaics to evaluate film type. The first maps were prepared from the black and white prints, the second from the color prints, and the third from the color infrared transparencies. Two scales were used on the final engineering soils photo-maps as shown in Figures 4 and 5. The same type of map was produced from each film type.

When comparing the maps produced from black and white and color aerial photographs, only minor differences were found. These differences primarily concerned the location of soil boundaries. This is explained by the fact that engineering soils mapping has been developed on the basis of land form-parent material relationships, and not on intrinsic colors of the soils. However, color is an asset for mapping engineering soils in that soil boundaries are located with greater precision and the interpretation is more accurate. The color assisted in locating and identifying muck basins, depressional conditions with various degrees of moisture, and minor land forms. Sinkholes in limestone terrain were detected more readily on color, and land forms under the leafless trees were more easily identified. With color, a greater number of soil features such as silt mounds and subsoil revealed by plowing were located and explained. Soils in several instances were readily distinguished on the basis of color. The red residual clay developed from limestone and the light yellow-grey silt in minor drainageways were identified by correlation of natural color with the photograph.

The color infrared was compared to black and white and color films. The main advantages of this film were concerned with accurate location of vegetation and bare soil (or bare rock) areas. The color infrared indicated the relative moisture conditions of the soils better than the natural color. The film was more difficult to interpret than natural color, partly because of a lack of experience in viewing objects recorded in this region of the spectrum.

The filter used with the color infrared film was a Wratten 12. The Wratten 12 filter, as compared with the Wratten 15, caused the color to shift toward the blue, the vegetation to purple-red instead of red, and the bare soil areas to hues of blue instead of green. The age of the film may also have affected the color infrared rendition. Aging is a critical aspect of color infrared and may be a factor in color as well as black and white. The effect of not aging the film is more obvious on the color infrared.

It was found that color infrared transparencies yield more information than color film or prints on soil surface drainage conditions, wet zones, and the like. It was found that on the bare soil areas the blue color darkened as the moisture increased. This was independent of soil type and color, except that light-colored soils had a tendency to be of a lighter blue.

Muck pockets and highly organic soils were not as easily detected on color infrared as compared to color. Highly plastic red clays in the limestone plains were rendered in different hues of green and different color values, depending on their reddishness and their moisture content. When considering color balance shift, these clays should show hues of greenish yellow to yellow for the light brown-red soils and the deep red clay soils respectively. Color and color infrared were of equal value in the identification of red clays developed as residual soil.

In this project a large number of photo-mosaics were prepared (28 separate 2- by 4-ft panels), and the time required for interpretation was carefully recorded. This allowed a measure of interpretation time differences in terms of film types and scales. The results indicated less time per unit area on color photos (at a given scale) than for any other type. They showed also that less time is required for the smaller scale photography per unit area, but much less detail was obtained. The comparative photo-interpretation times are given in Table 3. The gain in interpretation time for natural color varied between 23 and 40 percent when compared to black and white photos.

This economy of time is also reflected in the cost study that was conducted during this project. All costs and time of execution for each phase of the work were carefully recorded. The personnel of the Indiana State Highway Commission provided information on the costs for flying, processing, and printing photographic materials and costs of reduction and printing of the photo-maps. Costs for interpretation times, field

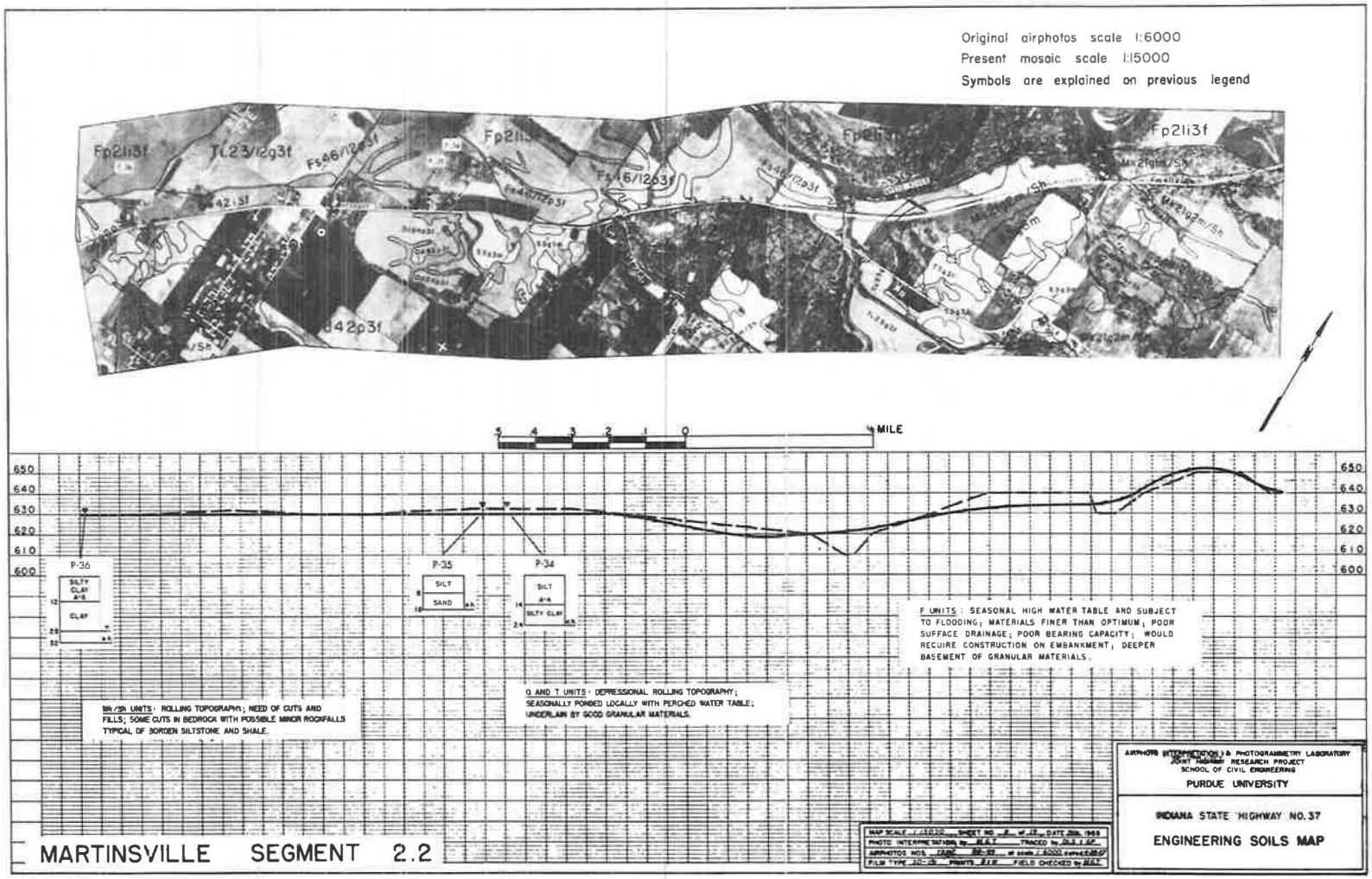

Figure 4. Example of engineering soils map.

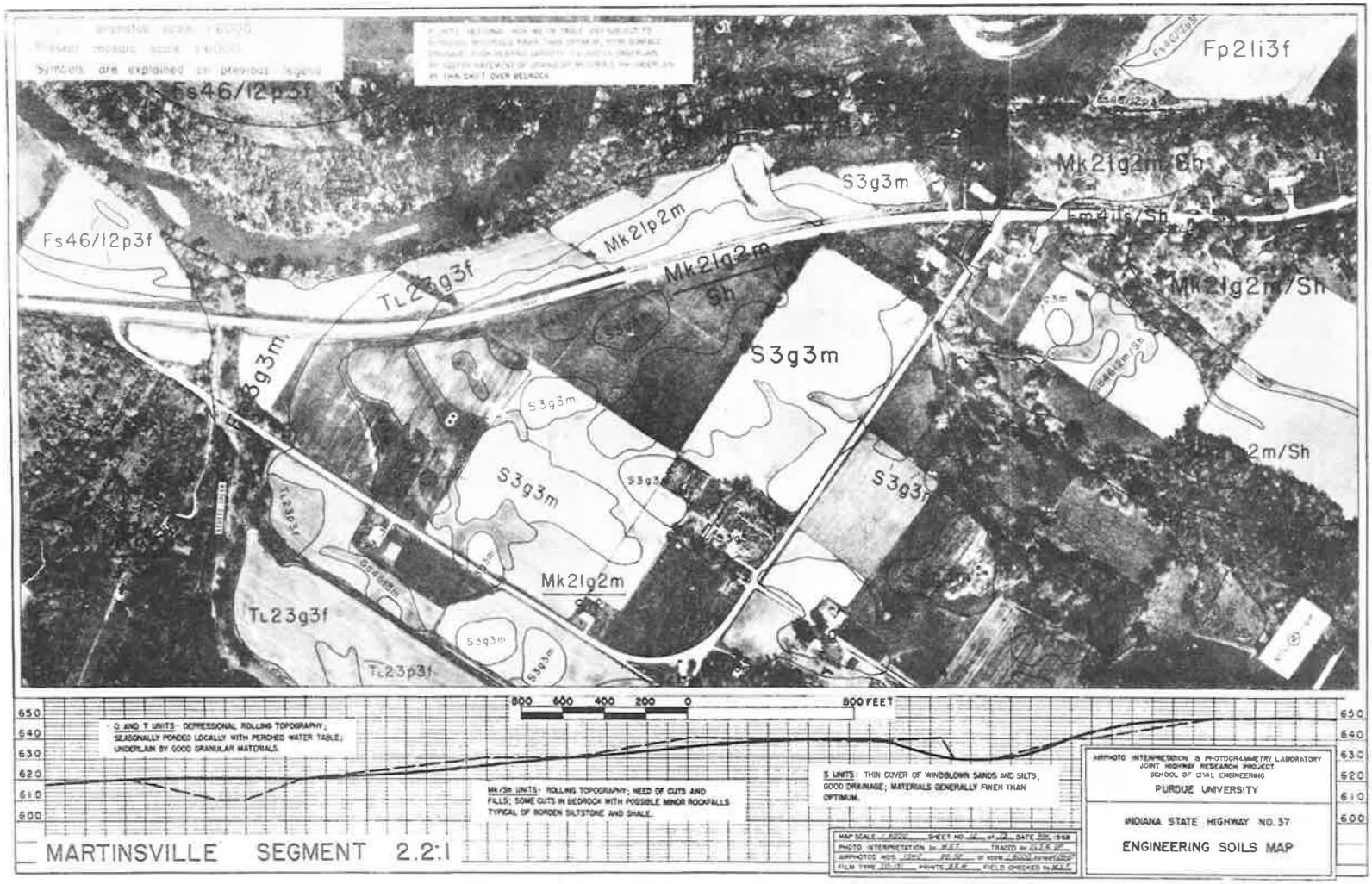

Figure 5. Example of large-scale engineering soils map.

TABLE 3

COMPARATIVE PHOTO-INTERPRETATION TIMES

Photo-Map No.	Scale (sq mi)	Area (sq mi)	P.I. Total Time (hours)	Normalized P.I. Time (hours/sq mi)
1 to 5	1:20,000	350.00	120.0	0.34
(9 photo-maps)	1:12,000	134.00	44.0	0.33
1.1	1:4,800	2.48	3.0	1.21
2.1	1:4,800	2.46	2.25	0.915
2.2	1:4,800	2.32	6.5	2.80
2.3	1:4,800	2.46	4.0	1.62
3.1	1:4,800	2.02	5.0	2.48
4.1	1:4,800	2.17	3.5	1.61
2.2.1	1:4,800	0.85	4.0	4.71
2.2.2	1:4,800	0.825	4.5	5.45
2.3.1	1:4,800	0.85	4.0	4.71
2.3(C)	1:4,800	2.02	2.5	1.24 (23.4 percent)
3.1(C)	1:4,800	1.70	2.5	1.47 (40.8 percent)
4.1(C)	1:4,800	1.80	2.0	1.11 (31.0 percent)
2.2.1(C)	1:4,800	0.72	2.0	2.78 (41.0 percent)
2.2.2(C)	1:4,800	0.85	2.75	3.24 (40.5 percent)

checking, sampling, and drafting of maps were noted. Costs used for soil testing were provided by personnel of the ISHC Materials and Testing Division.

The cost analysis is given in Table 4. These costs were based on the 70-mile route under study and the mapping of all the sections of this route as indicated. It is based on costs for film purchased in the spring of 1967. The other items are based on prices during the period of 1967 to 1969. The black and white photography (BW) at a scale of 1:20,000 was for a corridor 5 miles in width and 70 miles long. All other photography was for a single flight line.

The item "Prints" indicated in parentheses is the additional cost of color prints from transparencies. This shows that the color transparencies and color infrared transparencies if prints are included are more expensive than the others. The cost of field checking and sampling was approximately 30 percent less when using color photography. This was based on an evaluation of the actual borings made to assist in the interpretation of the black and white film and the estimated number that could be eliminated if color photographs were used. Figures in this table should not be quoted out of

TABLE 4

COMPARATIVE COST STUDY OF ENGINEERING SOIL MAPS OBTAINED FROM AERIAL SURVEYS

Item	BW Prints 1:20,000	BW Prints 1:12,000	BW Prints 1:4,800	Color Prints 1:4,800	Color Transparencies 1:4,800	Color Infrared Transparencies 1:4,800
1. Flying	N.A.	0.70	1.26	1.26	1.65	1.65
2. Films	N.A.	0.81	1.92	11.34	8.24	9.43
3. Chemicals	N.A.	0.02	0.04	2.72	1.03	1.03
4. Prints	3.76[a]	0.24[b]	0.73[c]	8.36[c]	None[c] 18.00[d]	None[c] 18.00[d]
5. Processing-printing	N.A.	0.33	0.98	3.93	2.29	2.29
6. Mosaics (uncontrolled)	1.57	1.89	3.29	3.29	3.29	3.29
7. Photo interpretation	2.14	2.05	11.70	8.40	8.40	8.40
8. Field checking and sampling	12.25	12.25	12.25	8.75	8.75	8.75
9. Soil samples testing	41.80	41.80	41.80	28.00	28.00	28.00
10. Photo-maps tracing	4.10	4.72	6.31	6.31	6.31	6.31
11. Reduction and printing	1.71	3.41	6.83	6.83	6.83	6.83
Total unit cost	67.33	68.22	87.19	89.19	74.79 92.79[d]	75.98 93.98[d]

[a]For a 5-mile wide corridor, 70 miles long.
[b]For a 9,000-ft wide strip, 70 miles long.
[c]For a 3,600-ft wide strip, 70 miles long.
[d]Additional cost when color prints are used in addition to the positive transparencies.

Note: Amounts in dollars per linear mile.

their context, because these costs did not include capital expenses, depreciation, taxes, and other related items. For example, the cost for processing-printing of the color prints is the cost of the processing of the color negative from which the prints were made. The cost for prints of the color prints is the cost of materials and labor as contracted by a commercial firm. The cost for BW 1:12,000 prints is only for materials; the cost for labor is included as a separate item.

Table 4 also gives a comparison in overall mapping costs using color or black and white at the same scale. It shows a very small increase in cost when using color prints prepared from color negative film. The reduction in interpretation time and amount of sampling when color is used tends to offset the higher cost of the color prints.

It was found that color is the best single source of information for engineering soil mapping when atmospheric conditions are good. The best combination of 2 films is color and color infrared. This combination enables the interpreter to determine the relative moisture conditions of the soils and the intrinsic color of the soils. The black and white infrared film was of little value for engineering soils mapping, with the filtering that was used.

The optimum scale was found to be 1:12,000 when the interpretation is not to be reported on standard engineering plans and profiles. If reported on plans and profiles, the scale should be at least 1:6,000, or as large as 1:2,400 depending on the scale used for the particular project.

Time of interpretation was found to increase rapidly with an increase of the photo scale. The use of color was found to decrease the time of interpretation from 20 to 40 percent, at a scale of 1:4,800.

ENGINEERING SOILS MAPS FROM MULTISPECTRAL DATA

The multispectral information on the study route was obtained in 2 single flight lines, one flown north to south at an altitude of 3,200 ft, the other flown south to north at an altitude of 1,600 ft. The imagery was obtained in 15 different bands of the electromagnetic spectrum as given in Table 1.

The purpose of this discussion is to present the results of 3 different approaches used to interpret the multispectral imagery. The 3 approaches are (a) interpretation by visual examination using conventional air-photo interpretation methods with the additional concept of a spectral signature of materials, (b) densitometric measurements to establish signatures of materials, if possible, and (c) the automatic method of multispectral data classification developed by the Laboratory for Applications of Remote Sensing at Purdue University. In each case the purpose was to determine the method most applicable for the production of soils maps useful to civil engineers in site selection studies.

Interpretation by Visual Inspection—The visual examination involved the following techniques: (a) examination of the original 70-mm negative film strips on a light table with and without magnification, and (b) examination and interpretation of contact prints and enlarged (2 diameter) prints made from the negatives.

It was determined that the maximum number of bands that could be handled and examined simultaneously in a convenient manner was six and ideally only four. Attempts were made to visually examine 12 bands simultaneously, but the information obtained on the first few bands was forgotten by the time the 10th, 11th, or 12th band was being examined.

This visual examination enabled the sorting of bands that were very closely related and thought to be essentially similar. The following 6 bands were determined to be most valuable for further examination:

Band	Microns
Thermal infrared	8.0-13.5
Reflective infrared	0.8-1.0
Red	0.62-0.66
Green	0.52-0.55
Blue	0.40-0.44
Ultraviolet	0.32-0.38

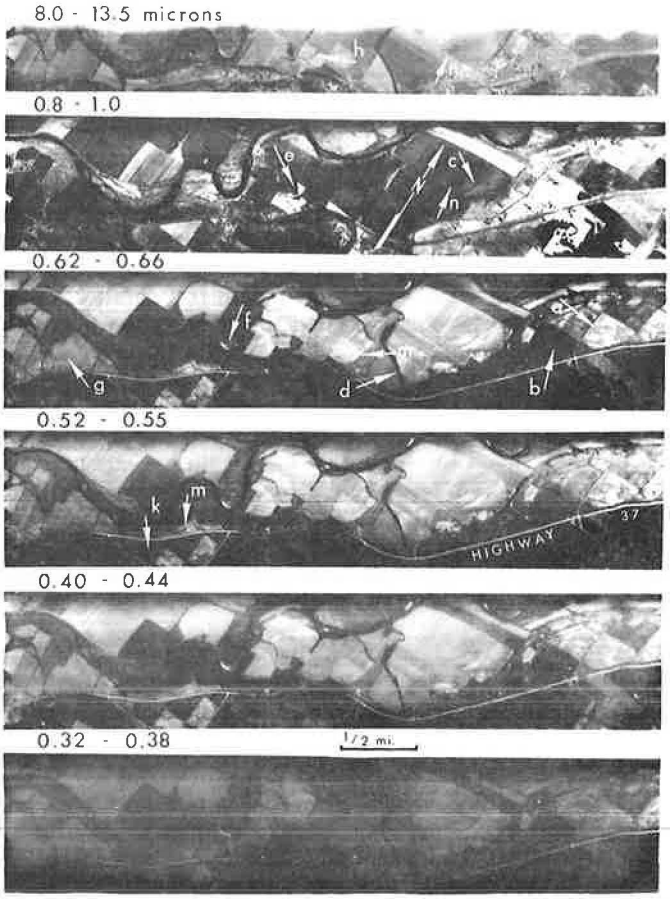

Figure 6. Example of multispectral imagery (area 4).

Figure 6 shows an example of the imagery produced in the wave-length regions. These are reproductions of the high-altitude imagery (3,200 ft) at a scale of 1:28,800 (1 in. = 2,400 ft). The low-altitude imagery (1,600 ft) at a scale of 1:14,400 (1 in. = 1,200 ft) was also examined but is not illustrated.

This figure shows the 6 bands considered to be most informative and shows 2 main land forms: a flood plain and a glacial moraine. Several bare soil conditions, drainage conditions, and various soil tones can be observed. A careful examination of each band revealed the following:

1. The thermal infrared band—The thermal infrared (8.0-13.5 μ) band was particularly useful in detecting surfaces that were relatively hot and emitting strongly and surfaces that were relatively cool. Water bodies and vegetation are considered relatively cool and show as dark areas or items on the imagery. Most soil areas were a similar intermediate grey tone except for a few special features normally due to drainage condition or moisture condition. Item h on Figure 6 is a soil drainage feature that could not be detected at all on the other bands nor on the photography, even on the color infrared. Tonal variations in this band will change over a 24-hour period in a drastic way as the surface temperature of materials changes and eventually may result in tonal inversions on imagery obtained at night. This may be of value in evaluating the causative factor.

2. The reflective infrared band—The reflective infrared (0.8-1.0 μ) imagery was very useful in determining areas of vegetation, e, in contrast to bare soil, c, areas. On this band, water bodies are very dark and uniform in tone, bare soils, c, and road systems are intermediate grey tones, wet soils are dark grey, and the crops and vegetation are very light grey to white. Coniferous trees are medium grey to dark.

3. The visible red band—The red (0.62-0.66 μ) imagery was found to be most useful for soil studies. Soil contrasts were shown better on this band than any other except the 0.52-0.55 μ band. In the red band, water bodies are dark, and soils are of various shades of grey from light, f, to medium dark, a. Bare dry soils are light, m on Figure 6. Wet soils are darker, c and n on Figure 6. Vegetation is dark. It is important to note that the tone inversions for soils and vegetation occur in the 0.8-1.0 and 0.62-0.66 micron bands. These 2 bands in combination yield extremely significant information as discussed in the section on automatic classification.

4. The visible green band—The visible green (0.52-0.55 μ) imagery is quite similar to the previous one but soils were not as distinct; however, the important soil features recorded on the 0.62-0.66 μ band were present. For instance the mottled tones of the ground moraine, a, and current scars, m on Figure 6, still show.

5. The visible blue band—The visible blue (0.40-0.44 μ) band is definitively not as interesting in terms of soil mapping. Much of the contrast between dark and wet soils and light colored soils is gone, c, m, and n on Figure 6. Because of a reduction of the overall contrast and the greater reflectance of pavement materials in this range, the road systems show much better. Water bodies are all of the same dark grey tone and cannot be distinguished from the vegetation.

6. The ultraviolet band—Only a few features show as bright tones on the 0.32-0.38μ band. Certain ultraviolet reflectors are recognized such as roofs, concrete pavements, some bituminous concrete pavements (because of the aggregates), limestone quarries, and river sand bars, f on Figure 6.

General Conclusions Based on the Visual Inspection—There is a change in reflectance as revealed by color of soil evidenced in bands 0.8-1.0, 0.62-0.66, and 0.52-0.55 μ and in a subdued manner in the 0.40-0.44 μ band. If an appreciable change in the drainage of soils or if a highly saturated zone occurs, the 8.0-13.5 μ band reveals a different temperature regime in comparison to the surrounding soils that are warmer.

The different bands treated separately are not as significant as when grouped, such as contrasts shown on the 0.8-1.0 μ and 0.62-0.66 μ bands. From the visual examination the following conclusions were drawn:

1. The best combination of imagery was obtained by grouping the 8.0-13.5 μ, the 0.8-1.0 μ, the 0.62-0.66 μ, and either the 0.40-0.44 μ or the 0.32-0.38 μ bands.
2. Soil contrasts were best detected on the 0.62-0.66 μ and 0.52-0.55 μ bands.
3. Water bodies showed best in the 8.0-13.5 μ and 0.8-1.0 μ bands. The 0.8-1.0 μ band appeared to be the best because of contrasts of the high reflectance of vegetation and the strong absorption of water in that band.
4. The imagery suffered from lack of resolution even for the low altitude imagery.
5. No information about the topography was obtainable either directly or indirectly from the imagery. Topography is an important element in engineering soils mapping by remote sensing techniques. It is obvious that multispectral imagery cannot replace aerial photography. It should be considered as a supplement to aerial photography.
6. Certain soil features and soil conditions are enhanced and more easily detected on the imagery than on aerial photography.

Recommendations for Visual Analysis of Multispectral Imagery—From the experience gained through this investigation, the following recommendations are made for future projects involving multispectral imagery:

1. The scale on the final imagery should be larger than 1:12,000, ideally between 1:10,000 and 1:6,000.
2. The geometric distortion or "sigmoid" distortion necessitates the use of the central two-thirds of the imagery for practical purposes. This is tolerable but attempts should be carried further to develop equipment for distortion-free restitution.

3. To use the far infrared 8.0-13.5 μ band to the maximum, the imagery should be obtained both during the daytime and at night in the hours before dawn. This would allow much better insight on infrared behavior and emissivity of materials.

Interpretation by Densitometric Measurements—In an attempt to study the validity of the spectral signature concept, a series of density measurements of the multispectral imagery was obtained. The approach involved the measuring of the transmission density on a calibrated transmission densitometer (1-mm aperture) for items of interest on the imagery. The density reading was normalized against a standard grey scale. Each of the imagery sections in each band and the respective calibration grey scale level were made comparable. Figure 7 shows the results for the 0.66-0.72 μ and 0.80-1.00 μ bands of a sample area (area 1-A). All the prime density levels that appear on these figures were normalized against a standard grey scale. Most of the changes in reflectance levels are due to changes in vegetative cover (i, n, t, v on Figure 7).

Fields d and g were dark, wet silty soil area as revealed by ground truth. The multispectral response for these fields as shown in Figure 8 are similar in terms of relative intensity within one band to the nearest 0.15 unit of normalized density. Figure 8 also shows the multispectral signatures for 2 contrasting terrain types. Fields h and t represent an area of dry, pale yellow-brown silt and an area of wet muck. These extremes were selected to emphasize the contrast in spectral signatures. The signature for the dry soil (Fig. 8) shows a very high response in most bands except the middle and far infrared, while the signature for the wet muck shows the overall low returns except for the far infrared, which is affected by water content. The relative

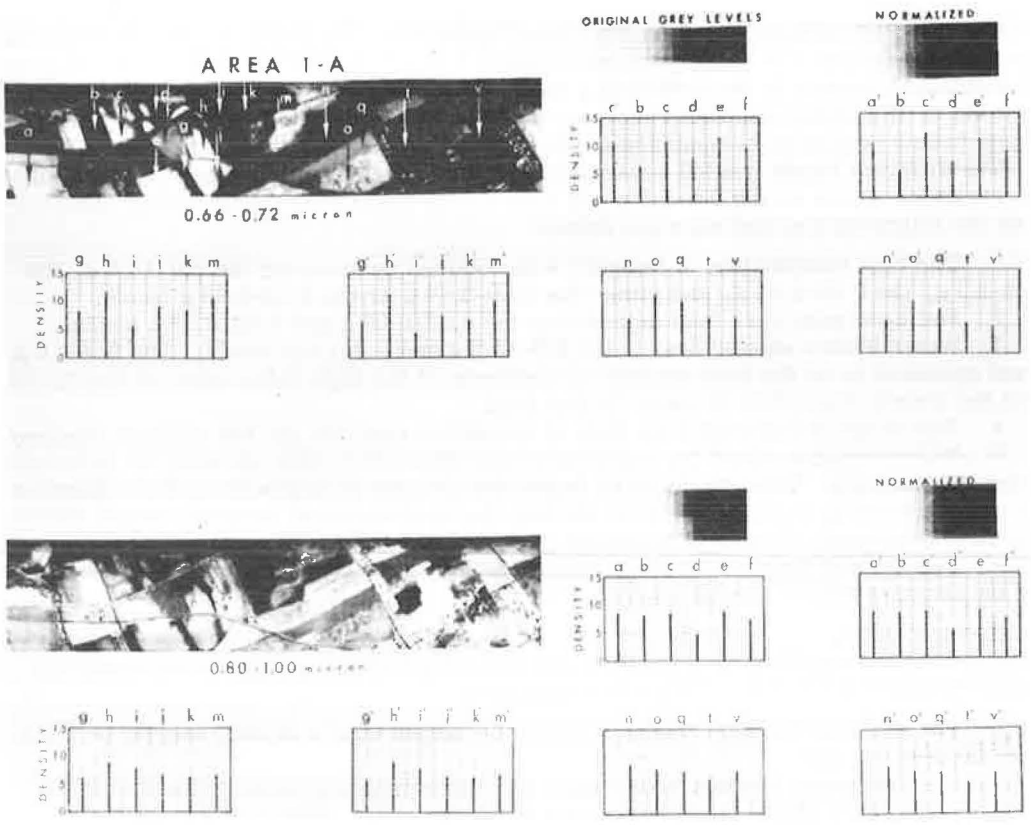

Figure 7. Normalized signatures by densitometric measurements.

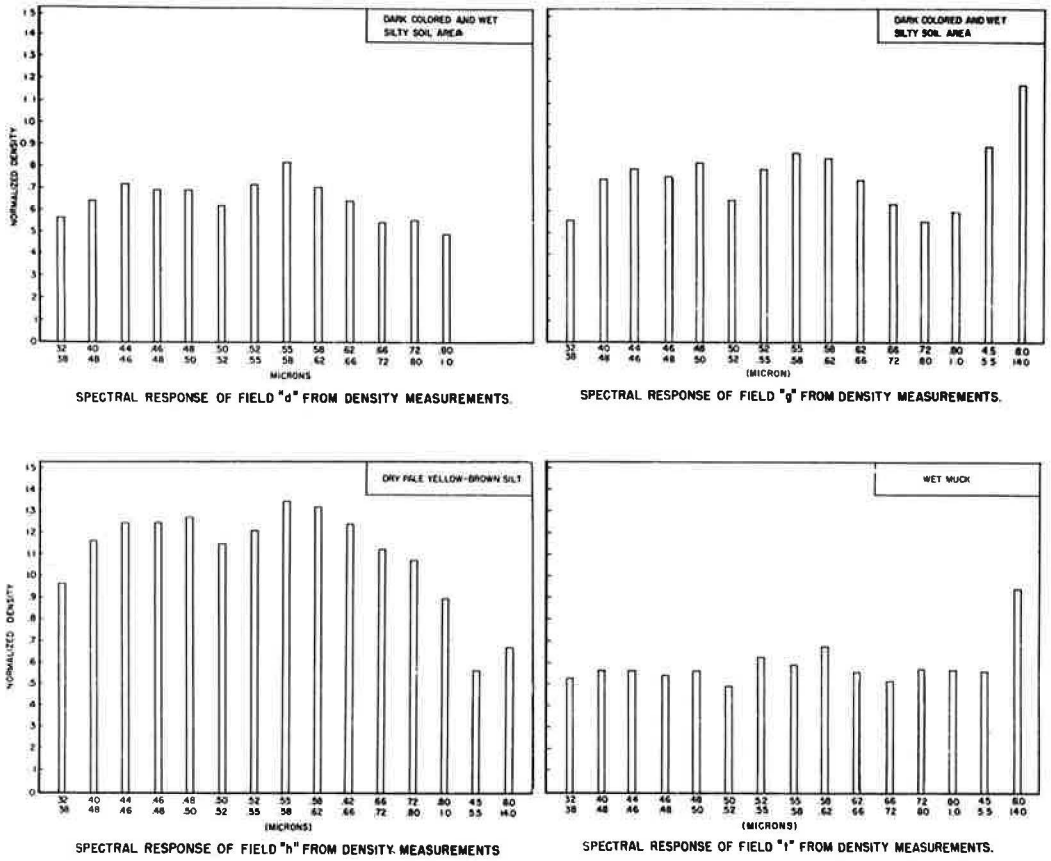

Figure 8. Spectral signatures from normalized density measurements.

responses shown in Figure 8 can be compared. They show that 3 different materials with different engineering characteristics in terms of texture and moisture content have different spectral signatures. These results and other measurements made during the research confirmed that the concept of multispectral signature of first surfaces is a valid premise in remote sensing. This correlates with Rib's research on this subject (5, 6).

This research showed the problems associated with the densitometric approach. It is slow and cumbersome. Long strips of imagery have to be searched. It is a tedious job to measure the densities point by point and to normalize and plot the results. If the data can be adapted for use in conjunction with a computer, there is really little point in using this approach and its use is not encouraged except for very special reasons.

AUTOMATIC CLASSIFICATION OF MULTISPECTRAL DATA BY COMPUTER

A system of computer programs has been developed over the past 3 years by the Laboratory for Applications of Remote Sensing for purposes of analyzing remote multispectral data for various agricultural applications. The studies include automatic crop identification and mapping, and studies of relative crop moisture and disease of crops as well as other related agricultural applications. This research effort is sponsored by the National Aeronautics and Space Administration in conjunction with the U.S. Department of Agriculture and Purdue University. LARS serves as a focal point for

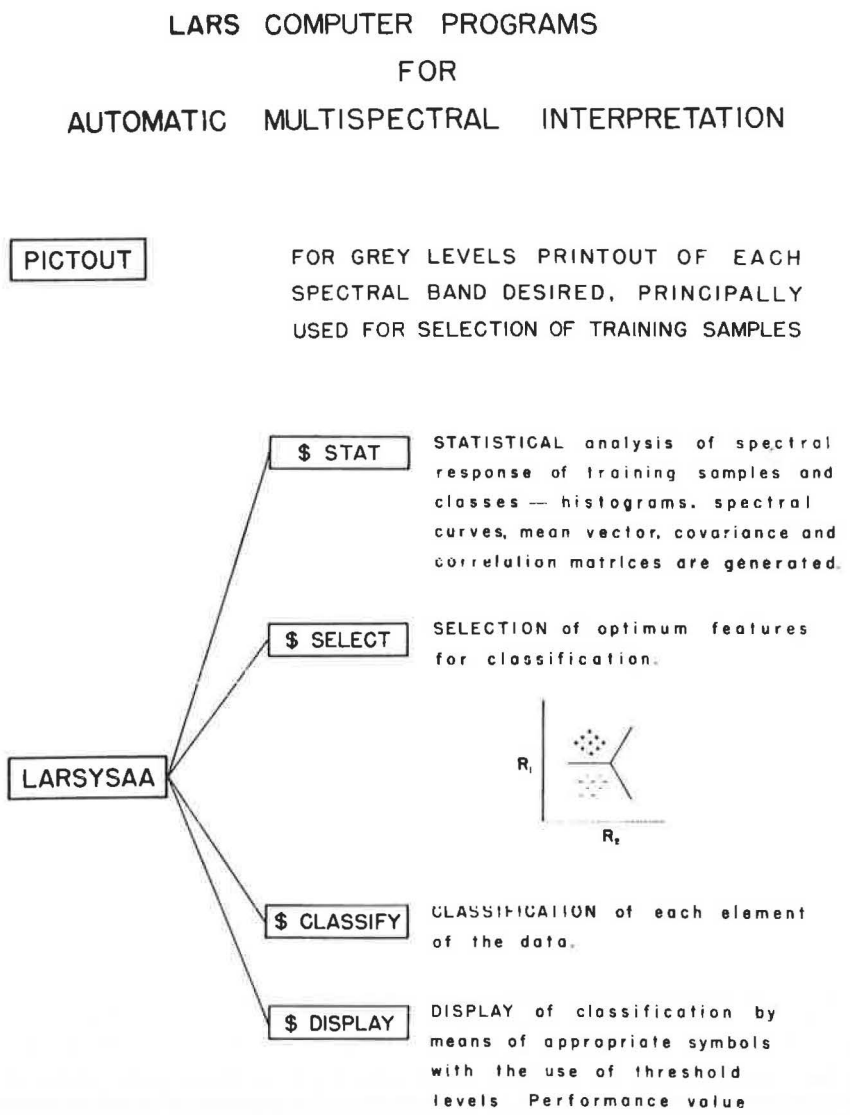

Figure 9. Computer programs for classification of scanner data.

research into the applications of modern remote sensing techniques for the benefit of national and state programs in natural resources.

Two LARS computer programs, LARSYSAH and LARSYSAA, were used to determine if the automatic classification procedures developed for agricultural purposes could be applied to engineering soils mapping. The facilities at LARS were made available to this Joint Highway Research Project to investigate the potential for engineering applications.

The LARS programs are shown in Figure 9. The approach involves a spectral pattern recognition technique in which training samples are used as a basis for classification. The computer is "trained" to recognize all areas having similar spectral signatures and to automatically classify these unknown areas into one of the categories designated by the researcher. The PICTOUT programs reproduce the multispectral data

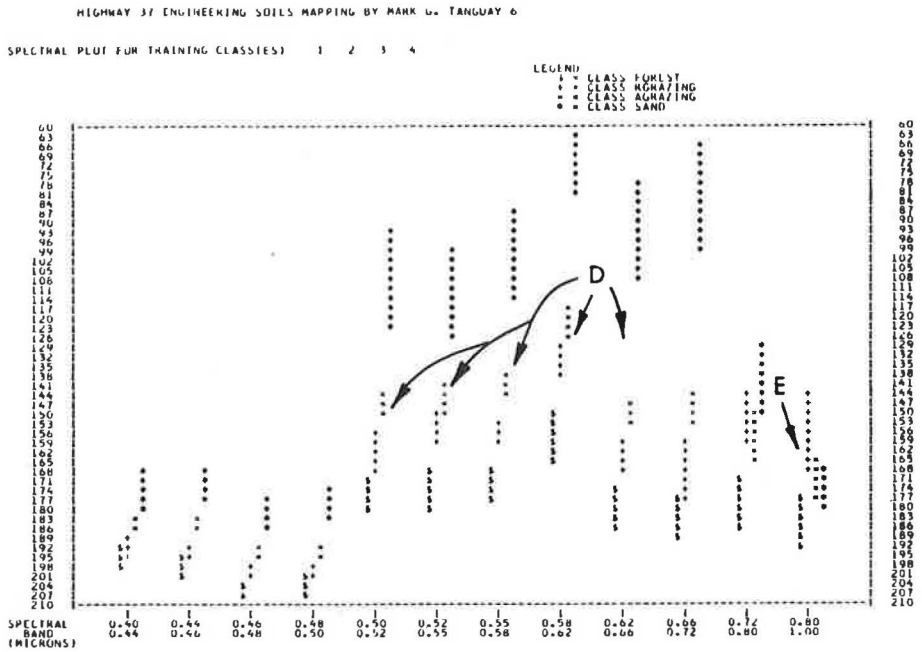

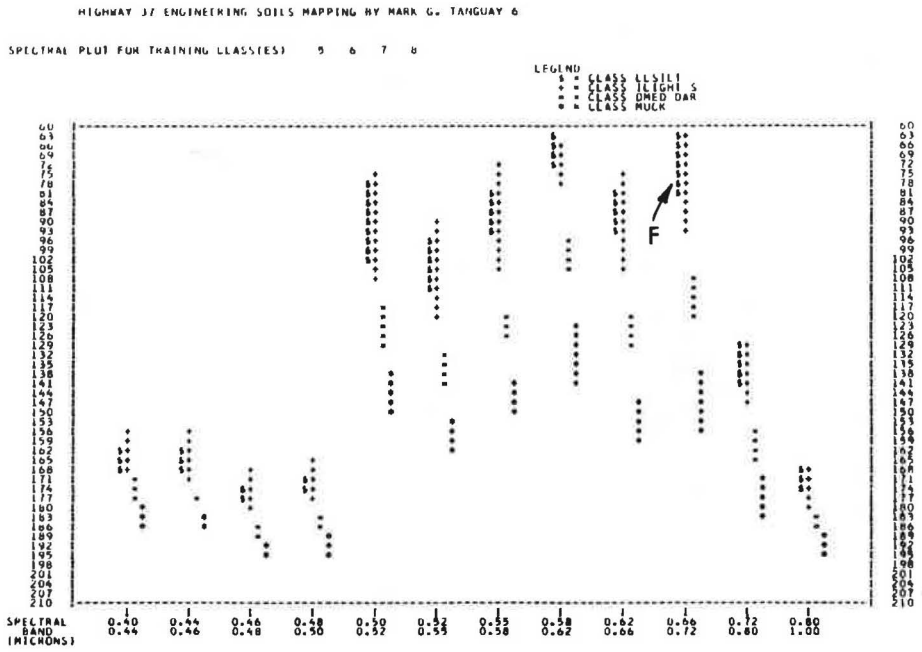

Figure 10. Spectral plots for 8 training classes.

as computer printouts similar to the imagery film strip. The imagery grey levels are represented by printer characters. This program also produces histograms of the grey levels for each band. One or several bands of the grey scale printouts can be used to select training samples.

Training samples should be conceived of as a set of spectral data, representative of a given ground object or ground feature and identified on the computer printouts by a system of coordinates. The material represented by a set of training samples is referred to as a "class."

The theory and development of LARSYSAA is discussed in the literature by Swain et al. (7), Landgrebe et al. (8), Landgrebe and Phillips (9), and others in LARS publications (10, 11, 12).

Once the training samples and their coordinates are selected, the statistics are obtained on the reflective characteristics of each class. The statistics include the mean vector of each class and the covariance correlation matrices. Histograms of each sample and/or class and their spectral response graphs can also be printed to assist the researcher in verifying the quality of each training sample and each class. To determine if the classes are easily separable, an option prints a series of combined spectral plots for the training classes. Figure 10 shows 8 classes. In the upper half, point D indicates that the 4 classes would be equally well distinguished in the 5 bands indicated by the arrows. In the 0.80-1.00 μ band, 3 classes would be similar (point E), and class AGRAZING is difficult to distinguish from class SAND.

In the lower half of Figure 10, point F indicates that 2 classes are difficult to distinguish in the 0.66-0.72 μ band. The class LLSILT (for very light-colored silt) has the same response as the class ILIGHTS (for intermediate light-colored silt). The other 2 classes have lower responses and are distinguishable. By visual inspection of the statistics, these 2 classes, LLSILT and ILIGHTS, obviously show similar response. The training samples for these 2 classes could be grouped under one class.

Examples of automatic multichannel data classification are shown in Figures 11 and 12. They indicate potential applications for engineering soil classification. Figure 11 shows 6 maps and a photo-mosaic for area 1-A. The 6 maps were produced by using the 12-channel (visible range) scanner data. They do not include the ultraviolet or the thermal infrared.

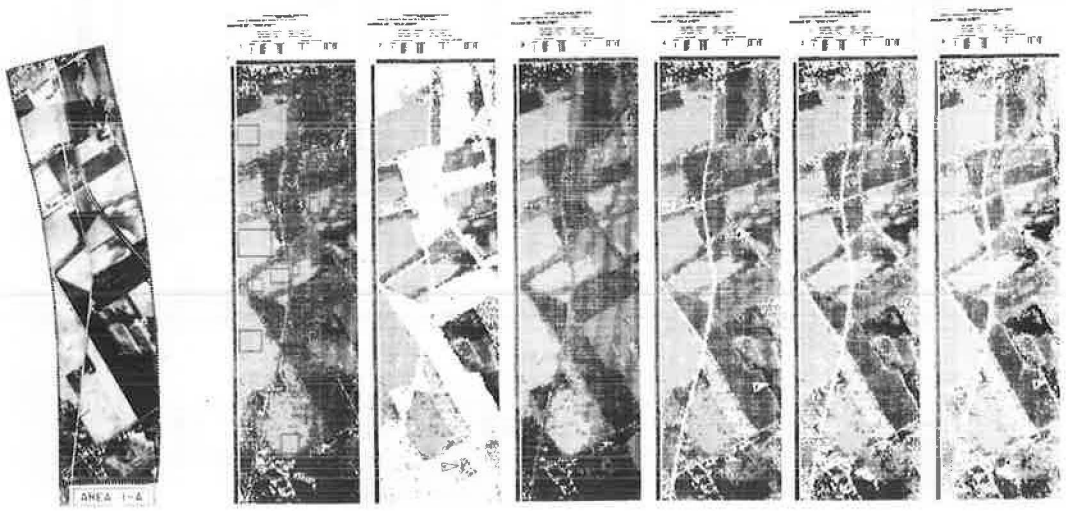

Figure 11. LARSYSAA printouts for general classification (map 1), 3 soils (map 2), soils, crops, forest, and roads (map 3), and examples of thresholding (maps 4, 5, and 6).

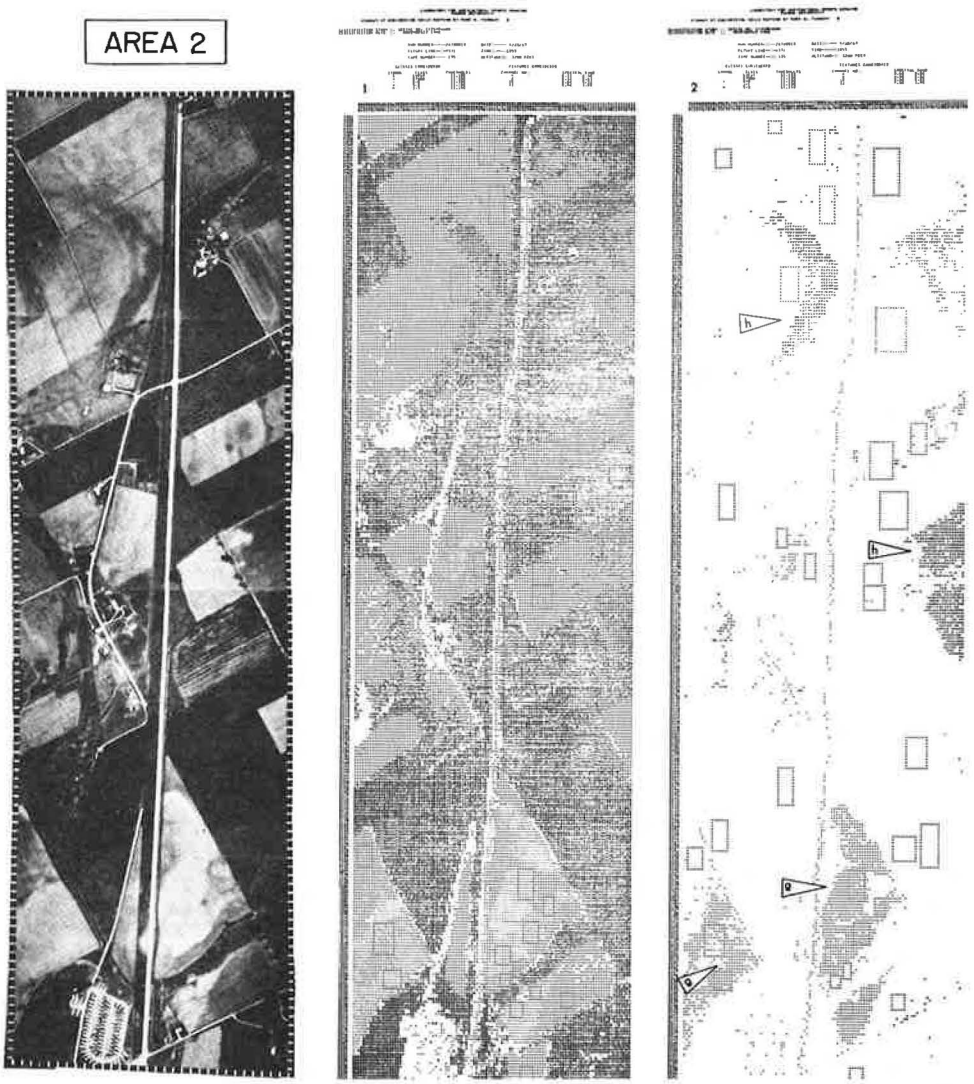

Figure 12. Printouts delineating 2 soil types.

Map 1 of Figure 11 shows a general classification of 7 classes for area 1-A: 3 different soil conditions as well as crops, forests, water, and roads. Map 2 shows the areal distribution of soils. It shows the location of light-toned soil, SOILD, the medium dark soil, SOILW, and wet dark-colored soil, SOILWW. Map 2 readily shows the distribution of the dark wet ground. The ground conditions of each soil class were verified in the field. This last soil class would require special treatment if an engineering facility were developed.

Map 3 of Figure 11 is a general interpretation of all the data. It illustrates a different character enhancement to locate the classes of materials. Maps 4, 5, and 6 show the effect of different threshold levels. The use of thresholds is made possible in the $ DISPLAY processor. A high threshold level is restrictive, and only the data points having very close spectral resemblance are displayed. A low threshold value is useful to display, in this case, all the light-toned soils of an area that may vary

slightly in spectral signature but are similar for engineering purposes. On the other hand, a high threshold value is useful in locating potentially troublesome areas as is the case for the SOILWW class, d and f. No training sample was taken for the area marked e, but this muck area was classified in the class for adverse soils, SOILWW. This shows the potential of this automatic classification based on spectral reflectance but also the need for ground control.

The maps of Figure 12 show other potential uses of this multichannel approach. The printout on the right side (map 2 for area 2) shows soils of engineering significance. The areas designated with the plus sign, g, indicate kame moraine. This portion of the moraine is underlain by sands and gravels as revealed by ground-checking. Special training samples were selected to show the location of these granular materials. The letter h points out a meander scar filled with highly organic soil as revealed by ground truth. This depressional soil condition would require special treatment or should be avoided. It is emphasized by overprinting by the letter M and by blanking out all other soils except the kame moraine.

In summary, the automatic computer classification as implemented by the LARS system and as tested in this research project is an important advance in automatic interpretation. This method of using training samples and a computer can produce, very rapidly, sets of soil maps useful to the engineer. The method can detect and classify reflectance of surfaces that indicate main soil classes, drainage conditions, muck area, and bare rock areas. The final interpretation and overall significance has to be assessed by an engineer competent in soils evaluation. The information will assist in planning boring programs.

CONCLUSIONS

This research project is concerned with the use of different aerial films and multispectral imagery as a source of data engineering soils mapping. Based on the results obtained for a 70-mile highway project in Indiana, conclusions are as follows:

1. In terms of developing annotated aerial photographs as detailed engineering soils maps, color photography is the best and most reliable source of information. Natural color photography enabled the mapping of a greater number of soil areas and soil conditions but did not allow full assessment of all soil conditions.
2. The combined use of color prints and color infrared transparencies is the best combination of 2 sources of remotely gathered information. This combination provided information on relative moisture conditions of soil areas.
3. Multispectral imagery obtained in 15 bands, UV to IR, provided some information on soils and soil conditions as a supplement to aerial photography.
4. If the multispectral data are to be processed by computer, the maximum number of bands should be obtained. The automatic classification of terrain features can be based on the optimum set or combination of bands.
5. If the imagery is to be analyzed by visual means, the minimum number of bands should be four and the maximum six. The 4 bands include the far infrared (8.0-13.5 μ), the reflective infrared (0.8-1.0 μ), the red (0.60-0.66 μ), and the green (0.52-0.55 μ). The 6 bands should include the 4 bands just named plus the blue (0.40-0.44 μ) and the ultraviolet (0.32-0.38 μ). The number of bands is restricted because of the inherent limitation of the human mind to analyze a very large number of images.
6. The best method of examination and interpretation of multispectral imagery is accomplished by automatic classification using a computer. The methods developed at the Laboratory for Application of Remote Sensing are applicable. The computer programs permitted (a) classification of the land surface in terms of vegetation, water, and various visible soil reflectance groups; and (b) delineation of unique soil conditions on a single map, emphasizing the distribution of adverse soil conditions.
7. The limitations of multispectral imagery for engineering soils mapping include vegetation masking the spectral data on soils and the lack of pertinent information about the topography.
8. Engineering soils plans and profiles, prepared from color aerial photographs, can be incorporated in soil surveys for highway projects. By this method boring sites

can be located to obtain more representative samples. The added expense of color is offset by the more reliable information obtained and the shorter period of time required for interpretation.

ACKNOWLEDGMENTS

This research project could not have been accomplished without the assistance and support of many organizations and persons. The study was sponsored by the Indiana State Highway Commission; the U.S. Department of Transportation, Federal Highway Administration, Bureau of Public Roads; and the Joint Highway Research Project, Engineering Experiment Station, Purdue University. Special thanks are due personnel of the various organizations who were especially helpful, including Aerial Photography Section, Indiana State Highway Commission; Infrared and Optical Sensor Laboratory, Institute of Science and Technology, University of Michigan; and Laboratory for Applications of Remote Sensing, Purdue University. Special thanks are due H. T. Rib of the Bureau of Public Roads, who monitored the project.

REFERENCES

1. Lueder, D. R. A System for Designating Map-Units on Engineering Soil-Maps. HRB Bull. 28, 1950, pp. 17-35.
2. Miles, R. D., Grabau, W. E., and Rula, A. A. Forecasting Trafficability of Soils–Air Photo Approach. U.S. Army Engineer Waterways Experiment Station, Corps of Engineers, Vicksburg, Miss., Tech. Memo. 3-331, Rept. 6, Vols. 1 and 2, 1963.
3. Moultrop, K. Engineering Soil Survey of Rhode Island. Eng. Exp. Station, Univ. of Rhode Island, Kingston, Bull. 4, 1956.
4. Holman, W. W., et al. Practical Applications of Engineering Soil Maps. Rutgers University, New Brunswick, N.J., Eng. Soil Survey of New Jersey Rept. 22, Eng. Research Bull. 36, 1957, 114 pp.
5. Rib, H. T. An Optimum Multisensor Approach for Detailed Engineering Soil Mapping. Purdue Univ., Lafayette, Ind., PhD dissertation, 1967, 406 pp.
6. Rib, H. T., and Miles, R. D. Multisensor Analysis for Soils Mapping. HRB Spec. Rept. 102, 1968, pp. 22-37.
7. Swain, P. H., and Germann, D. A. On the Application of Man-Machine Computing Systems to Problems in Remote Sensing. Presented at the Eleventh Midwest Symposium on Circuit Theory, Notre Dame Univ., South Bend, Ind., May 13-14, 1968; LARS Information Note 051368, 1968, 10 pp.
8. Landgrebe, D. A., Min, P. T., Swain, P. H., and Fu, K. S. The Application of Pattern Recognition Techniques to a Remote Sensing Problem. Presented at the Seventh Symposium on Adaptive Process, Univ. of California, Los Angeles, Dec. 16-18, 1968; LARS Information Note 08568, 1968.
9. Landgrebe, D. A., and Phillips, T. L. A Multichannel Image Data Handling System for Agricultural Remote Sensing. Computerized Imaging Techniques Seminar, Society of Photo-Optical Instrumentation Engineers, Washington, D. C., June 1967.
10. On Pattern Recognition. Laboratory for Agricultural Remote Sensing, Purdue Univ., Lafayette, Ind., LARS Information Note 101866, 1966.
11. Hoffer, R. M. Interpretation of Remote Multispectral Imagery of Agricultural Crops. Laboratory for Agricultural Remote Sensing, Purdue Univ., Lafayette, Ind., Research Bull. 831, Vol. 1, 1967.
12. Remote Multispectral Sensing in Agriculture. Laboratory for Agricultural Remote Sensing, Purdue Univ., Lafayette, Ind., Vol. 3, 1968, 240 pp.
13. Min, J. P., Landgrebe, D. A., and Fu, K. S. On Feature Selection in Multiclass Pattern Recognition. Proc. Second Annual Princeton Conference on Information Sciences and Systems, Princeton Univ., N.J., March 25-26, 1968.
14. Tanguay, Marc G. Aerial Photography and Multispectral Remote Sensing for Engineering Soils Mapping. Joint Highway Research Project, Purdue Univ., Lafayette, Ind., PhD thesis, Rept. 13, 1969, 308 pp.

Photogrammetric Data Acquisition for a Freeway Ramp Operations Study

JAMES I. TAYLOR, Pennsylvania State University; and
ROBERT G. CARTER, HRB-Singer, Inc.

This paper is concerned with the photogrammetric technique utilized to measure traffic kinematics of interest in an investigation of the effects of environmental conditions (weather and illumination) on a ramp driver's decisions to accept or reject a mainstream gap. A ramp providing access to the Long Island Expressway West in New York City was selected as the study site. Photographs were taken from the roof of a nearby apartment building using 2 Mitchell NC 35-mm motion picture cameras equipped with stop motion motors, set to run at a rate of 2 frames per second. The photo coordinates of each of the vehicles imaged on each photograph were measured at the Pictorial Data Transducer and transformed to ground coordinates. These ground coordinates, in turn, were used to calculate vehicle length, the spacing between successive vehicles on each photograph, and the velocity of each vehicle that appeared on 2 successive photographs. A total of approximately 3,400 vehicle trajectories were computed and filed in the data bank for the ensuing gap acceptance/rejection analyses. Although no precise information is available as to the overall error derived from the operator, the reduction system, and the transformation methods, analysis of the trajectory data indicates the error in the computed position of a vehicle for any given frame averages approximately ±2.5 ft. Trajectory smoothing was utilized to provide better estimates of vehicle positions.

• FREEWAY CONGESTION that results from peak traffic demands has become a widespread problem in all large metropolitan areas and is becoming increasingly critical as the demand for freeway travel continues to outstrip new construction. It is essential that maximum operational capacity of existing systems be obtained. Ramp metering devices to adjust entrance ramp traffic volumes to the available expressway capacity have been in operation for several years in Chicago, Detroit, and Houston. The initial ramp metering devices utilized a simple fixed-cycle traffic signal to control the rate of traffic entering the expressway. Some of the more advanced devices are responsive to measured macroscopic expressway traffic conditions (usually volume).

The research and development of merging control systems have now progressed to the point where sophisticated combinations of mathematical models and adaptive control technology are being applied in hopes of further increasing the operational effectiveness. "Traffic-responsive" systems promise greater efficiency, but their effectiveness will be a function of the compatibility between the control logic and the driver's risk-taking behavior.

Identification of relevant environmental factors, establishment of the relationships that exist between them and driver risk-taking strategies, and isolation of the time-space dynamics that can be measured efficiently for real-time control are a few of the

Paper sponsored by Committee on Photogrammetry and Aerial Surveys and Committee on Pavement Condition Evaluation.

parameters that must be quantified before traffic-responsive control systems can be developed.

To this end, a study entitled "Environmental Requirements for Merging Control Systems" is being conducted by HRB-Singer, Inc., under the sponsorship of the U.S. Department of Transportation, Federal Highway Administration, Bureau of Public Roads. More specifically, the purpose of this study is to investigate the effects of environment conditions (weather and illumination) on a ramp driver's decision to accept or reject a mainstream gap. The methodology employed relies on an assessment of the degree of correlation between gap acceptance/rejection and psychologically effective measures of gap size. Although these psychological gap sizes are subjective, they are defined by a series of alternative mathematical expressions involving observable vehicle kinematics that are available to the driver at the point in time where he is required to render a decision to merge or not to merge.

This paper is concerned with the photogrammetric techniques utilized to measure the traffic kinematics in a manner appropriate for the mathematical expressions utilized in the gap acceptance/rejection analyses.

OBJECTIVES AND PROCEDURES

Objectives

The study involves a comparison of gap acceptance/rejection under varying environmental conditions. The 4 "conditions" of interest can be visualized as the cells of a 2 by 2 matrix, with day versus night as one axis and wet versus dry as the other. In essence, then, it was necessary to collect all the physical situational data that might psychologically affect the decision of the driver of a vehicle entering from the ramp to accept a mainstream gap or not. As an integral part of the study consisted of the determination of which factors do affect the driver's decision, one of the initial project tasks was to develop a comprehensive list of alternative expressions for "g," the subjective gap size or index of acceptability of a gap, that might be critical to the decision reached by the ramp driver. In all, 43 expressions were developed and are being evaluated. For illustrative purposes, a few of these expressions are as follows:

$$\frac{G_{(i)}}{V_{F(i)} - V_R + 100}$$

$$\frac{D_{(i)}}{V_{D(i)}}$$

$$\frac{G_{(i)}}{D_{(i)}\left[V_{F(i)} - V_R + 100\right]}$$

$$\frac{LD_{(i)}}{\left[V_{LD(i)} - V_R + 100\right]}$$

$$\frac{D_{(i)}}{\left[V_{D(i)} - V_R + 100\right]} - \frac{0.75 + \left[V_{D(i)} - V_R\right]}{19}$$

The inputs for all of the 43 expressions can be evaluated from the measures shown in Figure 1.

For any time, t, the basic measures that follow were either recorded directly or calculated.

1. $X_{RF(i)}$ longitudinal coordinate of ramp vehicle, front;
2. $X_{RR(i)}$ longitudinal coordinate of ramp vehicle, rear;
3. $X_{LR(i)}$ longitudinal coordinate of lane vehicle, rear;

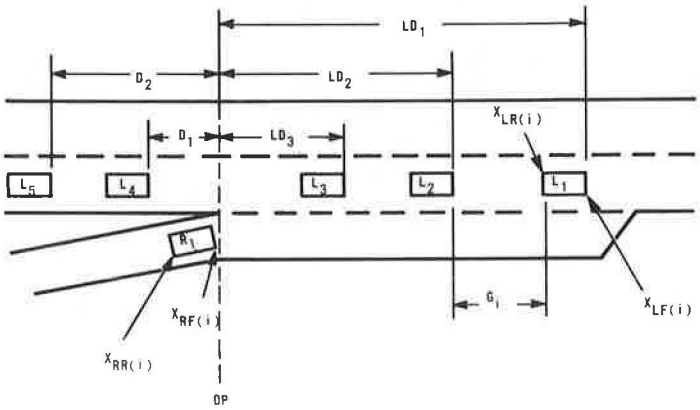

Figure 1. Schematic of typical vehicle configuration showing single ramp vehicle and basic measures used to formulate g expressions.

4. $X_{LF(i)}$ longitudinal coordinate of lane vehicle, front;
5. $L_{R(i)}$ length of ramp vehicle i;
6. $L_{L(i)}$ length of lane vehicle i;
7. $V_{L(i)}$ velocity of lane vehicle i;
8. $V_{R(i)}$ velocity of ramp vehicle i;
9. $G_i = X_{LR(i)} - X_{LF(i+1)}$ distance headway between any 2 lane vehicles;
10. $H_i = G_i - L_R$ distance headway less length of ramp vehicle at decision point;
11. $LD_i = X_{LF(i)} - X_{RF(i)}$ lead distance in which $X_{LF(i)}$ is downstream of $X_{RF(i)}$;
12. $D_i = X_{RF(i)} - X_{LF(i)}$ lag distance in which $X_{LF(i)}$ is upstream of $X_{RF(i)}$; and
13. $F_{(i)}$ following vehicle.

Hence, the basic problem was to derive these measures for each of the 4 environmental conditions, i.e., day-dry, night-dry, day-wet, and night-wet.

Site Selection Criteria

The process of choosing study locations for any field study effort is nearly always difficult, requiring the considered, but always compromised, matching of the experimental ideal with the physical limitations imposed by reality. In this particular effort, the site selection criteria fell into 3 main sets: geometric, operations, and photographic.

Geometric Criteria—In terms of physical restrictions placed by these criteria on the final selection of the study site, considerations of geometry were the least consequential. The conceptual design of the study did not call for a large sample of ramp designs and, therefore, any ramp that met certain minimum specifications could be expected to display "typical" merging behavior within the construct of the study.

Operational Criteria—The operational characteristics required of the ramp-freeway complex were related to traffic volumes on the main stream and ramp, and the requirement that no anomalous conditions affect flow in the vicinity of the site (i.e., no construction or detours).

Photographic Criteria—The conceptual study design requirements dictated a unique and rather stringent set of photographic criteria. Inasmuch as three-quarters of the data were to be collected under low illumination and/or inclement weather, the use of conventional aerial photography was precluded. The area coverage requirements, which extend considerable distances both up and downstream from the ramp nose, ruled out ground level photography. Hence, a fixed, elevated vantage point was required. The prime selection criterion, then, was the presence of such a vantage point, such as a tall building in close proximity to the ramp. Correlary requirements were as follows:

1. View of the entire site from the vantage point had to be virtually unobstructed.
2. The relative position of ramp and building could not introduce large distortions due to camera angle; i.e., obliqueness should be minimized to enhance photographic measurements.
3. The distance from the ramp to the building was constrained by the requirement to have as few cameras as possible while maintaining a scale such that measurement of the photographs was feasible.
4. "Appropriate" light conditions (i.e., "night" and "day") had to occur at the same hour of the day as a function of seasonal and time system change so that traffic characteristics would be similar under both conditions. Thus, a study site was required such that the study area would be in daylight in the summer at approximately 6 p.m. daylight saving time, and dark in the late fall at 6 p.m. standard time.

Characteristics of Selected Site

Freeways in Chicago, Detroit, Boston, and New York City were visited and surveyed for appropriate sites. As might be expected, very few ramps that satisfied the combined conditions outlined were found. The site finally selected was a ramp on the Long Island Expressway. This ramp provides access to the Long Island Expressway West from the North Service Road at a point between 99th Street and Junction Boulevard. The study site is shown in Figures 2 and 3. The characteristics are as follows:

Geometric—Ramp angle is $8\frac{1}{2}$ deg; acceleration lane is 554 ft long; acceleration lane is parallel to main roadway; grade of ramp and main roadway is nearly flat; main road up and downstream from ramp is on a tangent; and ramp is on a tangent.

Operations—Traffic volume is approximately 1,500 vph in each lane of the main stream; ramp volume is approximately 225 vph; no construction, rerouting, or other anomalous condition was present; and these conditions were met at the appropriate time of day.

Photographic—Apartment building downstream from ramp nose provided required photographic observation post. View of ramp and mainstream was free from permanent obstructions (minor problems of masking by large commercial vehicles did occur). Downstream view was adequate and ramp and upstream view were oblique but tolerable. Distance from building to ramp and acceleration lane was such that 2 camera set-ups provided adequate coverage. Ramp and merge area were illuminated at night by 400 watt, mercury-vapor luminaires, mounted 30 ft above the road. Distance between light standards varied from 65 to 220 ft. Sun angle was appropriate. Time/seasonal variation was as desired.

Figure 2. Upstream view of study site in daylight.

Figure 3. Downstream view of study site in daylight.

DATA COLLECTION

Time

As indicated earlier, the selection of the data collection time period was of concern because the design of the study required both day and night data. In addition, it was necessary that the driver population be relatively constant (i.e., it would not be desirable to have rush-hour traffic in the day condition and not at night). Further the time selected had to span a period when the prevailing conditions met the operational criteria The time period selected as satisfying the requirements was from 5:30 to 6:30 p.m. in May, June, July, and August for "day" and during November, December, January, and February for "night."

Equipment

The camera system employed in the majority of the data collection effort consisted of 2 Mitchell NC 35-mm motion picture cameras equipped with stop motion motors, set to run at a rate of 2 frames per second. Shutter synchronization was achieved by setting each camera's shutter manually to the same starting position. The cameras' motors were then started simultaneously by means of a common start switch. Shutter speed was set at $1/100$ sec. Lenses were 18.5-mm wide-angle Angnieux f/2.2. Figure 4 shows the placement of the cameras on the roof.

Film

Of necessity, prevailing light conditions varied widely among the 4 data collection "treatment" conditions, ranging from normal daylight through heavy, cloud-obscured sun, to the absence of any sunlight. This necessitated the use of 3 different types of film, depending on the existing ambient light conditions. The following summarizes treatment conditions, film types, and processing specifications:

Condition	Film Type	Processing	Remarks
Day-dry	Kodak double X	Effective ASA 320	
Day-wet	Kodak four X	Effective ASA 600	
Night-dry/wet	Kodak 2475 Recording	Rated ASA 400 Revised to ASA 1250	Large grain but acceptable

DATA REDUCTION

Reduction Device

The photographic data were reduced to numerical data (to allow evaluation of the space-time relationships) through the use of the Pictorial Data Transducer (PDT), an optical-comparator device. This device was interfaced with a Model 026 card punch. Normal machine functions were retained making it possible to use the card-punch keyboard for identification purposes. Moreover, the duplication function of the machine remained intact, allowing quick and efficient correction of punching errors.

Figure 4. View of the upstream (on left) and downstream (on right) camera positions.

Operator Procedures

Vehicle position data were taken on every photographic frame, i.e., at half-second intervals. The positional information obtained consisted of the location of all outside lane vehicles and ramp vehicles within camera view. No positional information was taken on vehicles in the middle or inside lanes because the study was

concerned only with the ramp vehicle's marge into the outside lane. Moreover, frames were skipped if all vehicles on the ramp had merged.

Vehicle numbers were assigned as a vehicle entered the camera's view either on the ramp or in the outside lane and were carried through from the upstream view to the downstream view in order to keep track of the vehicle and to facilitate the integration of the 2 views into one data record. Other identification data assigned to a vehicle were a number indicating whether it was a lane or a ramp vehicle (1 or 2 respectively); vehicle type identification (1 for passenger, 2 for commercial); and whether the vehicle data position was taken on the corner of the left front bumper, 1, or the corner of the left rear bumper, 2. In those cases in which a vehicle was hidden behind another vehicle, an estimated point was taken, and the data acquisition identifier was a 3, thereby flagging the need for replacement by an interpolated point.

To indicate merging by a ramp vehicle, the lane designation of a ramp vehicle was changed from a 2 to a 1 when its left front wheel crossed the lane divider line. It was felt that this point in time indicated encroachment into the next lane and signaled a driver's intention to merge.

Positional data were also taken within each photographic frame on 3 fixed reference points used for translating a "data" frame's points to a "map" frame for transposition to ground coordinates.

Determination of Ground Coordinates of Vehicles

The photo coordinates of each of the vehicles imaged on each photograph were transformed to ground coordinates. These ground coordinates, in turn, were used to calculate the spacing between successive vehicles on each photograph, and the velocity of each vehicle that appeared on 2 successive photographs.

The ramp and section of highway adjacent to it are essentially flat; i.e., the pavement surfaces can be considered to lie in a single plane. Because the photographs are also planar, transformation equations based on the projectivity between 2 planes can be utilized. The transformation equations used are as follows:

$$X_G = \frac{a_1 x_p + b_1 y_p + c_1}{dx_p + ey_p + 1}$$

$$Y_G = \frac{a_2 x_p + b_2 y_p + c_2}{dx_p = ey_p + 1}$$

where X_G and Y_G are ground coordinates, x_p and y_p are photo coordinates, and a_1, b_1, c_1, a_2, b_2, c_2, d, and e are the 8 required transformation coefficients. The space orientation, origin position, and scales of the ground coordinate and photo coordinate systems may be completely arbitrary (the coordinate systems must be rectangular, however).

The projectivity between the 2 planes (photograph and ground) is uniquely determined if the 8 coefficients are known. The determination of these 8 quantities requires at least 4 pairs of equations of the type shown. This equation system can be solved if the photo coordinates and ground coordinates of 4 points are known. These points, which for this study were objects on the ground in the area of interest (lamp post bases, storm sewer grates, and the like) and identifiable on the photographs, are commonly referred to as "ground control points."

After the coefficients of the transformation equations have been computed, utilizing the ground control points, the expressions may be used for computing ground coordinates for the vehicles from their respective photo coordinates.

(An intermediate step was employed to minimize the PDT operators' time. On the data frames the operators read 3 reference points in the area of the photograph that covered the ramp-expressway complex. A simple rotation/translation transformation was then used to transform the coordinates measured on the data frames to map frames on which were measured the 3 reference points and the 4 ground control points.)

PDT and Operator Accuracy

It is believed that the measurement of photo coordinates is the largest single source of error in the ground coordinate determination procedure. The method used for checking operator accuracy during data reduction was independent of ground measurements and was considered entirely from the standpoint of PDT encoder output units. The distances between the 3 reference points used on each photograph were calculated from the measured coordinates and noted in output units. The means and the standard deviations for each difference for an operator's group of frames were then calculated. An operator taking repeated positional measurements on a "clearly defined" point in the projected image could reliably locate the point with ±3 output units. (One output unit corresponds to approximately 0.000078 in. of travel on the film plane.) However, there is a distinct difference between testing for optimal accuracy and reducing a mass of data of average photo quality over long periods of time. In general, a standard deviation of ±15 units in the distance between reference points was obtained for the "data" photographs.

Operator accuracy, as discussed here, is in relation to PDT output units only. In the upstream view, on reference points near the entrance to the ramp, the conversion scale is 0.19 ft or 2.3 in. per PDT measurement unit. These points were furthest from the camera. For points at the other end of the upstream view, the scale conversion values were 0.02 ft or 0.24 in. per PDT unit. In terms of ground position error, then, ±15 PDT units means ±2.8 ft on the ground in the worst case, and ±0.30 ft at the near end of the photo coverage. The scale values obtained for points on the downstream photos near the end of the acceleration lane (furthest point from the camera) were approximately 0.06 ft (0.72 in.) per PDT unit on the X-axis of the expressway (i.e., along the road). Scale values for reference points near the camera are similar to those obtained for near points on the upstream camera, i.e., 0.02 ft (0.24 in.) per unit. Using these values, in the worst case ±15 PDT units correspond to +0.90 ft in ground distance and, in the other case, ±0.30 ft along the road.

Error Considerations

Although a detailed error analysis has not been made, it is reasonable to expect that the errors in the ground coordinates of the vehicles, as determined through this transformation procedure, will be somewhat larger, but not appreciably. Identification of the "measured point" on the vehicle (left corner of the front bumper) is not significantly more difficult than identification of the ground control points on the photographs, and hence errors in the measurement of the photo coordinates should be of comparable accuracy.

It is recognized that all vehicle bumpers are not at the same elevation above the roadway, and, hence, all vehicle points do not lie in a true plane. However, in velocity computations, the resultant errors will be very nearly self-canceling (i.e., the errors in the X- and Y-ground coordinates of the vehicle will be nearly equal in magnitude and direction in both photographs and, therefore, the change in ground coordinates from one photograph to the other will be essentially correct). In spacing calculations, the error will exist but will be of such magnitude that it will not materially affect the computation of the spacing between successive vehicles.

VEHICLE TRAJECTORIES

The data reduction procedure provides for the transformation of measured photo coordinates to ground positions. The transformation is such that the X-axis of the ground coordinate system is parallel to the centerline of the freeway. Because the angle between the ramp and the freeway is small, the X-ground coordinates of vehicles on the ramp can also be used to define their positions. As lateral position (within a lane) is not of concern in this study, the Y-ground coordinates can be dropped as they will not enter any of the ensuing analyses.

Each vehicle carries an identifying number. Hence, the position (relative to a line parallel to the centerline of the freeway) of each vehicle is known every time it appears on a photograph. As the time interval between photographs is known, it is possible to

construct a time-space trajectory for each vehicle through the length of freeway (and ramp) under observation. This collection of time-space trajectories constitutes the data base from which the gap acceptance/rejection analyses are made.

The velocity of a vehicle may be determined by noting its change in position from photograph to photograph, as the time base is known. The spacing between any 2 vehicles, at a given time, may be determined by noting the differences in their X-ground coordinates or positions on a given photograph.

Inaccuracies in the computed trajectories will occur because of mistakes in observations and incorrect measurements and operations. The first type, mistakes in observations, derive from 2 principal sources: mis-identification of vehicles, and loss of image of a vehicle (e.g., vehicle of interest hidden behind a large truck) on a specific photograph or series of photographs. This latter mistake is beyond the control of the photo coordinate reader, of course, and is due to the fact that oblique photography had to be used. In order to enter the identification number for a vehicle so hidden, the operator of the coordinate reading device was instructed to enter a fictitious position coordinate. When these coordinates are later used to establish ground positions, erratic trajectories result. By computing the velocity of each vehicle over each half-second interval, and then comparing consecutive velocities, rough estimates of the acceleration rates can be obtained. Limits are set for the maximum possible acceleration (deceleration) values to be expected in traffic operations. When these limits are exceeded, the computer rejects the specific vehicle position(s) creating these unrealistic conditions and inserts a new coordinate for that vehicle so that a relatively smooth trajectory is obtained through the "bad" photograph or series of photographs. These changes are noted and are part of the computer printout.

Minor erraticisms still remain in the trajectories after the elimination of the gross errors mentioned. The solid line in Figure 5 represents a plot of values of velocity

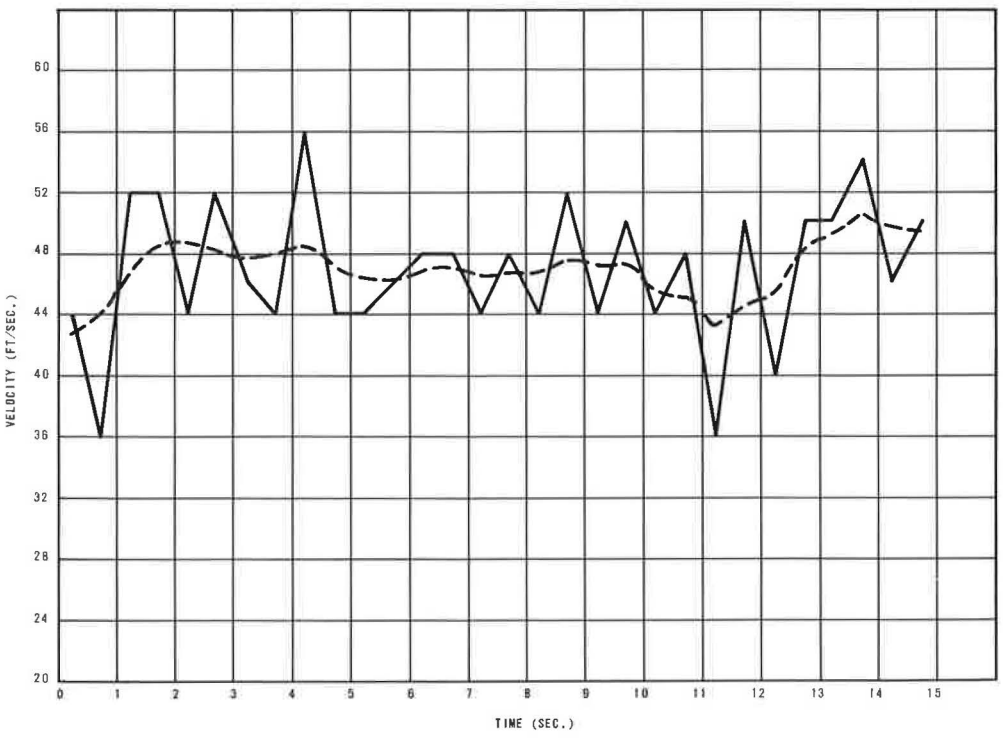

Figure 5. Single vehicle trajectory (before and after smoothing).

computed over consecutive half-second intervals over a total time period of 15 seconds (for a single vehicle). Note that although the trend is fairly obvious and reasonable, the acceleration/deceleration pattern represented by these values is quite erratic. In fact, it is still beyond the physical capabilities of any standard vehicle, as the limits set in the initial smoothing are quite broad. This erratic velocity pattern is caused by incorrect measurements and operations. The principal sources of these errors are lens and film distortions; simplifying assumptions in the transformation procedure; operator errors in the measurement of the photo coordinates of the ground control points and the vehicles themselves; slight variations in the vertical and horizontal alignment of the freeway and ramp; and basic inaccuracies (least count limitations) of the coordinate measuring device. Some of these errors are systematic (e.g., lens distortions, roadway alignment variations, and minor errors introduced through simplifying assumptions in the transformation procedure) and could be eliminated through calibration and correction equations. However, the development of the required equations would be expensive, and the resultant improvement would not be significant. As discussed previously, the overriding limitation in the data reduction system is the pointing ability of the operators of the photo coordinate reading device. Errors from this source are random in nature, and although the magnitude of such errors can be determined, correction is not possible.

In the ensuing analyses of gap acceptance criteria, only a few discrete points from any one trajectory will be utilized. In order that errors in the spacings and relative velocities of vehicles of interest do not obliterate gap acceptance relationships that may exist, it is imperative that the "most probable" values of velocities and positions at the specific times of interest be utilized. Hence, a trajectory-smoothing operation was carried out before further analyses.

As noted before, collectively, the raw data shown in Figure 5 present a reasonably clear indication of the velocity pattern of the vehicle. For any given half-second interval, however, the unadjusted velocity value may be considerably in error. If the information available from the overall pattern is synthesized through a curve-smoothing technique, a reasonable value may be estimated for each half-second interval. The technique utilized here calls for replacing the velocity value at any given half second by a new value obtained as follows:

$$V_{ia} = \frac{V_{i-2} + 2V_{i-1} + 3V_i + 2V_{i+1} + V_{i+2}}{9}$$

where

V_{ia} = adjusted value of the velocity at interval i, and
V_{i-2} = initial value of the velocity 2 intervals before i, and so on.

The results of this smoothing technique for the vehicle shown in Figure 5 are indicated by the dashed line. The technique for smoothing the velocity trajectories was carried out on all trajectories within the data bank before the trajectory data were used as input to the gap acceptance relationship analyses.

RESULTS

The basic measures used to formulate the g-expressions (shown in Fig. 1) can be derived from the smoothed trajectories. The accuracy has been determined to be suitable for the analyses to be performed, and the methodology has been successfully established.

From the photos available to date, covering a total time period of 4 hours, a total of approximately 3,400 trajectories have been constructed and filed in the data bank.

In essence, the position of each vehicle at ½-second intervals for the total period of time it was within the field of view of either camera (a total travel distance of 900 ft) has been determined. From these data, velocities of individual vehicles and relative velocities and spacings between sets of vehicles can be easily determined. In addition, the length of each vehicle is also available.

Although no precise information is available as to the overall error derived from the operator, the reduction system, and the transformation methods, trajectory data

indicate the error in the computed position of a vehicle for any given frame averages approximately ±2.5 ft. Occasional gross errors were also noted from the trajectory output and are a result of a number of factors, e.g., random PDT errors (dropped digits), misidentification of vehicles, estimated positions of hidden vehicles, and film distortion. Trajectory smoothing was utilized to remove the gross errors and minor erraticisms, thereby providing better estimates of vehicles' positions for the gap acceptance/rejection analyses to follow.